AD-A112 571 AUBURN UNIV ALA DEPT OF AEROSPACE ENGINEERING F/G 19/7
ROCKET LAUNCHERS AS PASSIVE CONTROLLERS.(U)
DEC 81 J E COCHRAN, R T GUNNELS DAAH01-80-C-0523
UNCLASSIFIED DRSMI/RL-CR-82-2 NL

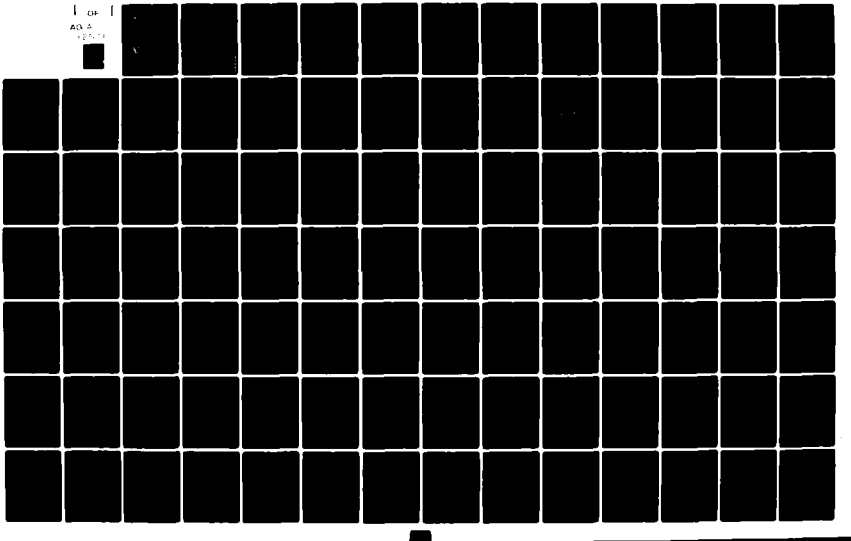

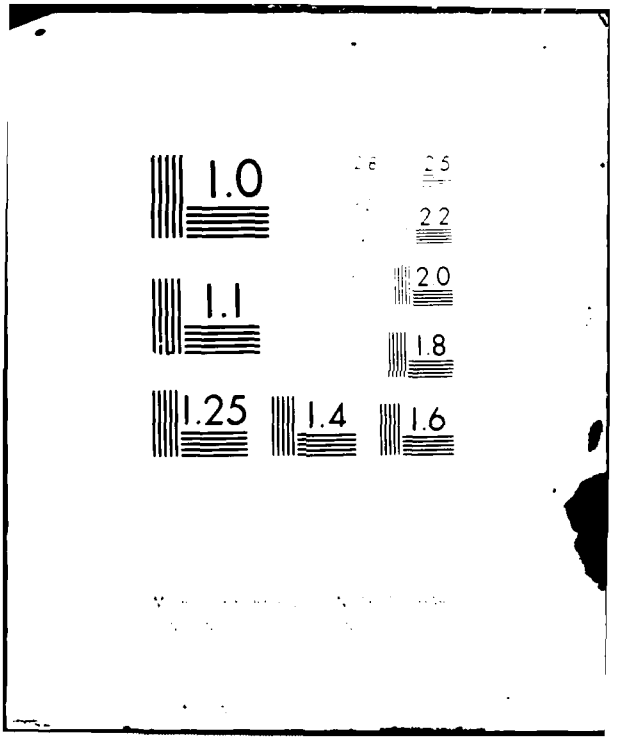
1.0
1.1
1.25
1.4
1.6
2.0
1.8
2.2
2.5

(2)

AD A112571

TECHNICAL REPORT RL-CR-82-2

ROCKET LAUNCHERS AS PASSIVE CONTROLLERS

by

John E. Cochran, Jr., Richard T. Gunnels and
Robert K. McCutchen, Jr.

Aerospace Engineering Department
Auburn University, Alabama 36849

U.S. ARMY MISSILE COMMAND
Redstone Arsenal, Alabama 35809

FINAL REPORT

under
Contract DAAH01-80-C-0523

Administered through

Engineering Experiment Station
Auburn University, Alabama 36849

31 December 1981

DISPOSITION INSTRUCTIONS

DESTROY THIS REPORT WHEN IT IS NO LONGER NEEDED. DO NOT RETURN IT TO THE ORIGINATOR.

DISCLAIMER

THE FINDINGS IN THIS REPORT ARE NOT TO BE CONSTRUED AS AN OFFICIAL DEPARTMENT OF THE ARMY POSITION UNLESS SO DESIGNATED BY OTHER AUTHORIZED DOCUMENTS.

TRADE NAMES

USE OF TRADE NAMES OR MANUFACTURERS IN THIS REPORT DOES NOT CONSTITUTE AN OFFICIAL INDORSEMENT OR APPROVAL OF THE USE OF SUCH COMMERCIAL HARDWARE OR SOFTWARE.

SECURITY CLASSIFICATION OF THIS PAGE *(When Data Entered)*

REPORT DOCUMENTATION PAGE		READ INSTRUCTIONS BEFORE COMPLETING FORM
1. REPORT NUMBER RL-CR-82-2	2. GOVT ACCESSION NO. AD-A112 571	3. RECIPIENT'S CATALOG NUMBER
4. TITLE *(and Subtitle)* ROCKET LAUNCHERS AS PASSIVE CONTROLLERS		5. TYPE OF REPORT & PERIOD COVERED FINAL 6. PERFORMING ORG. REPORT NUMBER
7. AUTHOR(s) John E. Cochran, Jr., Richard T. Gunnels, and Robert K. McCutchen, Jr.		8. CONTRACT OR GRANT NUMBER(s) DAAH01-80-C-0523
9. PERFORMING ORGANIZATION NAME AND ADDRESS Engineering Experiment Station Auburn University, Alabama 36849		10. PROGRAM ELEMENT, PROJECT, TASK AREA & WORK UNIT NUMBERS
11. CONTROLLING OFFICE NAME AND ADDRESS Commander, U.S. Army Missile Command Attn: DRSMI-RLH Redstone Arsenal, Alabama 35898		12. REPORT DATE December 31, 1981 13. NUMBER OF PAGES 103
14. MONITORING AGENCY NAME & ADDRESS(*if different from Controlling Office*) Commander, U.S. Army Missile Command Attn: DRSMI-RLH Redstone Arsenal, Alabama 35898		15. SECURITY CLASS. (*of this report*) UNCLASSIFIED 15a. DECLASSIFICATION/DOWNGRADING SCHEDULE

16. DISTRIBUTION STATEMENT *(of this Report)*

DISTRIBUTION STATEMENT A
Approved for public release;
Distribution Unlimited

17. DISTRIBUTION STATEMENT *(of the abstract entered in Block 20, if different from Report)*

18. SUPPLEMENTARY NOTES

19. KEY WORDS *(Continue on reverse side if necessary and identify by block number)*

Free Rockets
Rocket Launcher Dynamics
Passive Control
Dispersion
Launcher Response
Thrust Misalignment
Dynamic Imbalance

20. ABSTRACT *(Continue on reverse side if necessary and identify by block number)*

A concept is advanced for using the motion of launchers of a free-flight launcher/rocket system which is caused by random imperfections of the rockets launched from it to reduce the total error caused by the imperfections. This concept is called "passive launcher control" because no feedback is generated by an active energy source after an error is sensed; only the feedback inherent in the launcher/rocket interaction is used. Relatively simple launcher models with two degrees of freedom, pitch and yaw, were used in

DD FORM 1 JAN 73 1473 EDITION OF 1 NOV 65 IS OBSOLETE

SECURITY CLASSIFICATION OF THIS PAGE *(When Data Entered)*

conjunction with a more detailed, variable-mass rocket model in a digital simulation code to obtain rocket trajectories with and without thrust misalignment and dynamic imbalance. Angular deviations of rocket velocities and linear deviations of the positions of rocket centers of mass at burnout were computed for cases in which the launcher was allowed to move ("flexible" launcher) and was constrained so that it did not rotate ("rigid" launcher) and ratios of flexible to rigid deviations were determined. Curves of these "error ratios" versus launcher frequency are presented. These show that a launcher which has a transverse moment of inertia about its pivot point of the same magnitude as that of the centroidal transverse moments of inertia of the rockets launched from it can be "tuned" to passively reduce the errors caused by rocket imperfections. Additionally, results are presented which show that this reduction can be achieved if the imperfections are random. Hence, dispersion of free-flight rockets can be reduced by using passive control launchers. Reduction of dispersion by up to eighty percent appears possible.

PREFACE

This report contains the principal results obtained during an investigation of the passive control potential of launchers of free-flight rockets, under U.S. Army Contract DAAH01-80-C-0523, for the U.S. Army Missile Command, Redstone Arsenal, Alabama. The Contracting Officer's Technical Representative has been Mr. Dean E. Christensen. His advice and support are hereby gratefully acknowledged.

Graduate Research Assistants, Mr. Robert M. Watson and Mr. Fu-Chen Hwong, did most of the plots. Mr. Ping-Huei Shu, also a Graduate Research Assistant, rendered valuable assistance in computer programming. Their help is sincerely appreciated. Most of the other graphics work and some of the plots were done by Engineering Learning Resources Center staff.

For her expert typing, Mrs. Marjorie McGee deserves special recognition and thanks.

John E. Cochran, Jr.
Project Leader

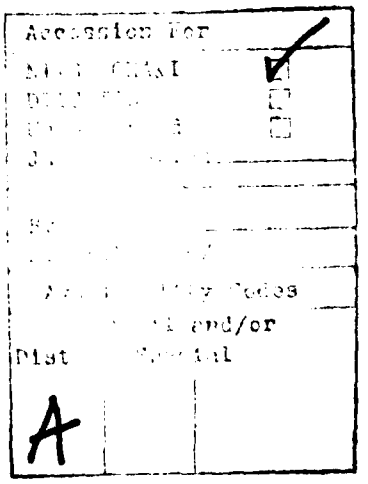

TABLE OF CONTENTS

TABLE OF CONTENTS (CONTINUED)

LIST OF FIGURES

LIST OF FIGURES (CONTINUED)

LIST OF FIGURES (CONTINUED)

LIST OF TABLES

SECTION 1. INTRODUCTION

1.1 Dispersion of Free-Flight Rockets

Free-flight, or "uncontrolled," rockets are very important tactical weapons because they can be used to rapidly deliver large payloads with good accuracy and at low cost relative to more sophisticated weapons. The characteristics of accuracy and low cost are conflicting ones. In keeping costs low, concessions must be made in manufacturing requirements. This results in rockets which are more imperfect than those which could be built if cost was not considered. These imperfections are random and of many types. They include, for example,[1,2] non-straightness dynamic imbalance, static imbalance, propellant imperfections, thrust misalignment, and geometric asymmetries. Since a free-flight rocket is not controlled after it leaves the constraints of its launcher, random imperfections cause random deviations of its actual flight path from the nominal, or expected, flight path. Given a group of rockets, the summation of the individual deviations is called "dispersion."

Of course, there are other causes of dispersion. For instance, one immediately thinks of random winds.[3] However, thrust misalignment and dynamic imbalance are two primary causes of dispersion of free-flight rockets.

In the literature (see, for example, Ref. 2, pp. 68, 149-156) the terms "mallaunch" and "malaim" are used for random transverse angular rates and angular rotations, respectively, produced by the launcher/rocket interaction. Although changes in its environment may cause a launcher to perform differently at different times, it may be considered much more deterministic

than the rockets launched from it. Hence, if the characteristics of a particular launch are well known, the major part of the "mallaunch" and "malaim" associated with it must be due to imperfect rockets which are generally the only energy source present.

If "mallaunch" and "malaim" are generated primarily by imperfect rockets, there is reason to believe that - as "mal" denotes "bad" - a "goodlaunch" and "goodaim" may exist. The grounds for this reasoning are that the trajectory of a free-flight rocket is significantly affected by the rocket's flight state when it leaves the influence of the launcher and that this state could, it would appear, be one which reduces the error produced by rocket imperfections in free-flight rather than one which increases such errors. The motivation for this investigation was provided by the hope that proper design of launchers will lead to the replacement of "mallaunch" and "malaim" by their antonyms, whatever they may be.

1.2 Scope of this Effort

Previously, the connection between the random part of the motion of a launcher and that of a rocket launched from it has been generally disregarded. Valid reasons for this are (1) that launchers are often much more massive than the rockets launched from them and (2) that mathematical simulations of the motion of rockets and of the motion of launchers have, for the most part, been pursued independently. This qualifier "generally" is used above because there have been investigations the objective of which was to design a launcher which compensated for rocket imperfections. The PADA[3] concept of compensating for dynamic imbalance is a case in point.

The goal of this effort was to determine whether a launcher can compensate for random imperfections of free-flight rockets. The objectives were

to model the launcher/rocket system mathematically, to use this mathematical model to determine qualitatively how rocket imperfections affect launcher motion and to produce quantitative numerical results which show how a launcher characteristic, such as launcher inertia and natural frequency of the launcher, affect its performenace as a passive controller.

This goal was partially achieved during the first phase of this investigation.[4] The results reported in Ref. 4 are qualitatively correct, but an error in the computer code which was found subsequent to publication of Ref. 4 renders the quantitative results for launcher/rocket systems given therein invalid. A later paper[5] presents more accurate results which somewhat substantiate the concept of launchers as passive controllers, but they are limited since only a few cases were studied.

In the next section, the concept of passive control as applied to rocket launchers is discussed and some practical considerations which are warranted by physical laws and intuition are stated. Section 3 provides descriptions of physical models of the launcher and rocket, as well as data used in the numerical portion of the investigation.

The rather extensive results contained in Section 4 include plots showing the effectiveness of a launcher in reducing dispersion due to thrust misalignment and dynamic imbalance. The effects of launcher frequency and inertia are illustrated and the effects of errors in rocket thrust profile are quantified to some extent. Conclusions and recommendations are given in Section 5.

Detailed descriptions of the mathematical models developed and used to produce the quantitative results are found in Appendix A. Finally, details of a "prototype" launcher model are given in Appendix B.

SECTION 2. PASSIVE CONTROL

2.1 The Concept

Passive, as opposed to active, control involves the use of an energy source, or sources, inherent within a system and/or its environment and "natural" feedback to produce a desirable response of the system when a disturbance acts upon it. A good example of the use of passive control is presented by gravity-gradient stabilized spacecraft.[6] Such satellites are designed so that the torque due to the gradient of the earth's gravitational field causes the spacecraft to rotate about a centroidal axis which is perpendicular to the satellite's orbital plane once each orbit thereby pointing one axis of the satellite toward the earth. In this example, the "control" torque is due to the environment and the satellite configuration.

Regarding launcher/rocket systems, the energy source is the rocket's motor, and in some cases, a spin motor. The feedback to the rocket is transferred through the launcher/rocket interface. All motion of the system is due to the rocket motion, spin motor, gravity and aerodynamic forces. The force due to gravity produces a tipping of the launcher which is essentially independent of the imperfections the rocket has except, of course, the propellant imperfections which result in different guidance times. Aerodynamic forces include those due to the flow field about rocket and launcher during guidance which are very difficult to define, and those on the rocket during free-flight, which can usually be determined quite well from wind tunnel tests.

The random forces and moments of interest herein are those due to thrust misalignment and dynamic imbalance. Moreover, the thrust misalignment is

assumed to be angular misalignment such as that due to a misaligned rocket nozzle. The dynamic imbalance is assumed to be due to a misalignment of the principal axis of least inertia and the geometric symmetry axis of the rocket.

It can be demonstrated[1,5,6] that the flight errors due to thrust misalignment and dynamic imbalance are manifested during the time of thrusting. These errors are of the same type as those generated by transverse angular rates of the rocket at the time it leaves the launcher. In fact, it can be shown[4] that, for a spinning rocket, thrust misalignment and dynamic imbalance result in transverse angular rates of the rocket during the first quarter of a revolution of the rocket after it leaves the launcher. These angular rates persist until damped out by aerodynamic moments. Because of the nature of the errors due to these two types of rocket imperfections; i.e., their equivalence to those due to transverse angular rates at end of guidance, it follows that if proper transverse angular rates of the system are caused by imperfections prior to the time the rocket leaves the launcher, then the adverse effects of rocket imperfections can be reduced. This is the passive control concept advanced herein. In simpler terms, if the imperfections cause the system to rotate or to be rotating in one direction when the rocket leaves the launcher and they cause the rocket to rotate in the opposite direction during free-flight, the total error will be less than if the launcher did not move.

2.2 Practical Considerations

There are two basic requirements for passive control by the launcher. First, the imperfections of the rocket must cause the system to rotate.

Second, the rotation must be in opposition to that which the imperfections cause during free-flight.

The first requirement dictates that either the entire launcher, or the part of the launcher in contact with the rocket, must be small enough that the imperfections can produce motion of it and the rocket. Hence, if the launcher (or the part of it) is much more massive than the rocket, one would expect little if any passive control to be possible. Figure 1 shows a concept of a passive control launcher in which the launch "tube" (which may not be closed, but could be a framework) can rotate transversely in response to rocket imperfections. To satisfy the second requirement, either the system must rotate to point the rocket in a direction in opposition to that it will rotate during free-flight, or the system must acquire an angular rate which is in opposition to that generated subsequent to launch. To get such a system response, one must design a launcher (or part of it) which is supported so that limited rotation is possible and, in the case of production of angular rates, has a natural frequency which causes its response to be out-of-phase with the post-launch response of the rocket.

An important fact to remember is that for a spinning rocket the angular rate produced by dynamic imbalance or thrust misalignment is 90° out-of-phase with the body-fixed torque caused by the imperfection. The launcher response must be determined accordingly. Furthermore, if the rocket is not spinning when it leaves the constraints imposed by the launcher, the duration of its powered flight must not be too much longer than the time it spent on the launcher; for, if it is, the angular rotation produced by thrust misalignment during free-flight will be much larger than any

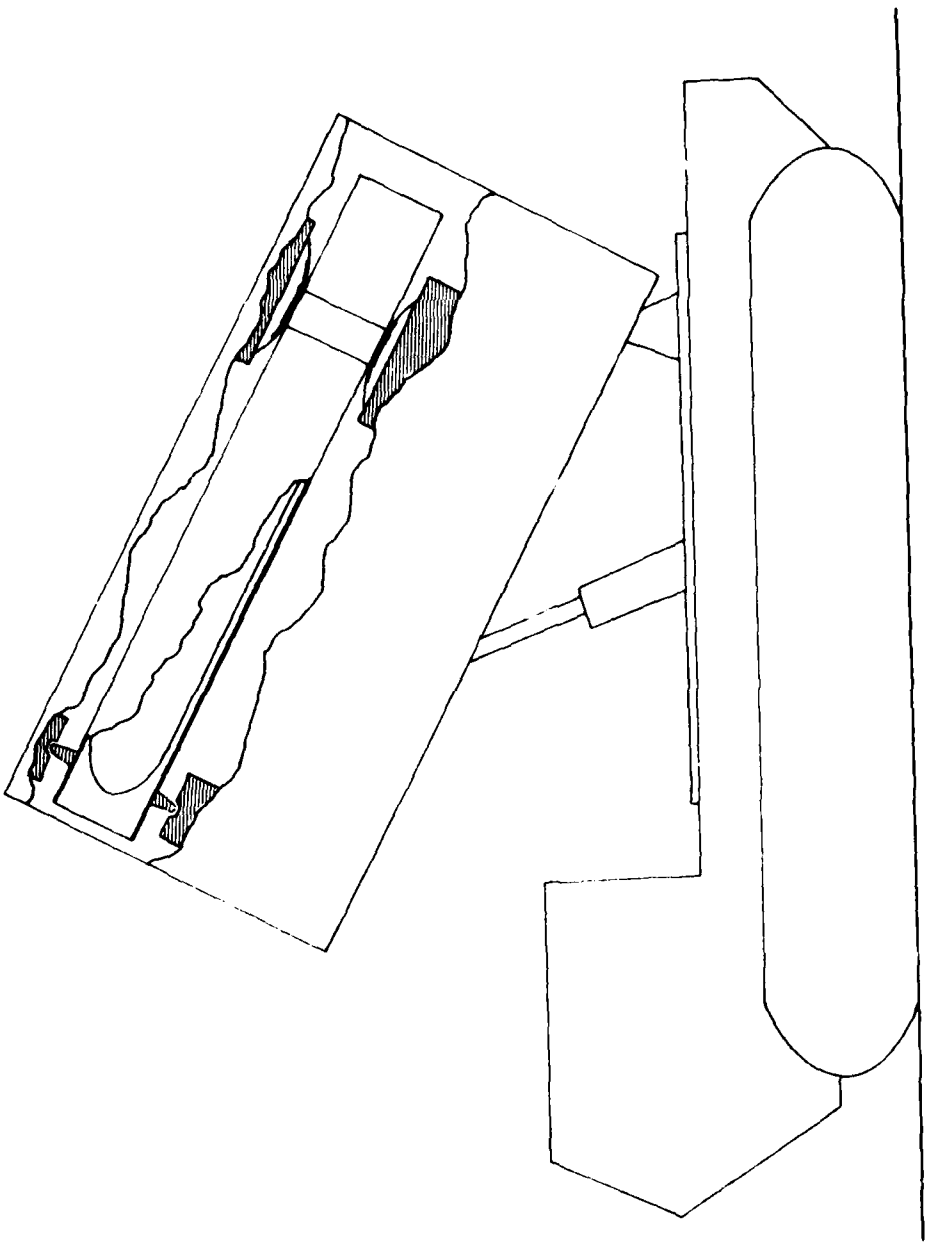

Fig. 1 Passive control launcher.

compensating rotation or angular rate that was produced by the imperfection prior to free-flight. Reference 4 contains additional discussion of the points.

In summary, intuition and physical reasoning dictate (1) a small launcher, or a small part of the launcher, which can respond to the imperfection and (2) proper phasing of the launcher and rocket motion.

SECTION 3. MODELS

3.1 General Comments

In this section the models of the launcher and rocket adopted for this investigation are described. Additional discussion of the models and the governing equations of motion are provided in Appendix A.

Although it is somewhat redundant, since similar comments are made in Appendix A, it is worth stating twice that the dynamical system of vehicle, launcher and rocket(s) is a complicated one. Moreover, the variety of vehicles, launcher configurations and types of rockets makes the construction of a model which would be sufficient for all such systems a very large task at best. Although the development of a fairly comprehensive model which incorporates major characteristics of launcher/rocket systems seems justified, it is generally more efficient for certain individuals to develop the skills needed to construct mathematical models of launcher/rocket systems and to apply these to the particular concept under study.

Often, simple models of a dynamical system yield extremely useful results. What must be modeled are the salient characteristics of the system, not all the details. The models described in what follows are of this type. They are relatively simple (especially the launcher model, and yet provide, we believe, a good idea of the dynamical behavior of the class of systems considered.

3.2 Launcher Model

The "launcher" model is actually a model of either a small light-weight single-round launcher, or what we term a "sublauncher." Due to the require-

ment that there must be a response to the relatively small forces and/or either the launcher must be small or there must be a relatively small part which responds. It is assumed that in the latter case the motion of the small part, or sublauncher, due to rocket imperfections does not cause significant motion of the main portion of the launcher. Regardless of whether it is a launcher or a sublauncher, we shall refer to it as "the launcher."

The model is a tube, or framework, which has two degrees of freedom, pitch and yaw. Two examples are shown in Fig. 2. Both of these are configured so that they rotate about a point on their longitudinal axes. The rotation is constrained by "leaf springs." In both, helical rails are assumed to provide a specific angular rotation of the rocket about its longitudinal, or roll, axis during guidance. *It should be emphasized that helical rails are not required.* However, specific roll angles were considered in obtaining results presented *infra* and helical rails are means of providing these. The results are valid if other methods for producing spin, such as spin vanes, are used as long as the angle of rotation can be controlled closely.

The launcher is assumed to have axisymmetric inertia characteristics and to have equal natural frequencies in pitch and yaw. Viscous damping is assumed.

The launcher is completely specified by M, its mass; I_L, its transverse moment of inertia about its center of mass C_L; $|R|$, the distance from C_L to the pivot point O (see Appendix A, Fig. A2); ω_{Ln}, its undamped natural frequency; and ζ_L, its damping ratio.

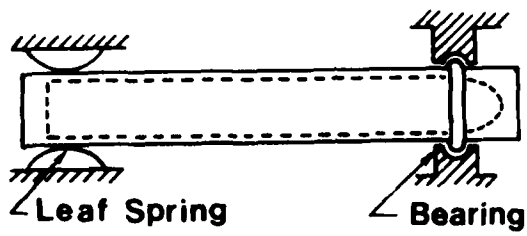

(a)

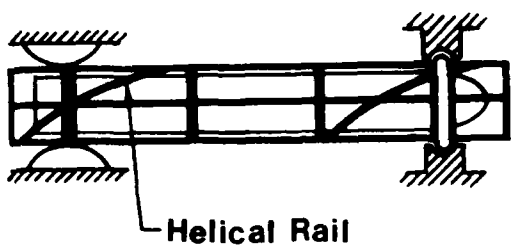

(b)

Fig. 2 Simple models of launchers.

The launcher's moment of inertia about its longitudinal axis is immaterial because it does not rotate about that axis. A value of $R<0$ implies that the pivot point is forward of the launcher's center of mass.

In the following section, several different pivot locations are considered. The launcher characteristics are given in Table 1. To simplify matters, in all cases except those for the prototype launcher, $R=0$ and the pivot location is determined by the vector $\underline{s}_a$, from the launcher center of mass to point a on the rocket.

3.3 Rocket Model

The rocket model is necessarily more detailed than that for the launcher. The main reasons for this are that (1) the mass of the rocket varies, (2) the rocket is subjected to aerodynamic forces which must be described in some detail, and (3) the rocket is the part of the system which has imperfections.

The rocket is modeled as a variable-mass body which is rigid except for the fluid within which is generated by burning solid propellant. Aside from the variation of the rocket's mass and moment of inertia with time, the variability of its mass is assumed to cause only thrust and a jet damping torque during free-flight. Other[7] reaction forces and torques due to internal combustion and fluid flow are assumed negligible.

The propellant charge is modeled as a right-circular cylinder with a cylindrical port for the purposes of determining the moments of inertia of the propellant at time t and obtaining an expression for the jet damping torque. The internal radius changes so that the mass of propellant at time t agrees with that computed from the thrust equation (pressure term omitted) $dm/dt = -F_T(t)/V_E$, where m is the rocket mass; F_T is the thrust

Table 1 Basic launcher characteristics

Guidance length (m): 1.524

Damping Ratio: 0.1 all axes

Transverse moments of inertia (kg-m^2): 54.24

Detent Force (Nt): 817

Helical rail pitch: as indicated by ϕ_{EOG}

Pivot point positions (m)

Aft: $\underline{s}_a = (0 \quad 0 \quad 0)^T$

Mid-point: $\underline{s}_a = (-5.66 \quad 0 \quad 0)^T$

Forward: $\underline{s}_a = (-3.048 \quad 0 \quad 0)^T$

Tip-off distances (m)

Small tip-off distance: 0.3048

Large tip-off distance: 1.524

Center of mass at launcher pivot point.

Table 2 Rocket physical characteristics

Length (m): 3.5

Diameter (m): 0.157

Initial Mass (kg): 113.35

Initial C.G. (m from nose): 5.84

Burnout Mass (kg): 76.08

Burnout C.G. (m from nose): 3.48

Inertia Matrix (kg-m^2)

Initial

$$\begin{bmatrix} 0.40 & 0 & 0 \\ 0 & 93.12 & 0 \\ 0 & 0 & 93.12 \end{bmatrix}$$

At Burnout

$$\begin{bmatrix} 0.26 & 0 & 0 \\ 0 & 39.3 & 0 \\ 0 & 0 & 39.3 \end{bmatrix}$$

Thrust Time Variation

Time (sec)	Thrust (Nt)
0	0
0.05	0
0.0647	6674
0.0794	67664
0.0912	70500
0.1147	69430
0.1400	69430
0.7014	122040
0.9585	116630
0.9944	2670
1.1000	0

magnitude, which is tabulated; and V_E is the characteristic exhaust velocity (speed) of the propulsive subsystem. The thrust profile, $F_T(t)$, used in this investigation as well as rocket mass, moments of inertia and dimensions are given in Table 2. They are typical data compiled from data for an experimental rocket.[7]

The aerodynamic forces and moments are modeled fairly simply. As explained in Appendix A, they depend on the flight Mach numbers, aerodynamic angles, the angular velocity of the rocket and its speed. No wind effects are considered. The aerodynamic coefficients used are listed in Table 3.

Table 3 Rocket aerodynamic characteristics

Reference Area (m^2): 0.01923 Reference Length (m): 0.157

Mach No.	C_{N_α}	C_{m_q}	x_{cp} (m from nose)
0.0	4.41	-1460	1.876
0.4	4.24	-1540	1.722
0.6	4.12	-1610	1.628
0.8	3.95	-1730	1.457
0.9	3.80	-1780	1.408
1.0	3.58	-1780	1.384
1.1	3.84	-1730	1.378
1.2	4.07	-1660	1.378
1.4	4.41	-1560	1.423
1.6	4.61	-1460	1.469
1.0	4.70	-1380	1.512
2.0	4.76	-1300	1.533
2.2	4.71	-1230	1.548
2.4	4.67	-1170	1.533
2.6	4.54	-1120	1.487
3.2	4.41	-1010	1.298

Mach No.	C_A
0.00	0.425
0.80	0.328
0.90	0.310
0.95	0.305
1.00	0.330
1.10	0.403
1.20	0.381
1.28	0.373
1.50	0.372
2.00	0.340
2.50	0.299
3.00	0.262
3.50	0.231
4.00	0.205

SECTION 4. PASSIVE CONTROL RESULTS

4.1 Definition of Imperfection

The effects of two types of imperfection, dynamic imbalance and misalignment of the thrust force, are considered in this section. The dynamic imbalance is defined by μ_2 and μ_3 (see Appendix A), which are small angles generated by rotating from a centroidal principal system, Cx*y*z*, to a rocket-fixed system, Cxyz, which has its x-axis parallel to the symmetry axis of the launcher. Figure 3 illustrates the angle μ_2. The linear misalignment of the thrust force with respect to the symmetry axis of the rocket is defined by the vector $\underline{r}_T$, from point "a" on the symmetry axis of the rocket to a point on the line of action of the thrust. Angular thrust misalignment is specified by the small angles α_y and α_z which are, effectively, rotations about the y and z rocket-fixed axes, respectively. In this report, $\underline{r}_T$ has only an x-component. Hence, all the misalignment is due to α_y and α_z. Figure 4 illustrates the angle α_y.

For all the dynamic imbalance results presented herein, except those in subsection 4.9, $\mu_2 = 0.001$ and $\mu_3 = 0$. Also, with the above exception, for all the thrust misalignment cases, $\alpha_y = -0.001$ and $\alpha_z = 0$.

4.2 Definition of Flight Errors

Since dynamic imbalance and thrust misalignment cause changes in the direction of flight of free rockets during the powered portion of free-flight, they result in two types of errors at burnout. One is in the direction of the velocity of an affected rocket. The second is in the displacement of its center of mass from the desired trajectory. The error

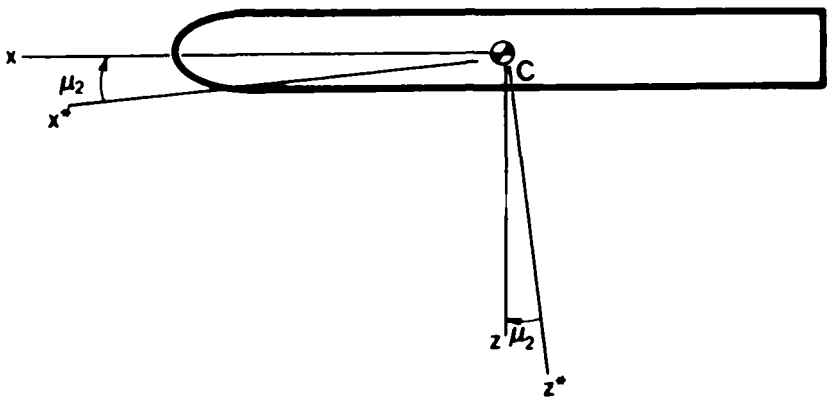

Fig. 3 Dynamic imbalance angle μ_2.

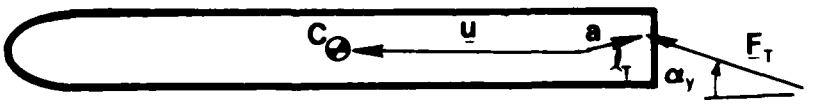

Fig. 4 Thrust misalignment angle α_y.

in flight direction is the most significant if the unpowered phase is much longer than the powered phase, since it propagates as a displacement error.

The direction of flight at any instant is defined by the angles γ and ψ_w, which orient the rocket's velocity vector (see Fig. 5). The angle γ is measured from the horizontal plane in the vertical plane which contains the rocket's center of mass and the velocity $\underline{V}_C$. The angle ψ_w is used to define the orientations of the vertical plane with respect to some reference line, perhaps the horizontal projection of the desired line of flight.

The position of the center of mass of a rocket is given by the coordinates X, Y and Z, where X is nominally measured along the desired direction of flight, Z is measured positive down (a flat earth is assumed) and Y is measured positive to the right of the desired flight direction.

In order to define errors using the angles γ and ψ_w and the displacements Y and Z, we must have a standard. The obvious one is the unperturbed or nominal trajectory; i.e., the trajectory flown by a perfect rocket. By letting a subscript N denote a nominal value and P a perturbed value of a state variable, we have the following errors as functions of time:

$$\Delta\gamma(t) = \gamma_P(t) - \gamma_N(t)$$

$$\Delta\psi_w = \psi_{w_P}(t) - \psi_{w_N}(t)$$

$$\Delta Y = Y_P(t) - Y_N(t)$$

$$\Delta Z = Z_P(t) - Z_N(t)$$

The total angular deviation or error, is $\sqrt{\Delta\gamma^2+\Delta\psi_w^2}$ and the total transverse linear error is $\sqrt{\Delta Y^2+\Delta Z^2}$. The purpose of passive control is to reduce these two errors at burnout regardless of the random nature of their cause and hence reduce the total dispersion of the rockets launched.

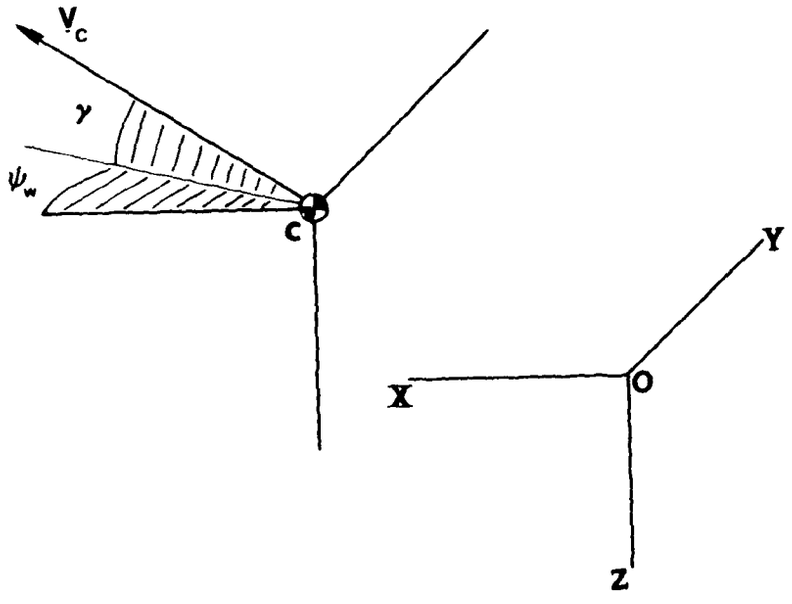

Fig. 5 Flight path angles γ and ψ_w.

4.3 Determination of Launcher Performance

Some method must be established for determining how well a given launcher performs in its passive control role. The following method has been adopted:

1. A specific launcher configuration is chosen.
2. A specific type of imperfection is chosen.
3. A nominal trajectory is generated by numerically integrating the equations of motion of the system with no imperfections and a rigid launcher; i.e., $\omega_{Ln} = \infty$, until burnout ($t=t_{bo}$).
4. A perturbed trajectory is generated by numerically integrating the equations of motion of the system with the specific imperfection and a rigid launcher until burnout.
5. Step 3 is repeated with ω_{Ln} equal to a finite number; i.e., a flexible launcher.
6. Step 4 is repeated with ω_{Ln} equal to the value in step 5.
7. The difference in the flight path angles γ_{bo} and $\psi_{w_{bo}}$ ($\Delta\gamma$ and $\Delta\psi_{w_{bo}}$, respectively) and of the lateral displacements Y_{bo} and Z_{bo} (ΔY_{bo} and ΔZ_{bo}, respectively) are calculated from the results of steps 3 and 4 (rigid launcher errors) and from the results of steps 5 and 6 (flexible launcher errors).
8. The ratios of $\sqrt{\Delta\gamma^2_{bo} + \Delta\psi^2_{w_{bo}}}$ and $\sqrt{\Delta Y^2_{bo} + \Delta Z^2_{bo}}$ for the flexible launcher to the same quantities for the rigid launcher are computed.
9. Steps 6 through 8 are repeated with other launcher frequencies to generate launcher response curves.
10. The entire process, steps 1 through 9, is repeated for a different launcher configuration and/or imperfection.

The foregoing procedure in no way guarantees that an optimal launcher configuration will be found. However, if enough of the parameter space

spanned by the physically possible values of I_L, ω_L, R and rocket rotation angle ϕ is searched at least we may obtain results which will support, or challenge, the passive control concept.

4.4 Passive Control of Dispersion due to Thrust Misalignment

Obviously, only a finite number of parameter sets could be considered in the finite amount of time available for this investigation. This is doubly true because of the amount of computer time required to produce nominal and perturbed trajectories. In all, six sets of thrust misalignment error ratio versus launcher natural frequency curves were produced for a fixed launcher transverse moment of inertia, $I_L = 54.24$ kg-m^2. This moment of inertia was fixed, so that the effects of geometry; i.e., launcher support location and rocket rotation angle could be studied.

The first set of curves for an aft launcher support location and a non-tip-off guidance length of 1.524 m are shown in Fig. 6. Three different rotation angles were used in producing the curves. The first thing to note about this set is that for an aft support location (s_a=0; see Appendix A) even the "best" launcher reduces the error by less than 10 percent. Since we have plotted error ratios for equal rotation angles at end-of-guidance (EOG) ϕ_{EOG}, the curves may be compared even though for the larger ϕ_{EOG}, the absolute error would be less because the rocket is spinning more rapidly at EOG. Note also that the curves for $\sqrt{\Delta\psi_{w_b}^2+\Delta\gamma_{bo}}$ and $\sqrt{\Delta Y_{bo}^2+\Delta Z_{bo}^2}$ error ratios are essentially the same.

When the support is moved to the front, the launcher becomes more sensitive to the imperfection. Evidence of this sensitivity can be seen in Fig. 7. Note that at a launcher frequency of around 18 Hz, the error ratio for $\phi_{EOG} = \pi/2$ is only about 0.2. Therefore, an error reduction of about 80 percent is predicted for such a launcher.

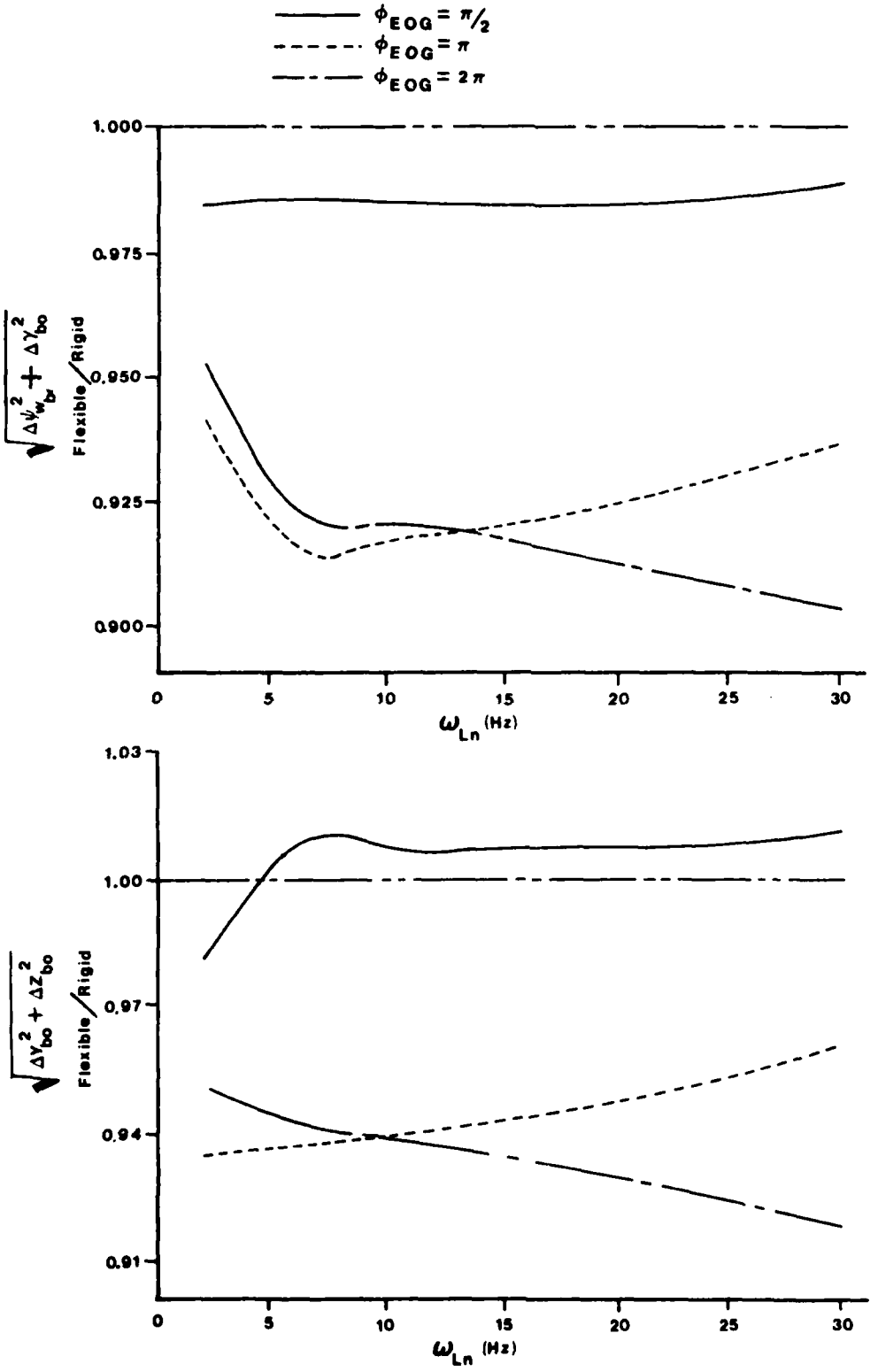

Fig. 6 Error ratios - thrust misalignment, aft pivot, non-tip-off.

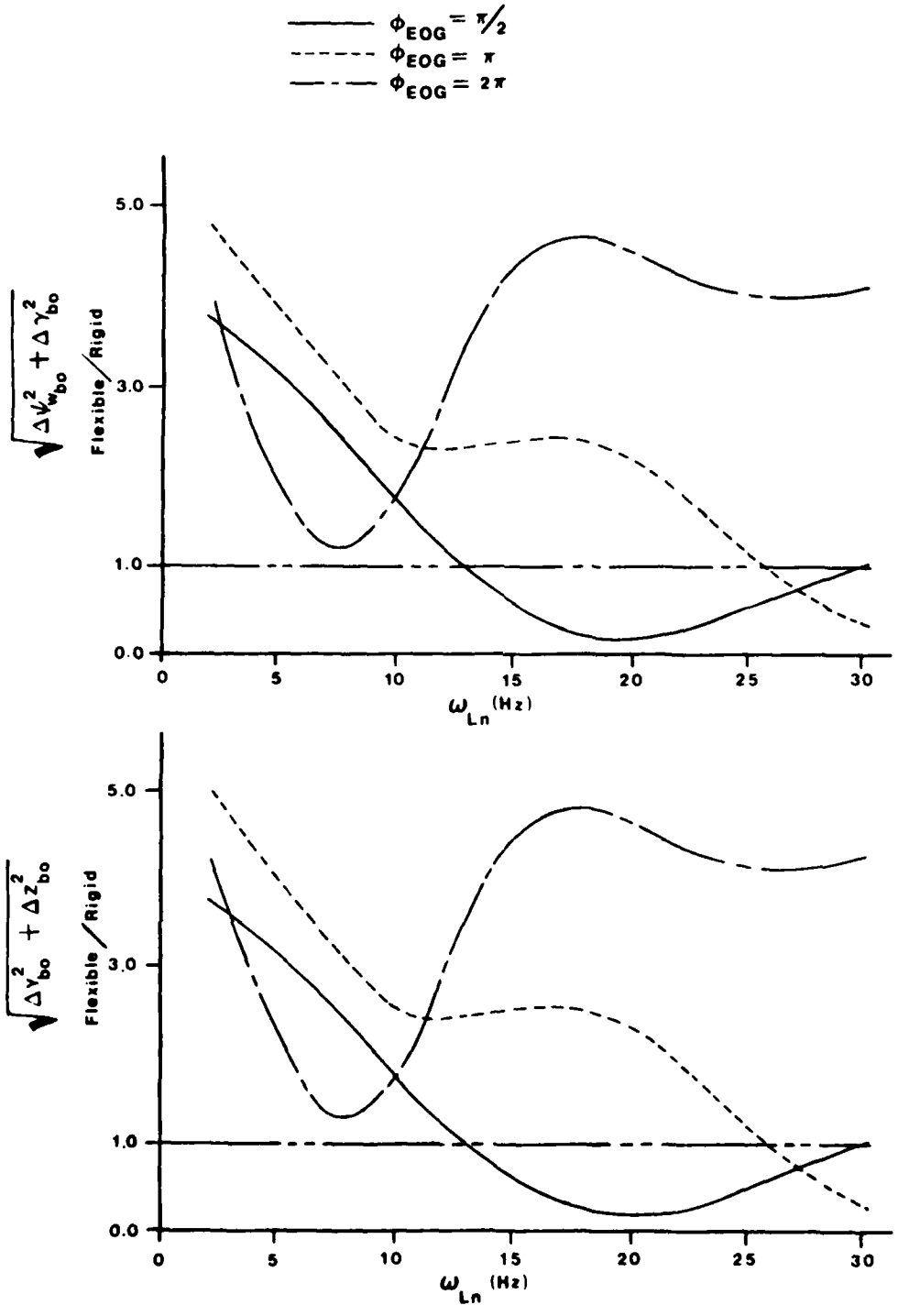

Fig. 7 Error ratios - thrust misalignment, forward pivot, non-tip-off.

Tip-off launcher results are given in Fig. 8. Curves for $\phi_{EOG} = \pi/2$ and π are given. The tip-off distance is 0.3048 m and EOG occurs at the beginning of tip-off. The launcher pivot point is again at the rear. Because the reduction for the $\phi_{EOG} = \pi$ case is greater than 10 percent for all launcher frequencies, the tip-off apparently is beneficial.

When the tip-off distance is increased (see Fig. 9) to 1.524 m, rocket rotation so that $\phi_{EOG} = \pi/2$ is more beneficial and the error ratio is drastically reduced to less than 0.5 at $\omega_{Ln} \doteq 12$ Hz.

The front-pivot, tip-off results shown in Figs. 10 and 11 are of interest also. The 0.3048 m tip-off curves look much like the corresponding non-tip-off curves of Fig. 6. However, the 1.524 m tip-off curves are very different from their non-tip-off counterparts and indicate that tip-off is detrimental if the launcher is pivoted near its front end.

In addition to the constant-moment-of-inertia results given in Figs. 6 throgh 11, results were obtained for the "prototype" launcher which is described in Appendix B. This launcher is basically a steel tube. Its centroidal transverse moment of inertia is 61.17 kg-m^2. Only non-tip-off results were obtained using this model. These are shown in Figs. 12, 13 and 14 which correspond to aft ($|x_{L_a}| = -3.48$ m), mid ($|x_{L_a}| = -1.454$ m) and forward ($|x_{L_a}| = 0.07$ m) point locations, respectively. The launcher pivoted at its front is obviously superior. Especially encouraging is that if $\phi_{EOG}=2$, a launcher with $\omega_{Ln} = 7$ Hz is a <u>very good</u> passive controller. The launcher supported at its center of mass also acts as a passive controller, but is less effective. Furthermore, the launcher which is pivoted near its aft end does not respond as well as the other two. A maximum error reduction of only about 12 percent was achieved with the aft pivot. This is at least

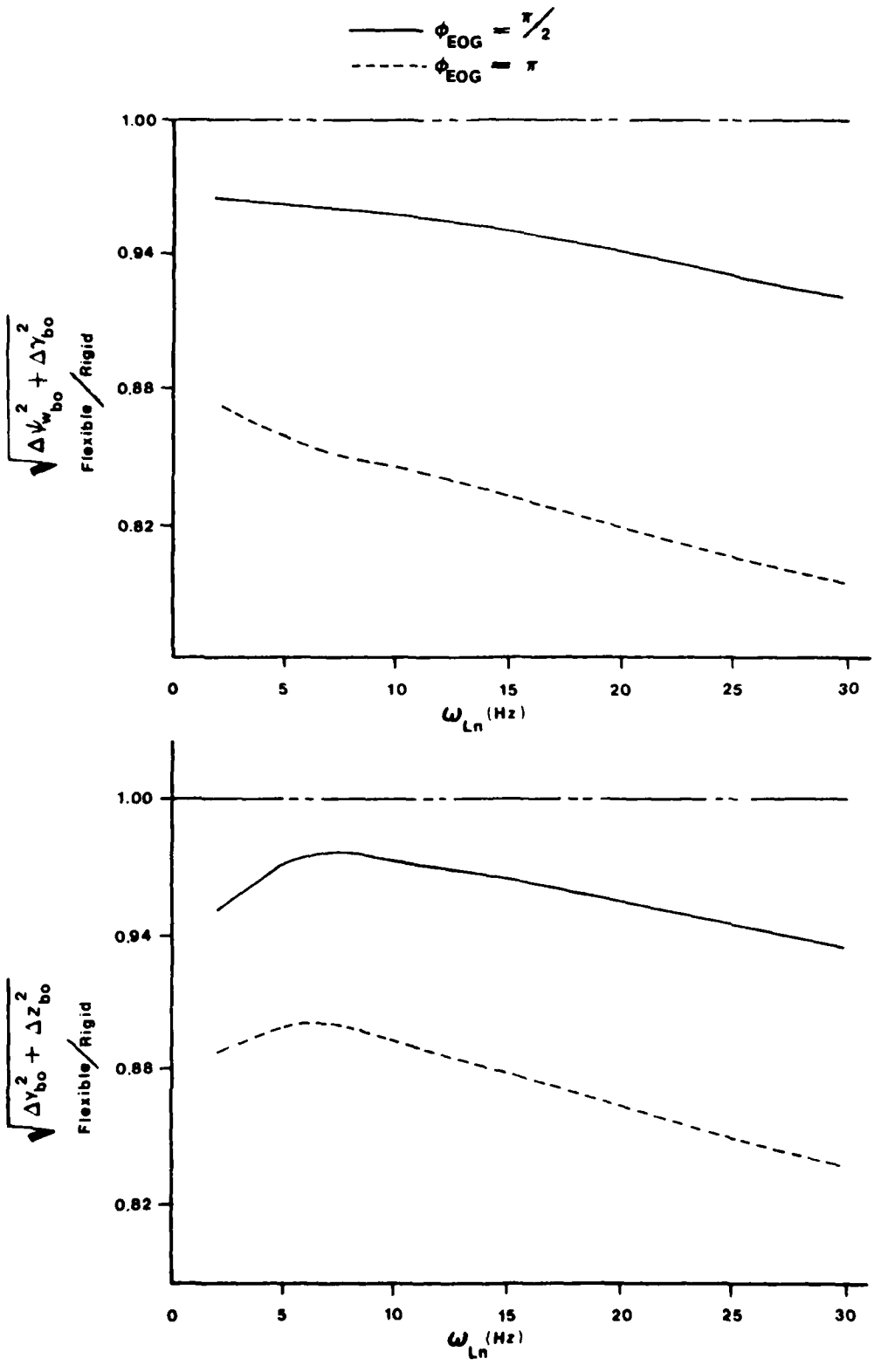

Fig. 8 Error ratios - thrust misalignment, aft pivot, small cut-off distance.

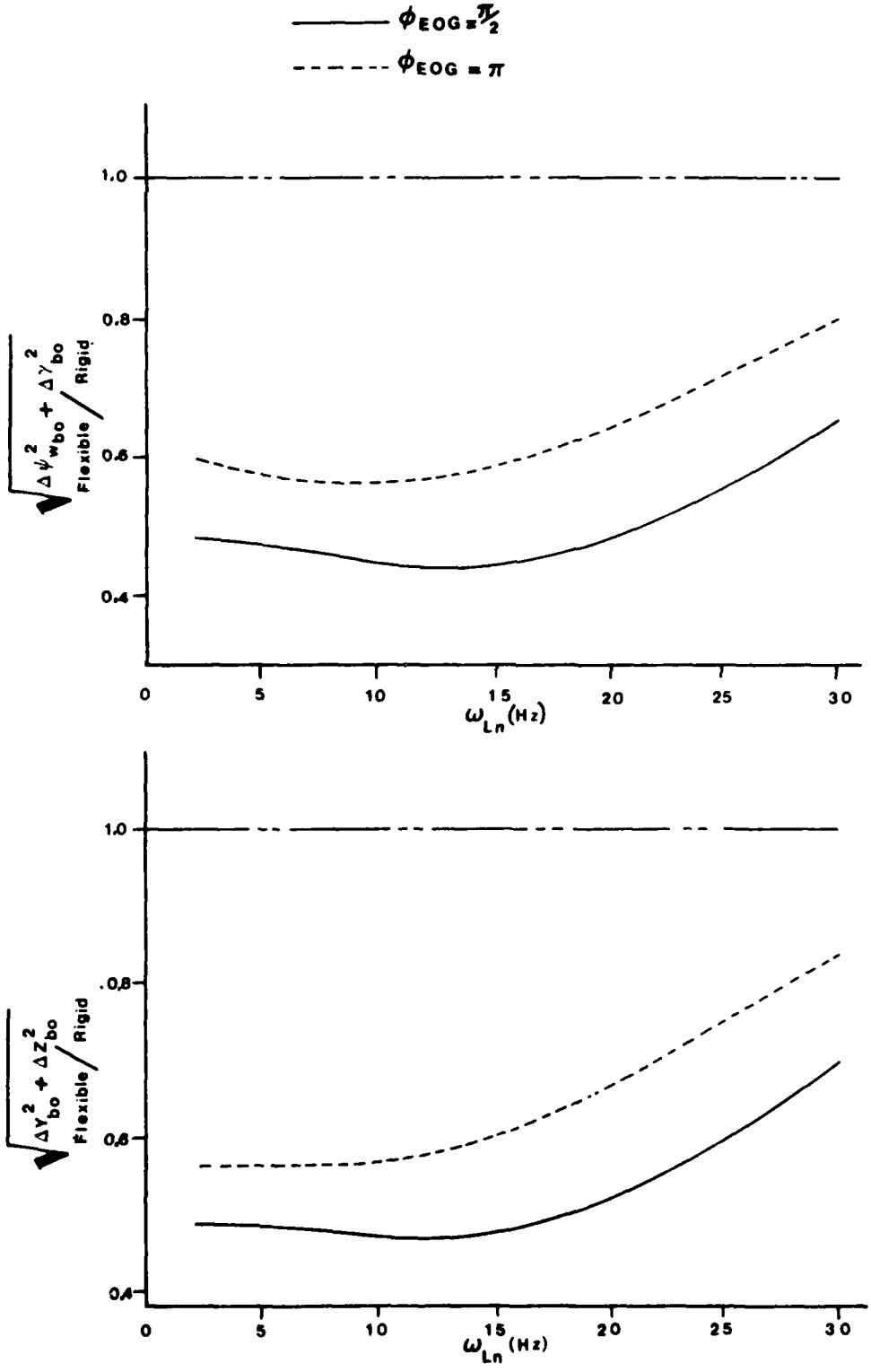

Fig. 9 Error ratios - thrust misalignment, aft pivot, large tip-off distance.

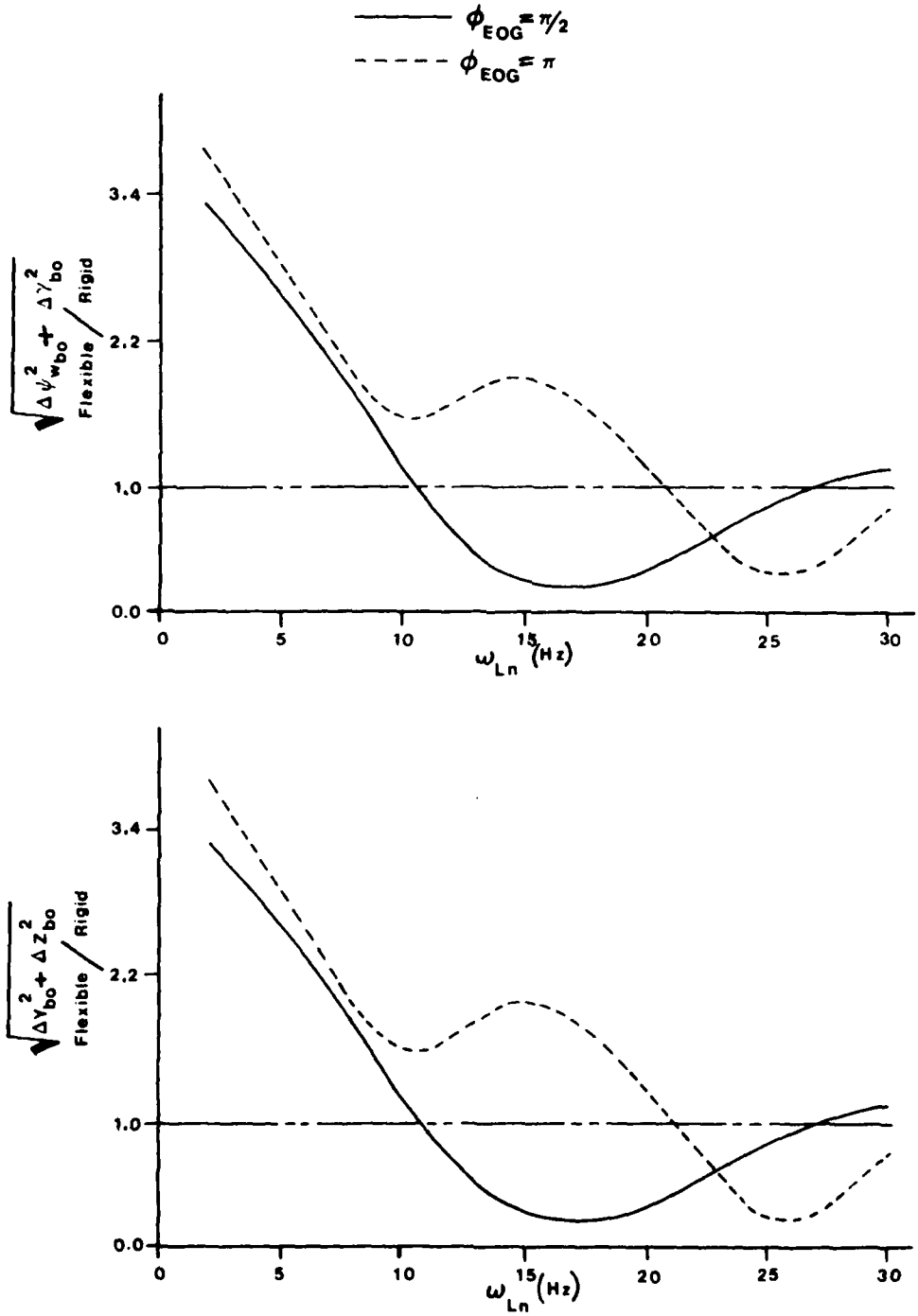

Fig. 10 Error ratios - thrust misalignment, forward pivot, small tip-off distance.

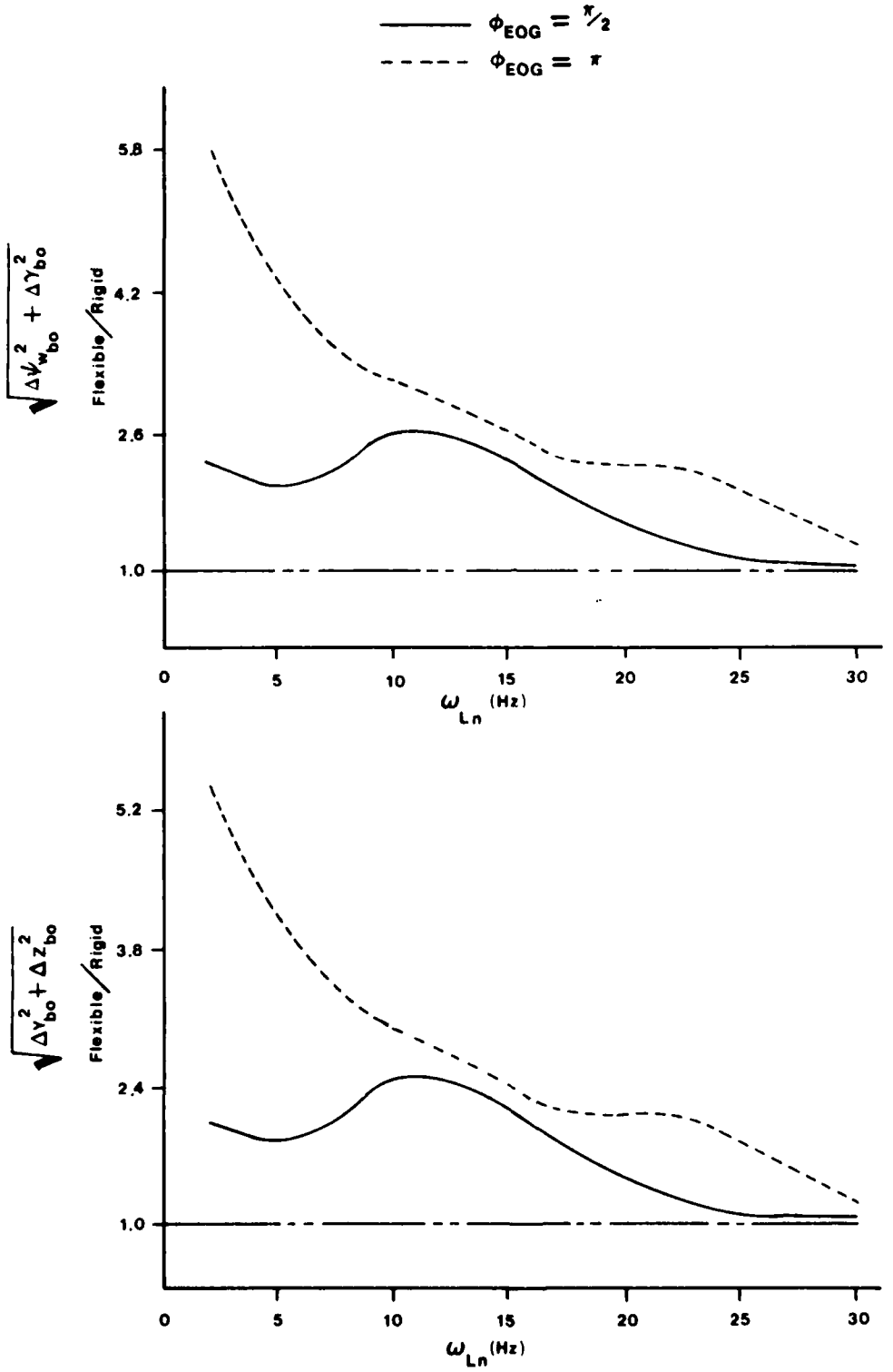

Fig. 11 Error ratios - thrust misalignment, forward pivot, large tip-off distance.

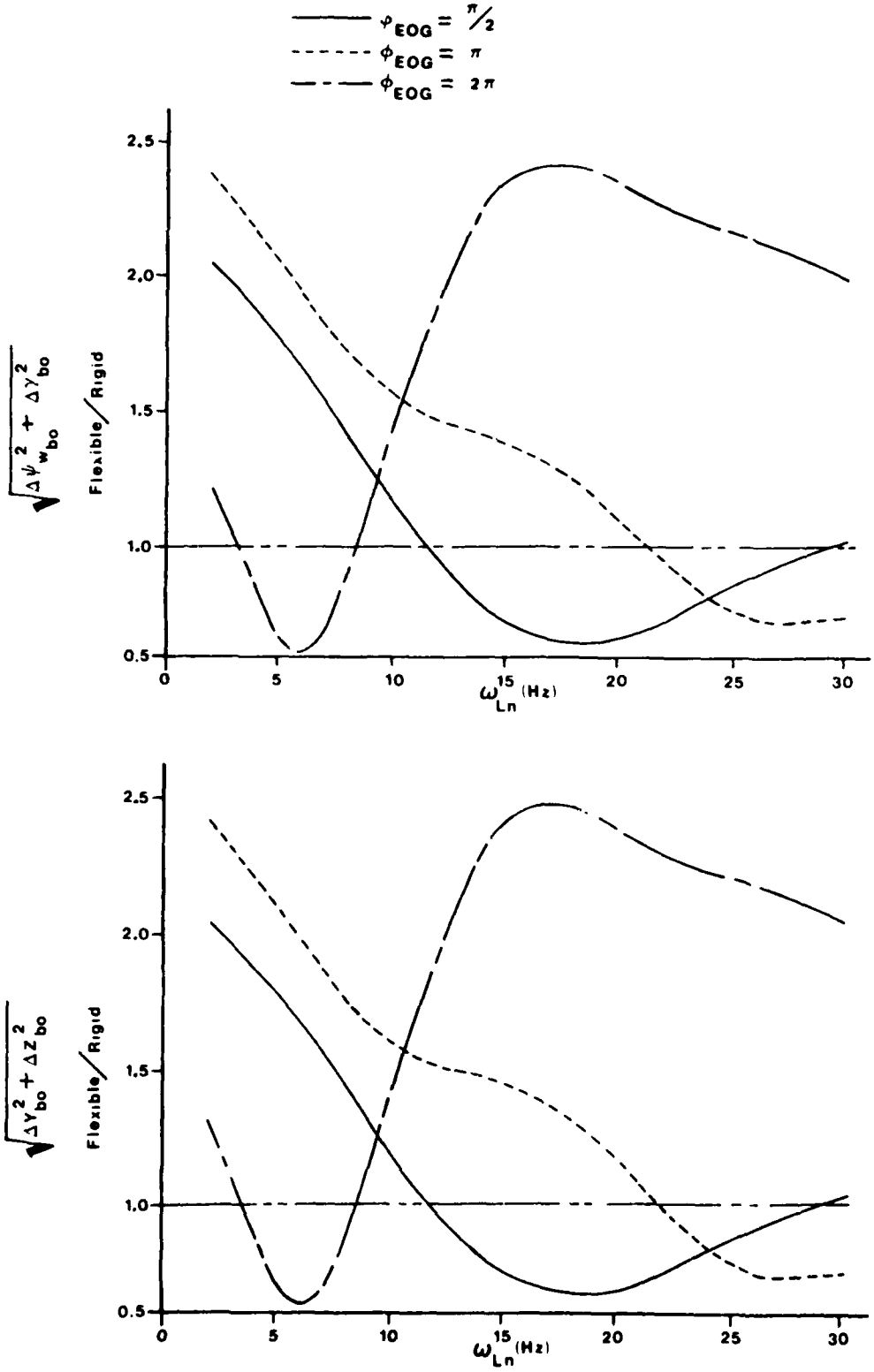

Fig. 12 Prototype launcher error ratios - thrust misalignment, aft pivot.

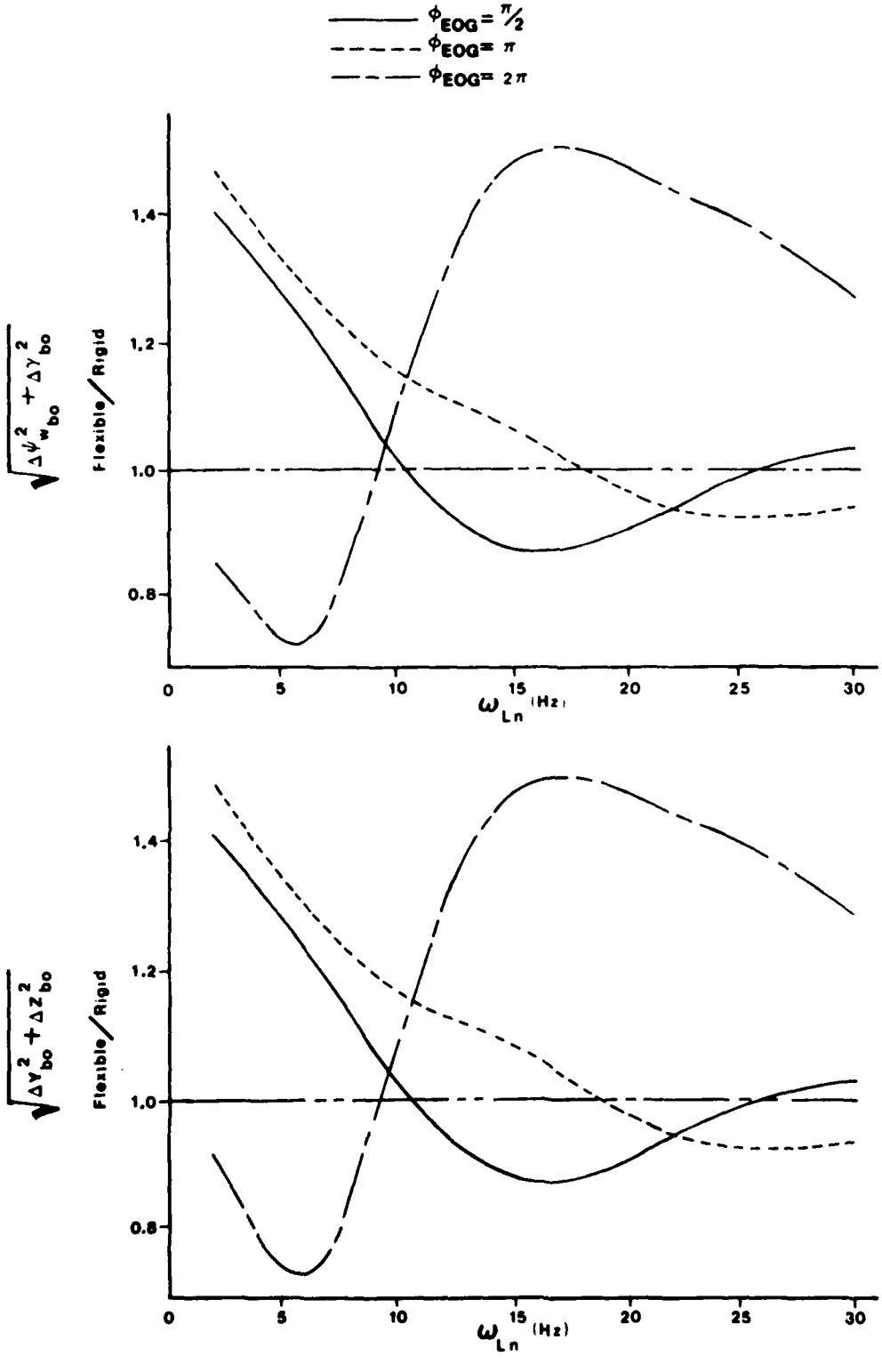

Fig. 13 Prototype launcher error ratios - thrust misalignment, mid-point pivot.

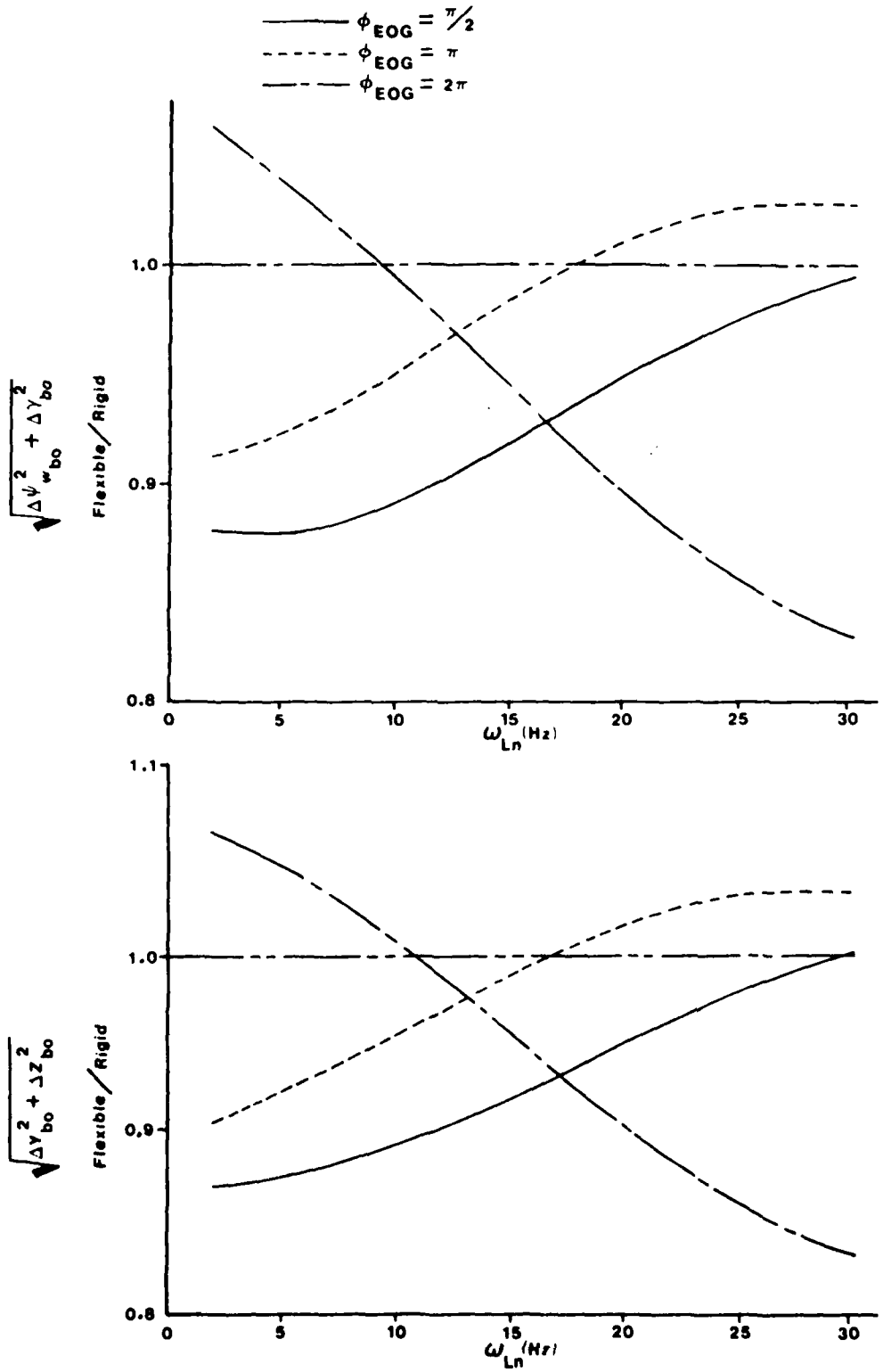

Fig. 14 Prototype launcher error ratios - thrust misalignment, forward pivot.

partially due to the increase of the inertia of the system during launch if the pivot point is at the rear of the launcher.

4.5 Passive Control of Dispersion due to Dynamic Imbalance

An axisymmetric rigid body which is constrained to spin about an axis which is not aligned with its axis of minimum or maximum centroidal moment of inertia and then released and allowed to rotate freely nutates and precesses.[8] The nutation has a period close to the spin period, but if the body is a very slender body of revolution, the precessional period is much longer than the spin period. In a rocket which is dynamically unbalanced the long period precession, coupled with the thrust force, causes the rocket to depart from its nominal trajectory.

Dynamic imbalance of a rocket which is rotating on its launcher produces a torque on the launcher. If the launcher is sufficiently responsive to this torque, beneficial motion of the system may be achieved.

Ten sets of launcher response curves for dynamic imbalance and fixed launcher moment of inertia are presented in this subsection. They are divided into non-tip-off and tip-off groups.

Non-Tip-Off Results

Figure 15 gives the response curves for $\phi_{EOG} = \pi/2$ and π of a launcher with an aft pivot point. A great deal of passive control is not evident. However, the ratios are always less than unity. Thus, the launcher's flexibility is beneficial regardless of its frequency.

A mid-point pivot was also considered. From Fig. 16 it appears that the mid-point pivot is considerably better than an aft pivot. However, the angles of rotation used to generate Fig. 16 are $\phi_{EOG} = 3\pi/2$ and 2π.

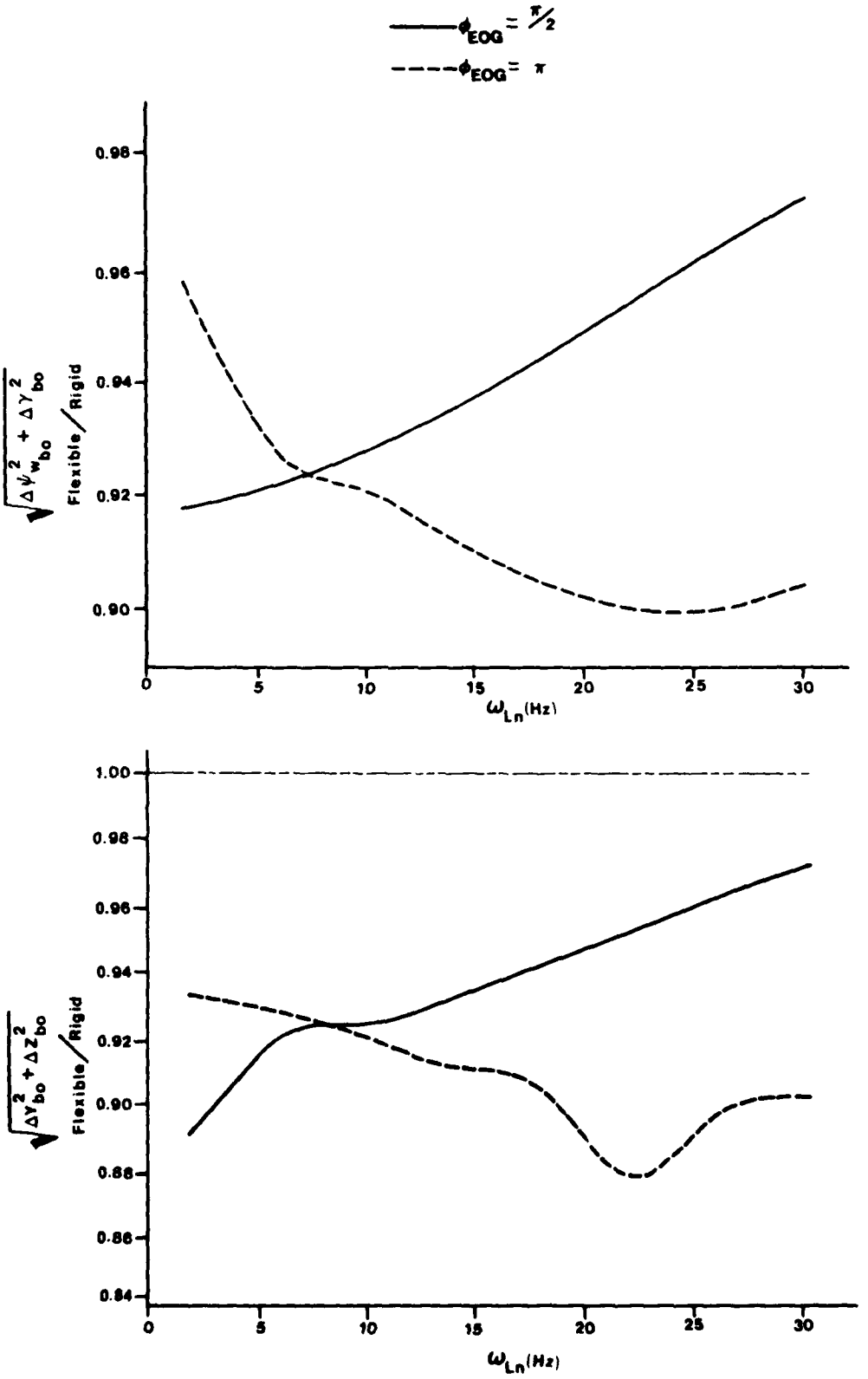

Fig. 15 Error ratios - dynamic imbalance, aft pivot, non-tip-off (set 1).

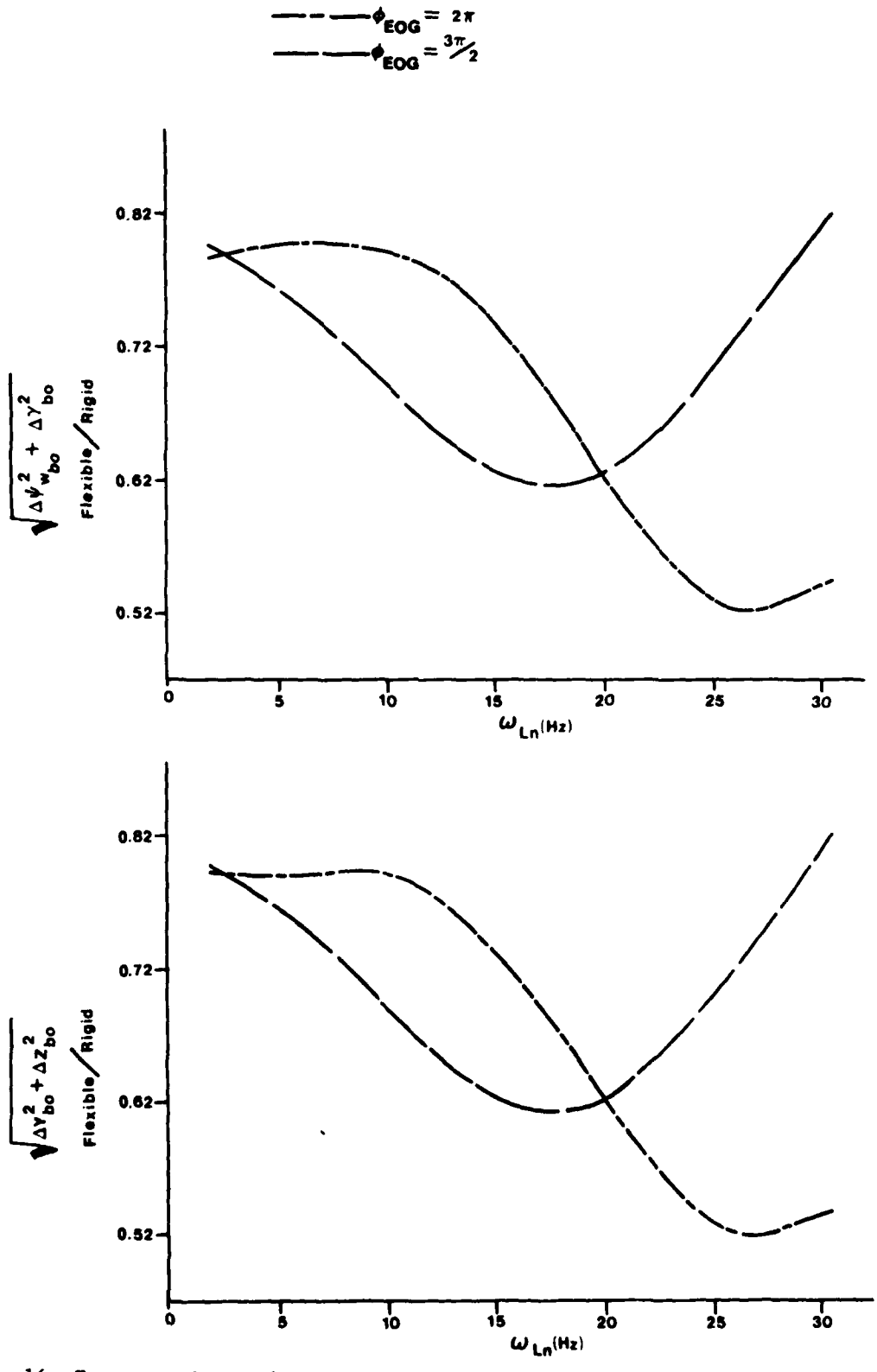

Fig. 16 Error ratios - dynamic imbalance, mid-point pivot, non-tip-off.

For direct comparison we need Fig. 17, the dashed curve of which can be compared with the solid curve of Fig. 16. Upon making this comparison, it is clear that a mid-point pivot is better than an aft pivot.

Use of a forward pivot also leads to positive results, as shown by Fig. 18. At low launcher frequencies, the error ratio is much less than unity. The minimum is about 0.3.

Tip-Off Results

The results for an aft pivot and a tip-off distance of 0.3048 m (see Fig. 19) are about as good as the corresponding non-tip-off results. However, the 1.524 m tip-off distance curves shown in Fig. 20 never pass below the break-even value of 1. The same statements hold regarding the mid-point pivot tip-off results shown in Figs. 21 and 22.

The forward-pivot results for 0.3048 m tip-off presented in Fig. 23 are not nearly as good as those shown in Fig. 18 (non-tip-off) except at very high frequencies and $\phi_{EOG} = \pi/2$. The 1.524 m tip-off results (see Fig. 24) are better. For $\phi_{EOG} = \pi/2$ and $\omega_{Ln} = 2$ Hz, the error ratio is about 0.5.

The "prototype" launcher results presented in Figs. 25, 26 and 27 clearly reveal the sensitivity of a launcher with a mid- or forward-pivot point to dynamic imbalance. These curves are all for non-tip-off launchers.

4.6 Passive Control of Dispersion due to Combinations of Imperfections

Generally, both thrust misalignment and dynamic imbalance will be present. Thus, to be successful, the launcher must passively control random combinations of these two types of imperfections.

The "prototype" launcher model was used to determine launcher performance in the presence of thrust misalignment ($\alpha_y = -0.001$, $\alpha_z = 0$) and

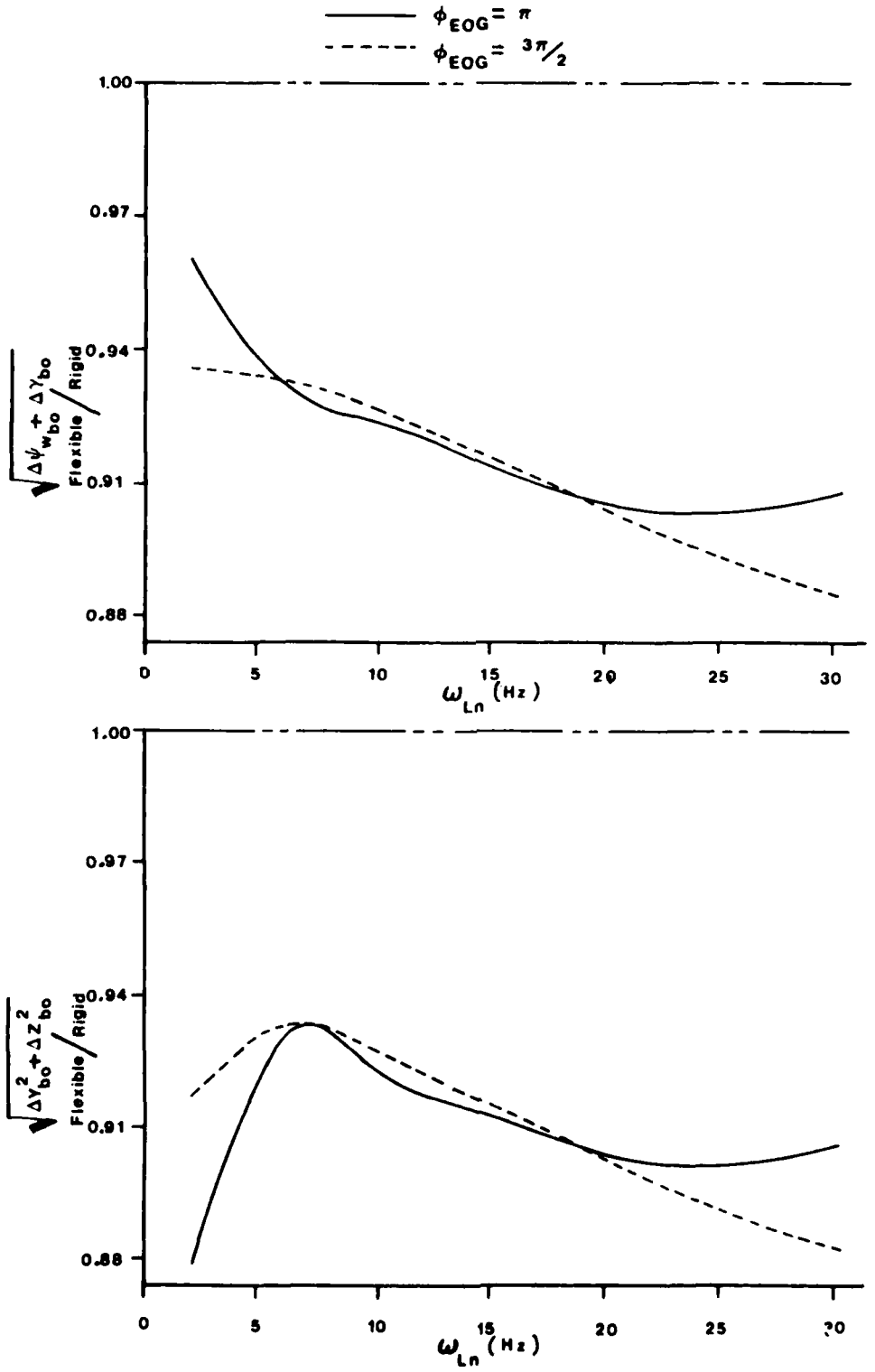

Fig. 17 Error ratios - dynamic imbalance, aft pivot, non-tip-off (set 2).

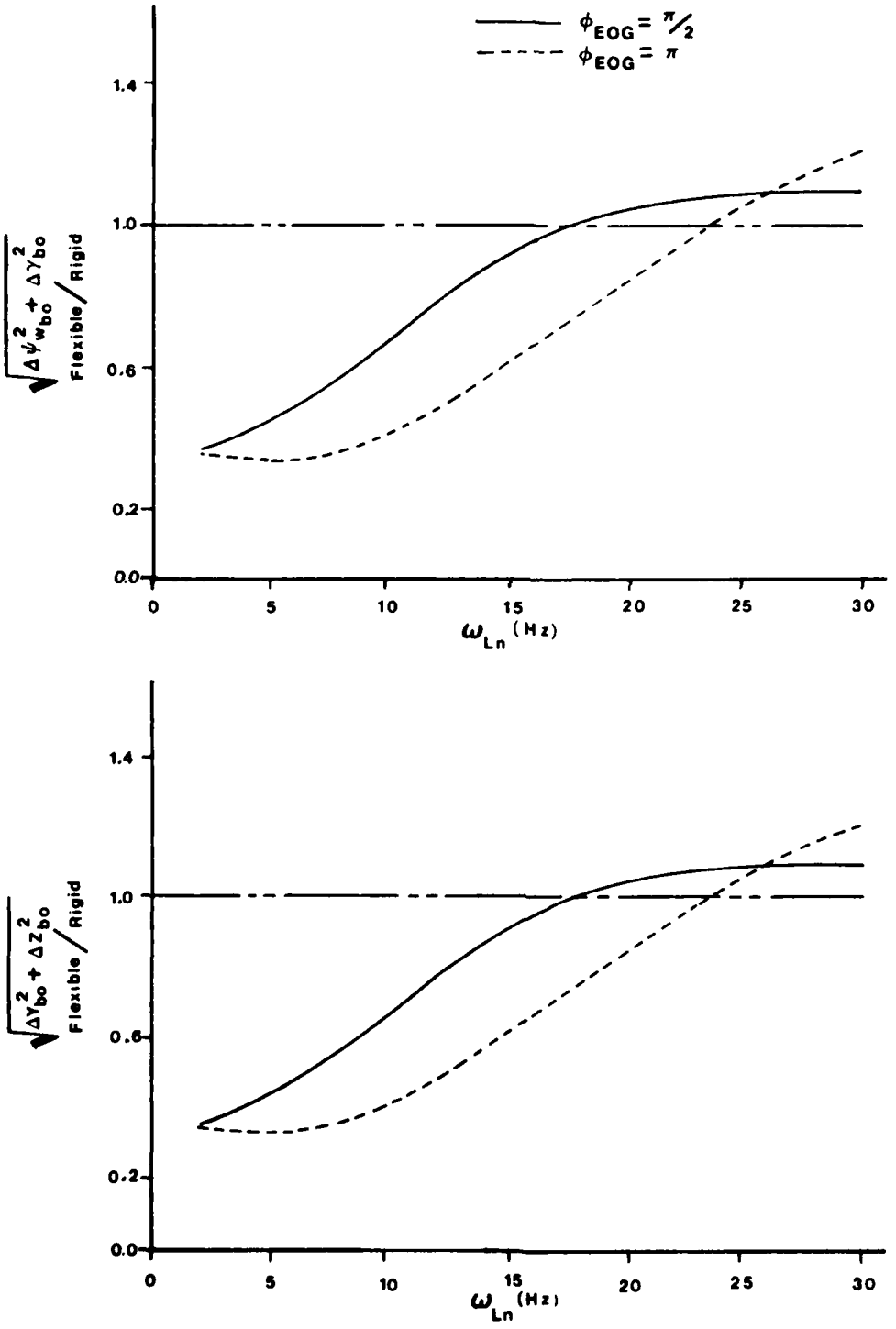

Fig. 18 Error ratios - dynamic imbalance, forward pivot, non-tip-off.

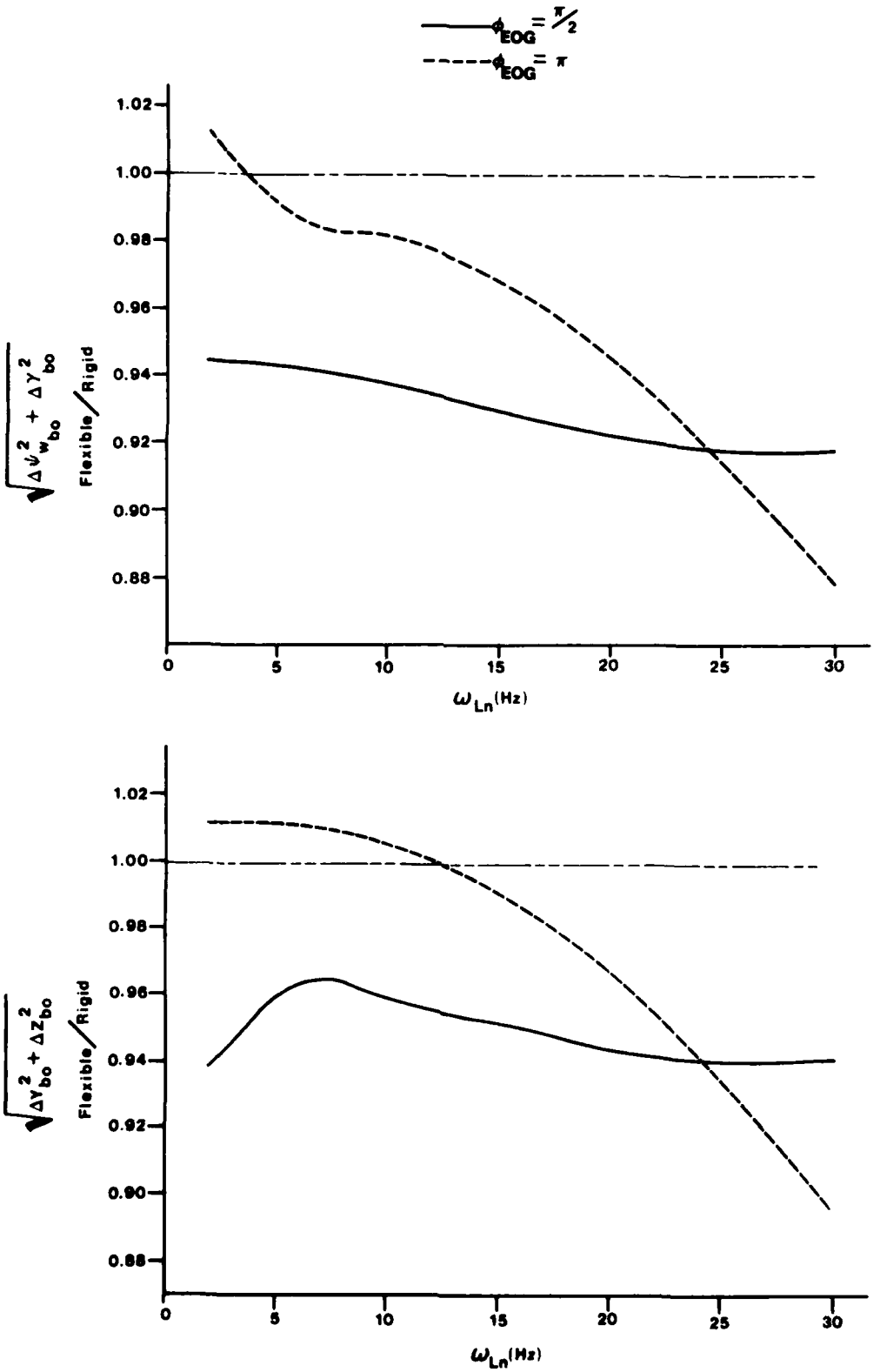

Fig. 19 Error ratios - dynamic imbalance, aft pivot, small tip-off distance.

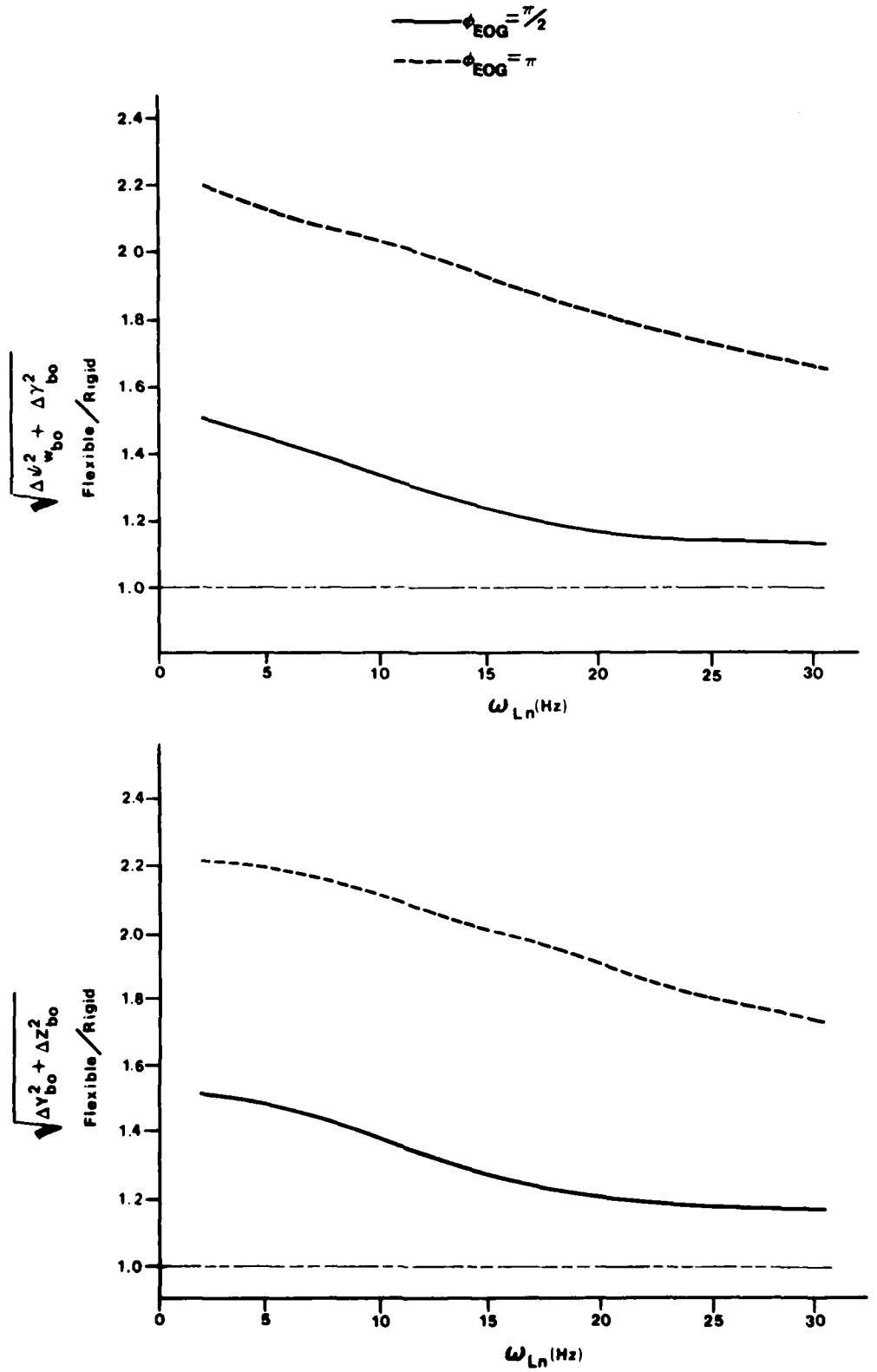

Fig. 20 Error ratios - dynamic imbalance, aft pivot, large tip-off distance.

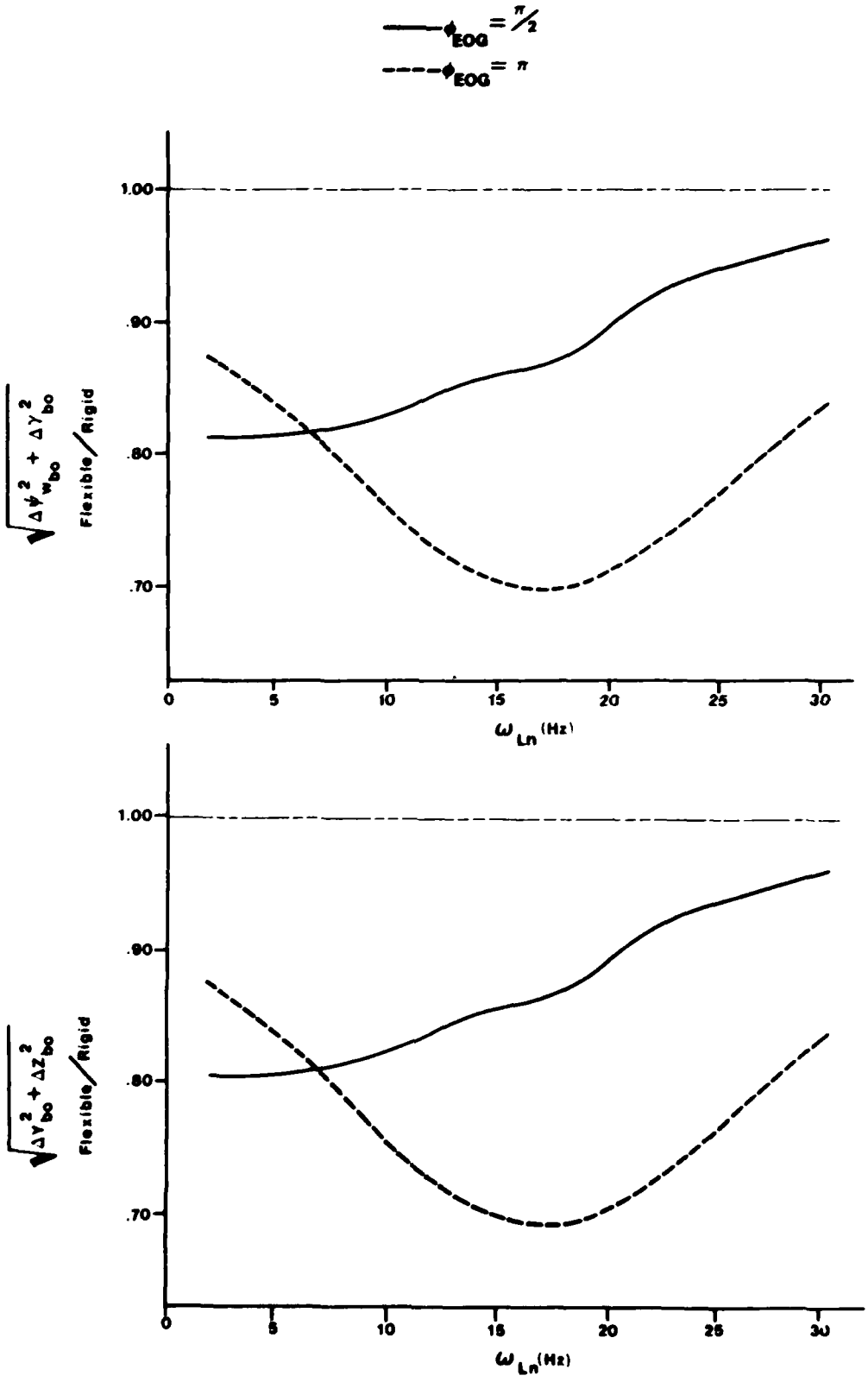

Fig. 21 Error ratios - dynamic imbalance, mid-point pivot, small tip-off distance.

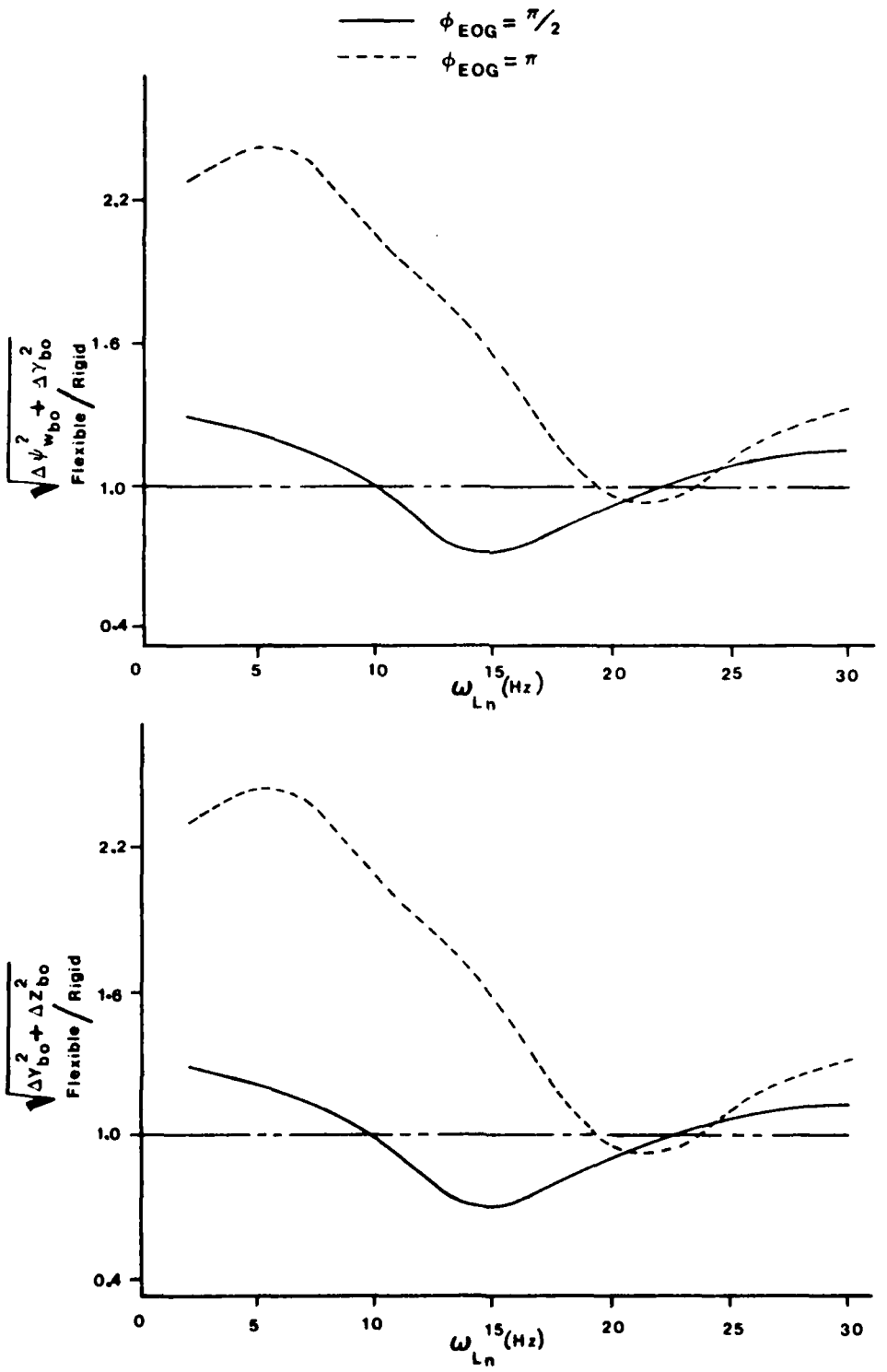

Fig. 22 Error ratios - dynamic imbalance, mid-point pivot, large tip-off distance.

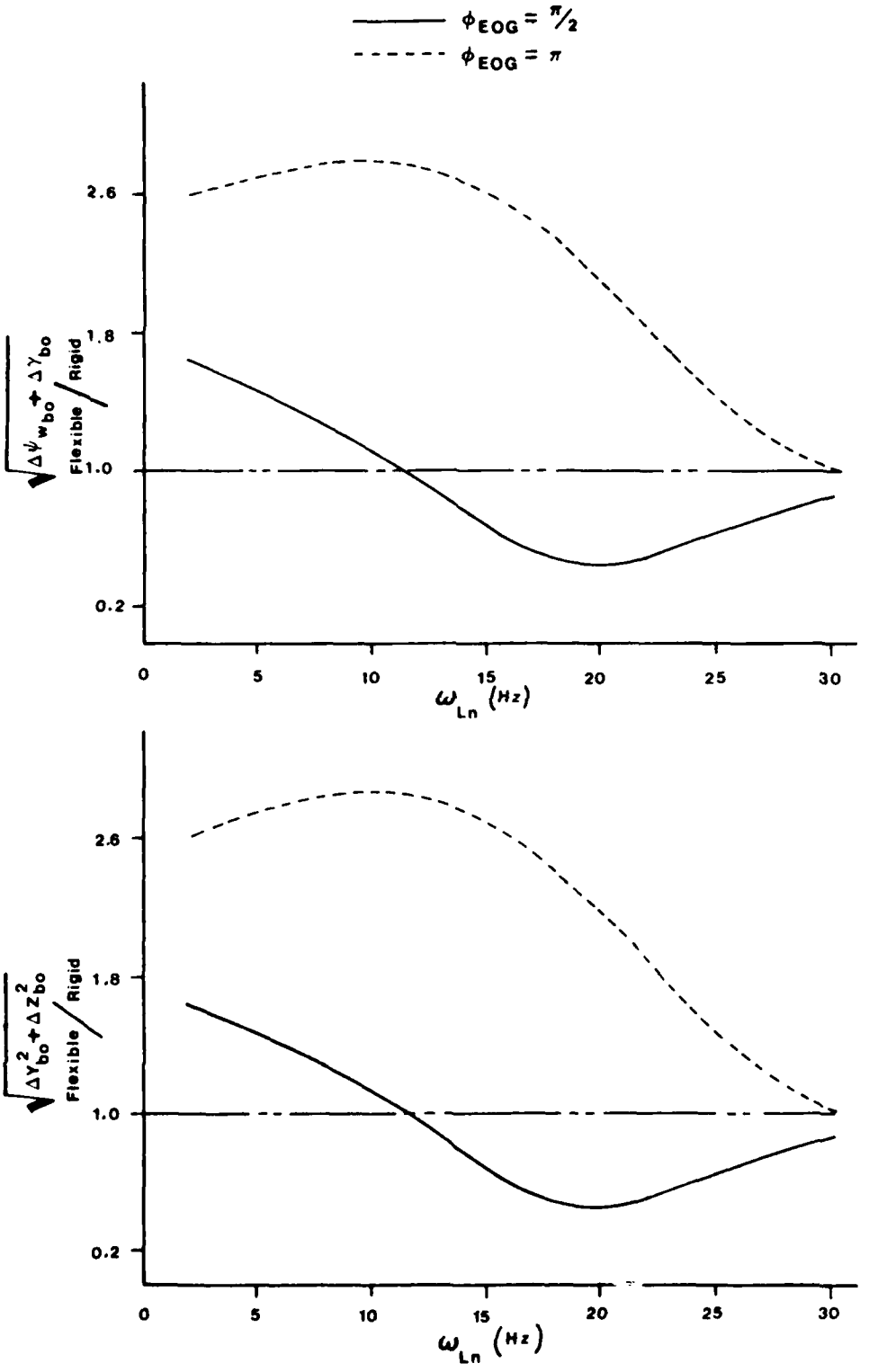

Fig. 23 Error ratios - dynamic imbalance, forward pivot, small tip-off distance.

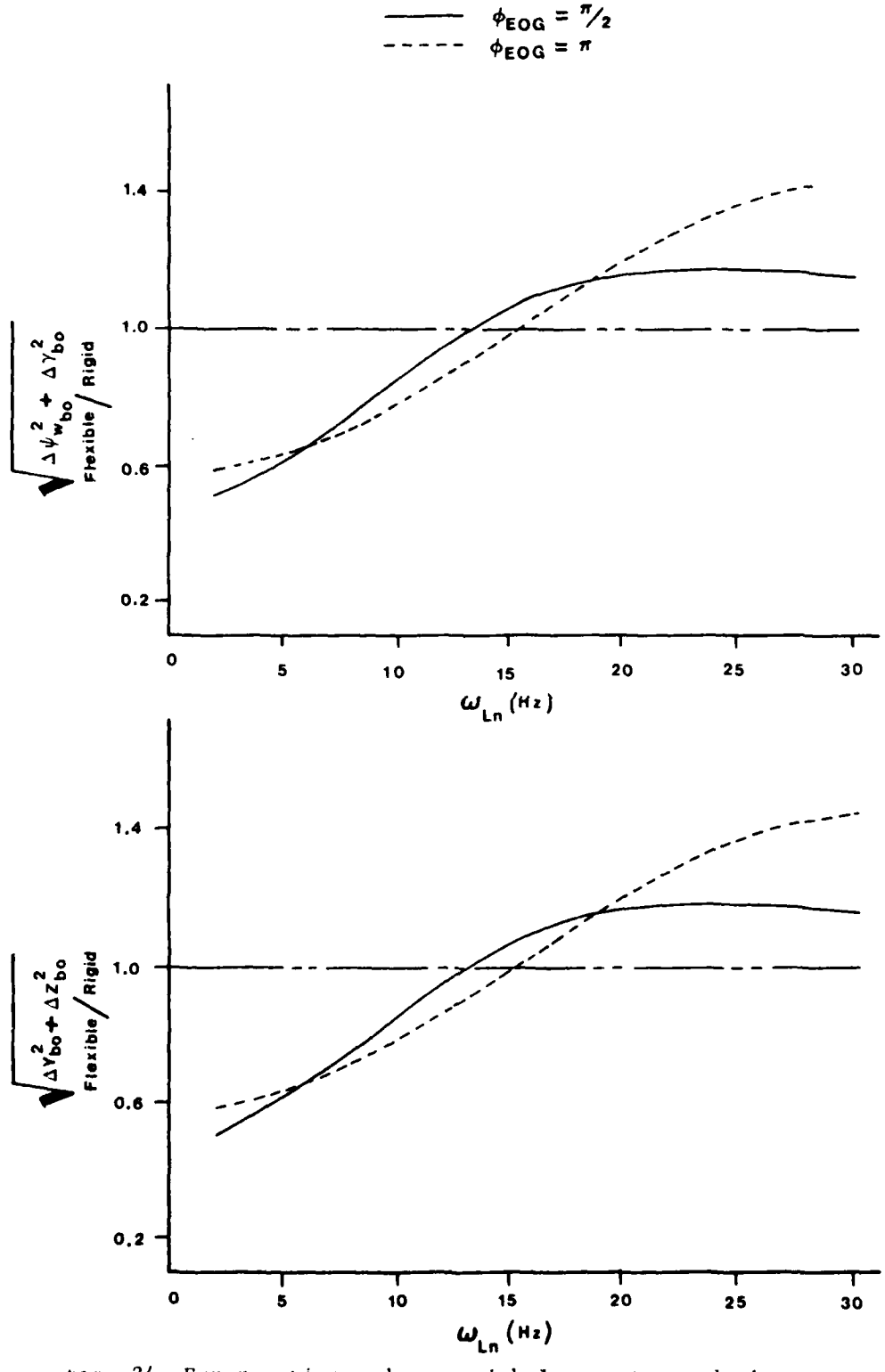

Fig. 24 Error ratios - dynamic imbalance, forward pivot, large tip-off distance.

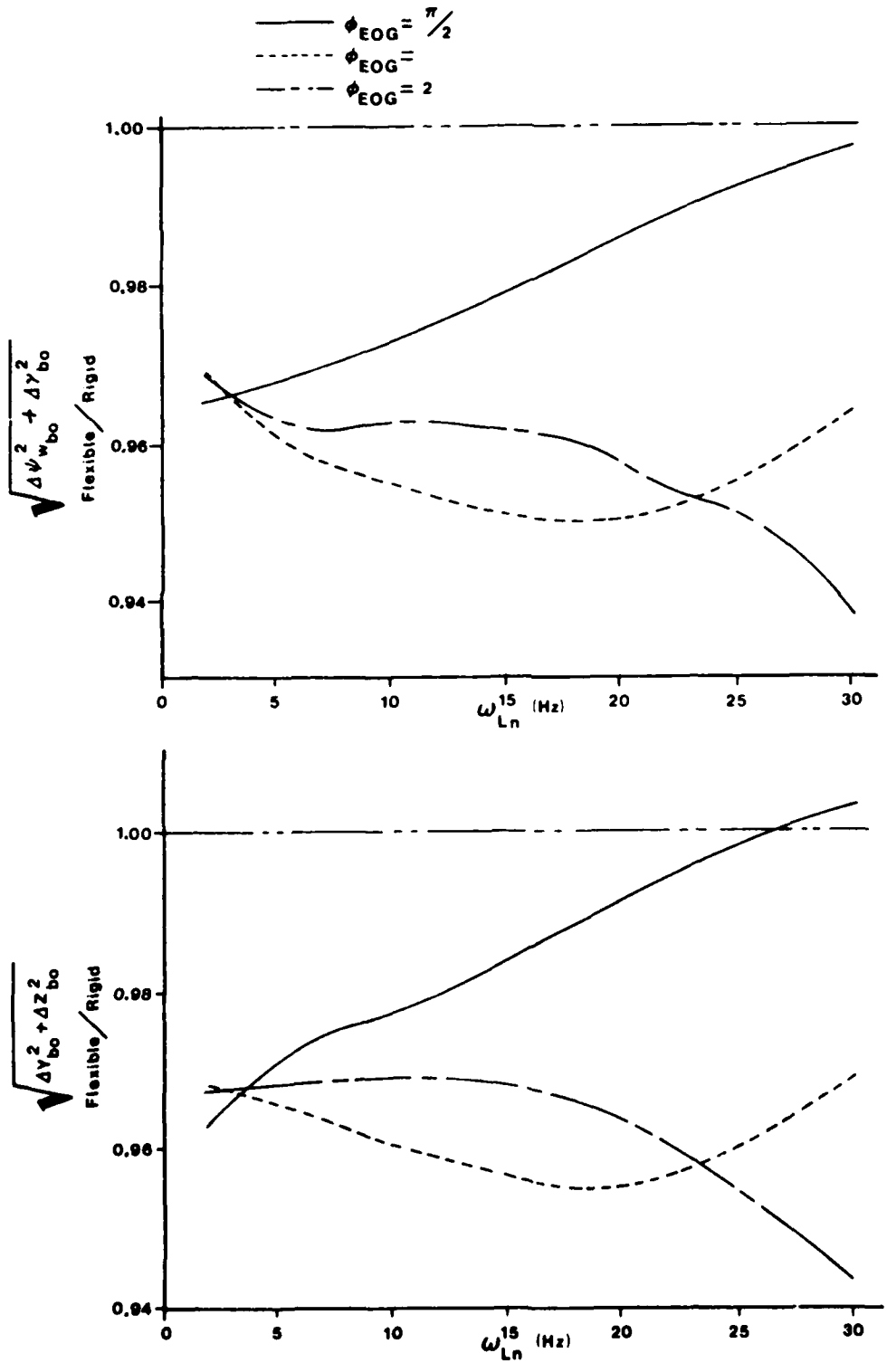

Fig. 25 Prototype launcher error ratios - dynamic imbalance, aft pivot, non-tip-off.

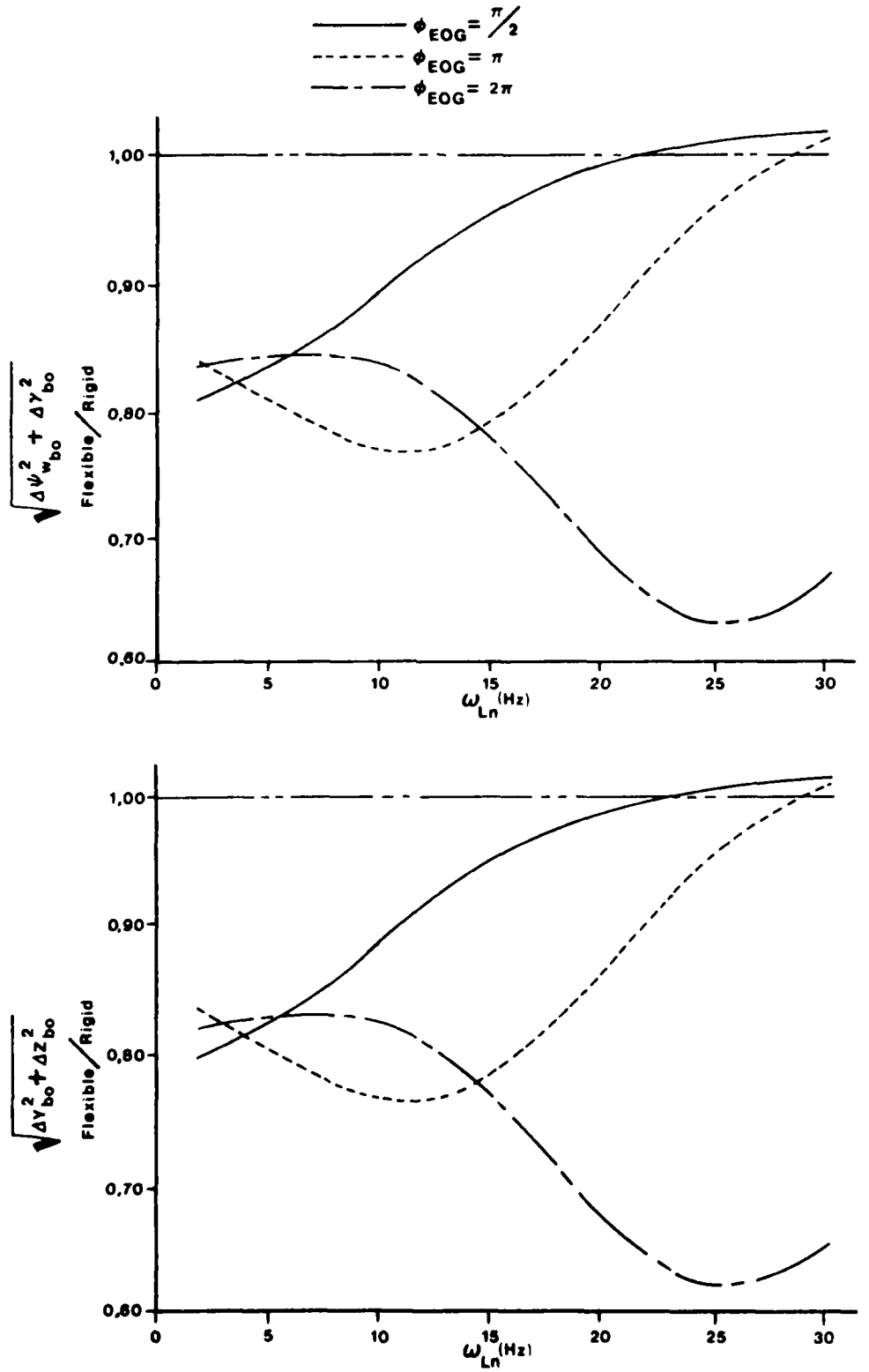

Fig. 26 Prototype launcher error ratios - dynamic imbalance, mid-point pivot, non-tip-off.

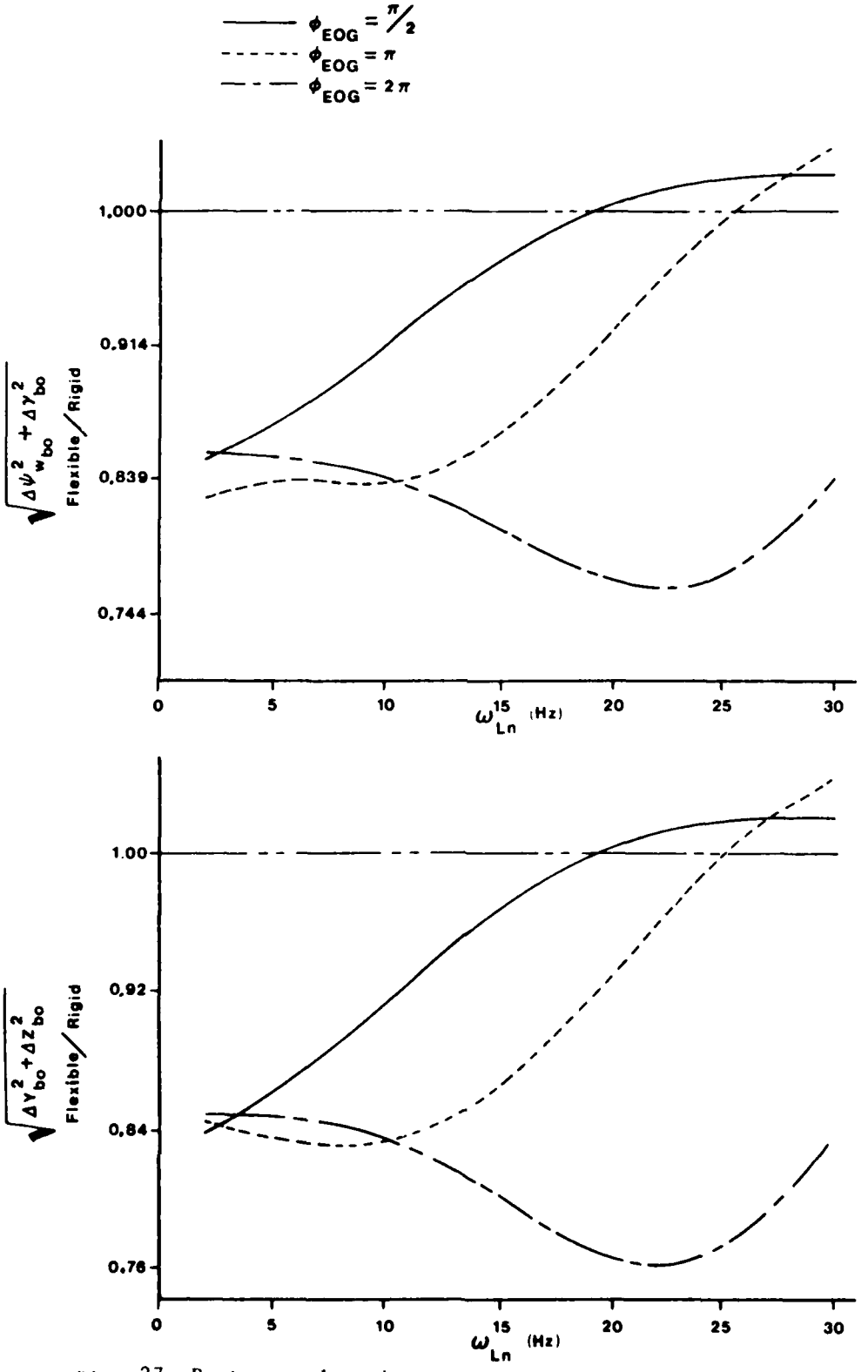

Fig. 27 Prototype launcher error ratios - dynamic imbalance, forward pivot, non-tip-off.

dynamic imbalance ($\mu_2 = 0.001$ and $\mu_3 = 0$). The curves in Figs. 28, 29 and 30 indicate that positive control is possible. A mid-point pivot is best for a range of values of ϕ_{EOG}.

Since dynamic imbalance effects increase with spin rate, while thrust misalignment effects decrease, the results for $\phi_{EOG} = \pi$ and 2π were principally produced by dynamic imbalance. It is not surprising therefore that they are very similar to those for dynamic imbalance only.

4.7 Effect of Launcher Inertia

Some indication of the effect of launcher moment of inertia can be derived from the "prototype" launcher model results. However, to delineate a range of moments of inertia for which passive control may be feasible, the best cases from several of the "constant-inertia" results error ratios were chosen and error ratios were determined for various values of I_L/I_R, where I_R is the initial value of the rocket's transverse moment of inertia. As can be seen from Fig. 31, in which results for several thrust misalignment cases are presented, the system performance rapidly deteriorates as the ratio I_L/I_R is increased. Figure 31 is for non-tip-off launchers. For a tip-off launch distance of 0.3048 m, the ratio I_L/I_R can be larger. Note, however, the high launcher frequencies which were used to obtain Fig. 32.

Figure 33, for non-tip-off launchers and dynamic imbalance, provides more encouragement as far as launcher size is concerned. If a mid-point pivot is used, it appears that a relatively large launcher will still respond significantly to dynamic imbalance.

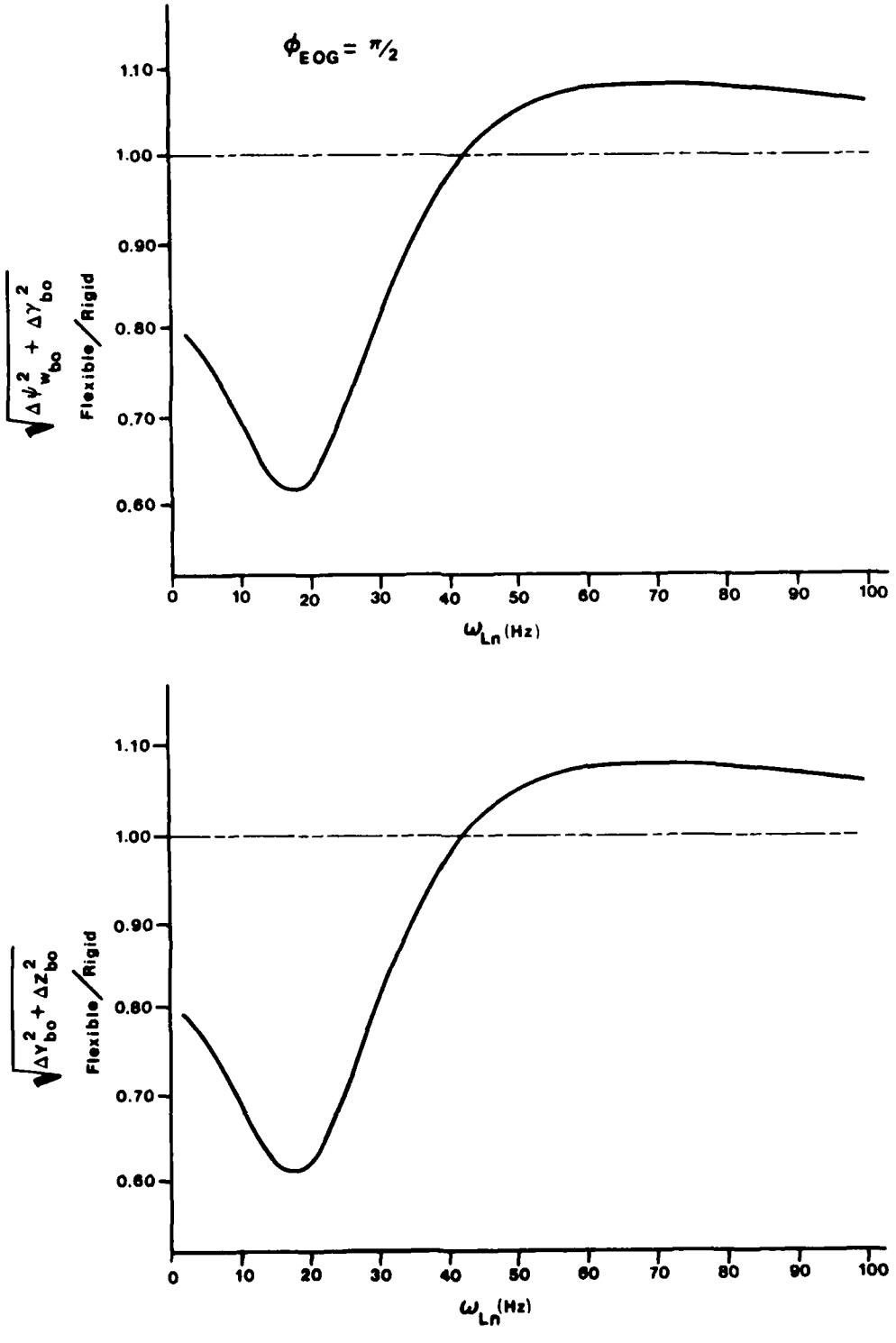

Fig. 28 Prototype launcher error ratios - combination of imperfections, aft pivot, non-tip-off.

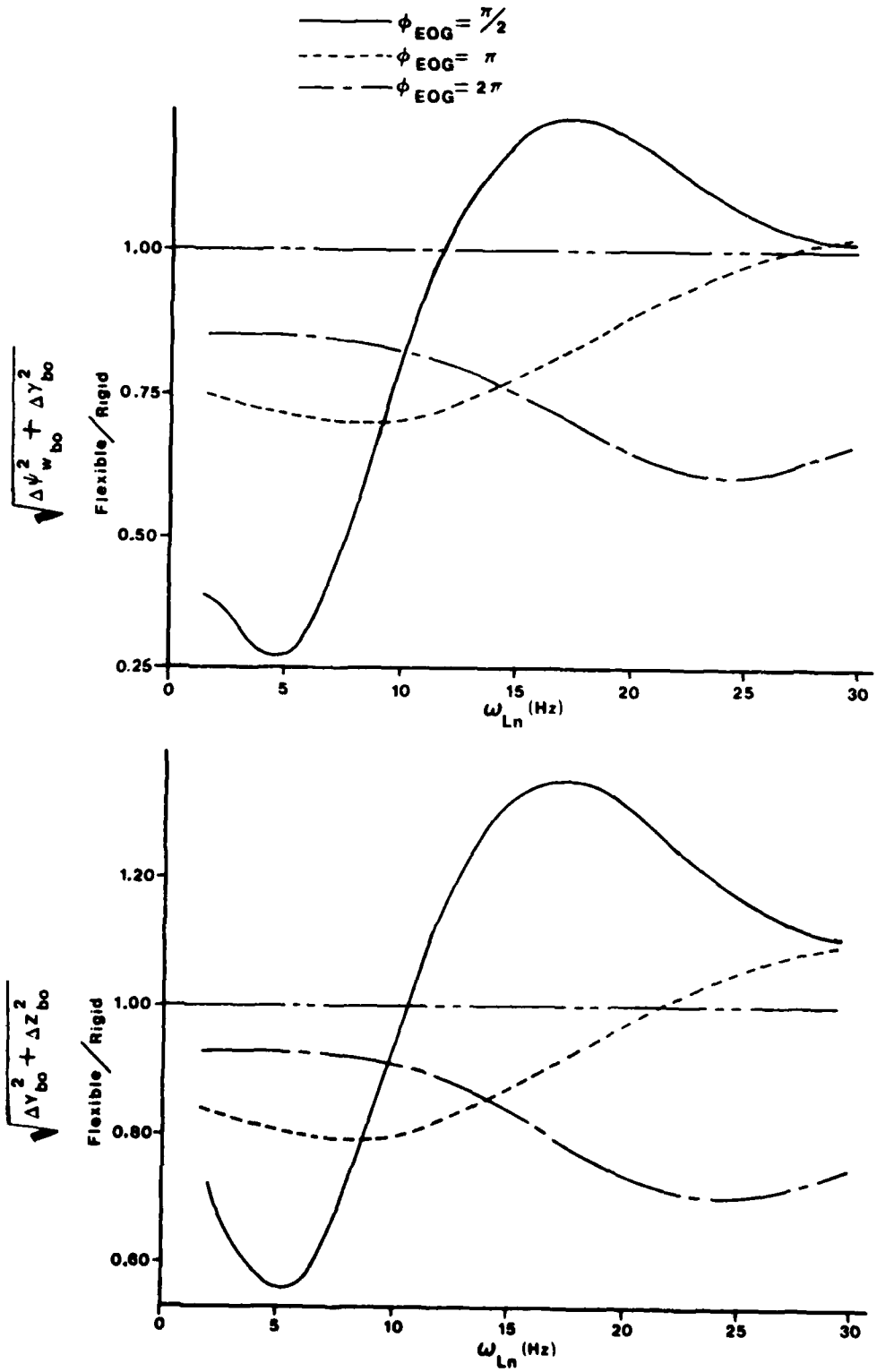

Fig. 29 Prototype launcher error ratios - combination of imperfections, mid-point pivot, non-tip-off.

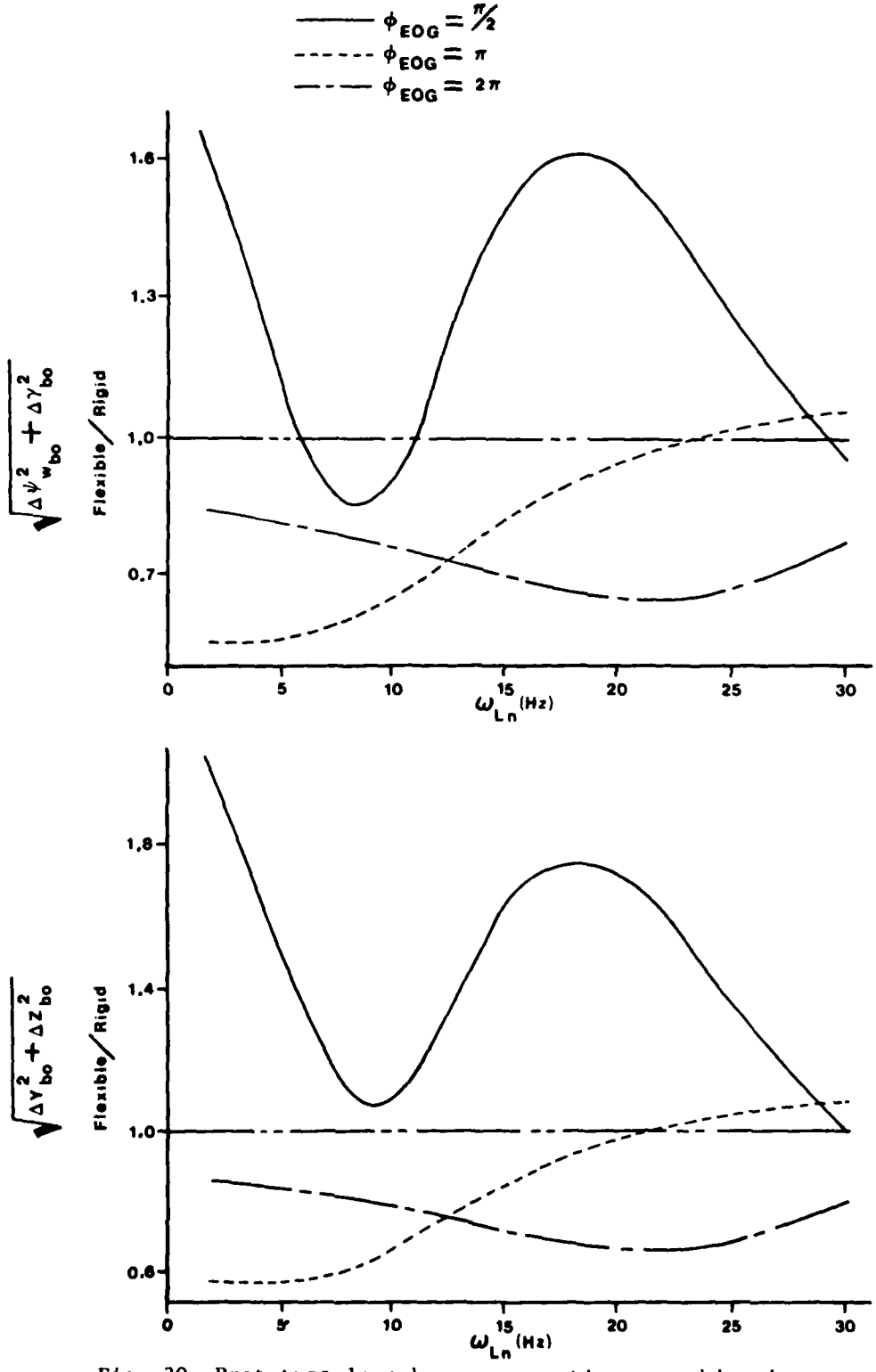

Fig. 30 Prototype launcher error ratios - combination of imperfections, forward pivot, non-tip-off.

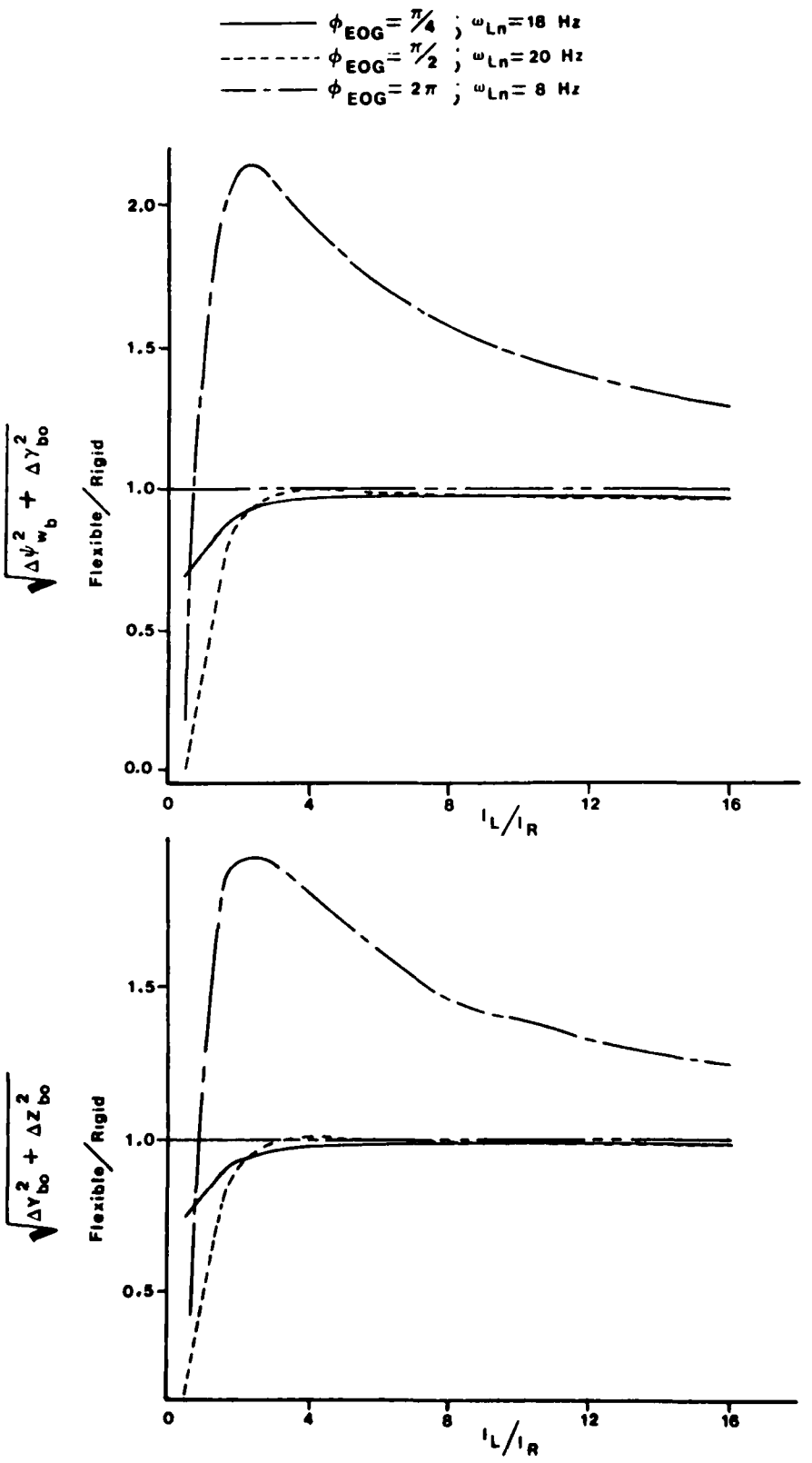

Fig. 31 Effect of launcher inertia - thrust misalignment, forward pivot, non-tip-off.

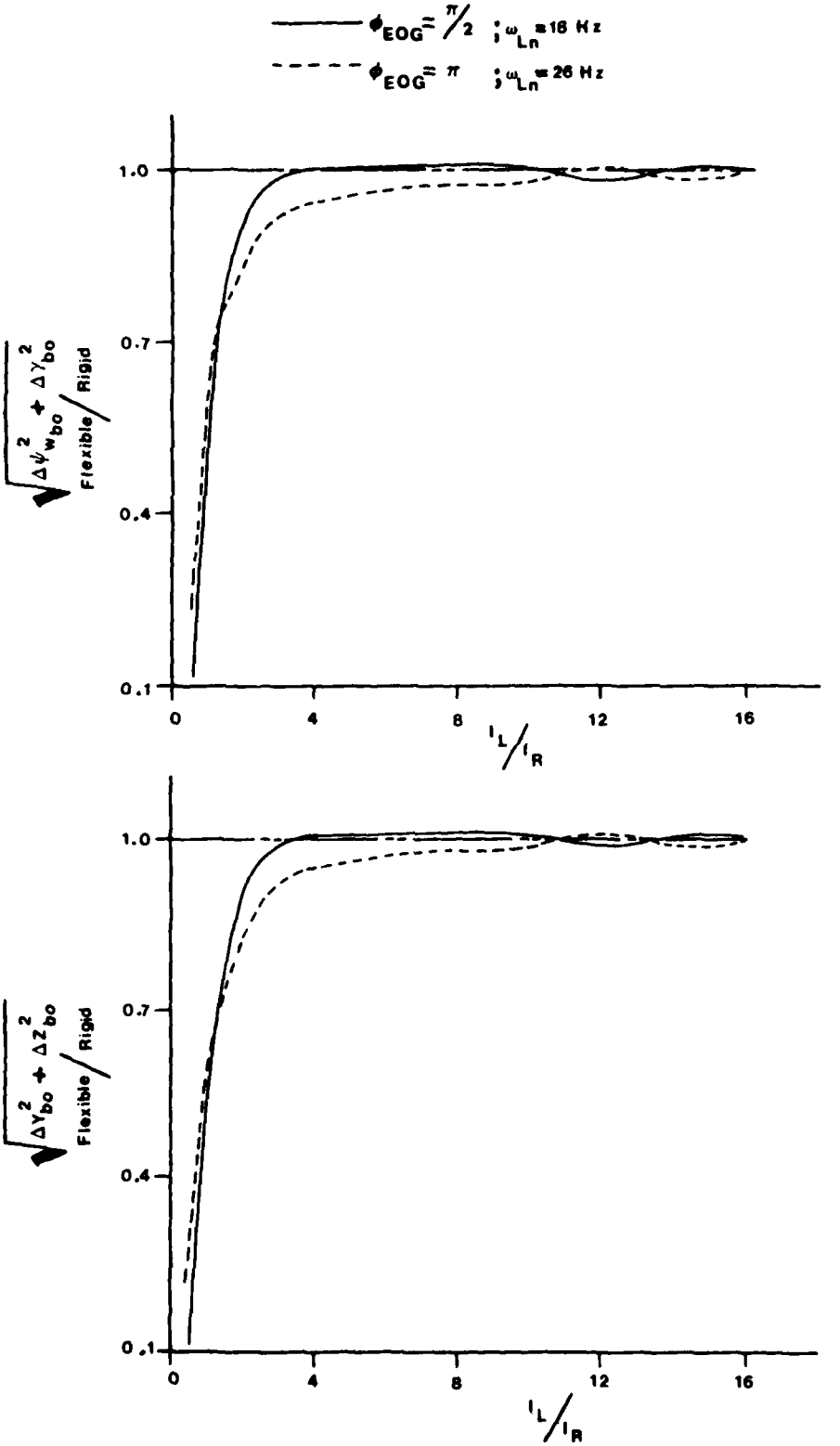

Fig. 32 Effect of launcher inertia - thrust misalignment, forward support, small tip-off distance.

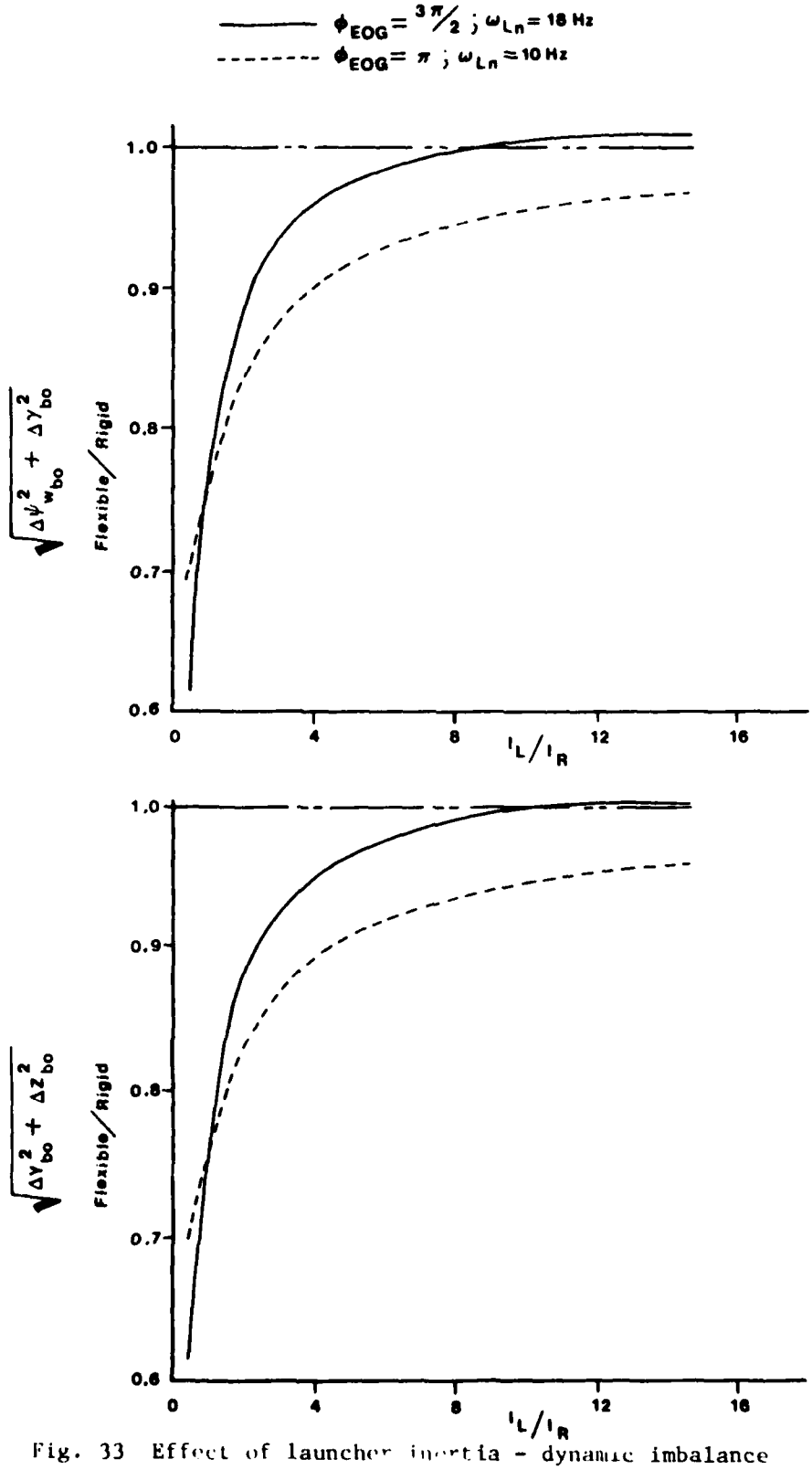

Fig. 33 Effect of launcher inertia - dynamic imbalance mid-point pivot, non-tip-off.

4.8 Effect of Thrust Profile Variations

A brief look was taken at the effects of thrust profile variations on launcher performance. A simple thrust profile (see Fig. 34) was assumed and the thrust rise time t_2-t_1, was varied while keeping the total impulse constant. The differences in error ratios from a nominal profile were determined for various launcher frequencies. Figure 35 contains plots of the percent error in the error ratios based on $t_2 = 0.06$ sec as the nominal value. For all cases, $t_1 = 0.005$ sec was used. Dynamic imbalance was the imperfection. The launcher was the basic one and had a forward pivot point. The launcher frequency was varied as indicated.

Note that even relatively large changes in the thrust rise time result in only small percentage changes in the error ratios. Thus, the passive control capability of the launcher should not be significantly affected by small random changes in thrust profile from rocket to rocket.

4.9 Effects of Randomness of Imperfections

Since the results presented in the previous subsections were obtained by using one or more specific imperfections, there is obviously a question as to whether they are valid for random imperfections. One way to check to see if they are is to vary the rocket-fixed orientation of the imperfection(s) through 2π and produce error "ellipses." These should, if the magnitude of the imperfection is not varied and there are no biases, be circles centered at the origin of $\Delta\gamma_{bo}$ vs. $\Delta\psi_{w_{bo}}$ and ΔZ_{bo} vs. ΔY_{bo}.

Figure 36a shows typical error curves. The solid curves were obtained for a thrust misalignment case for which:

$$\alpha_y = -0.001, \quad \alpha_z = 0, \quad \phi_{EOG} = 2\pi, \quad \omega_{Ln} = 8 \text{ Hz},$$

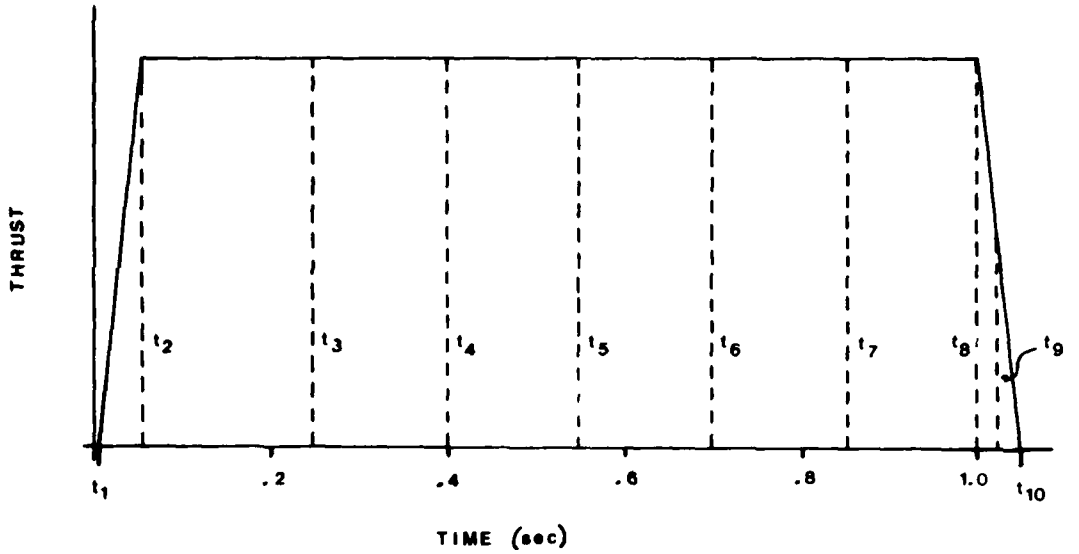

Fig. 34 Thrust profile for thrust variation effects study.

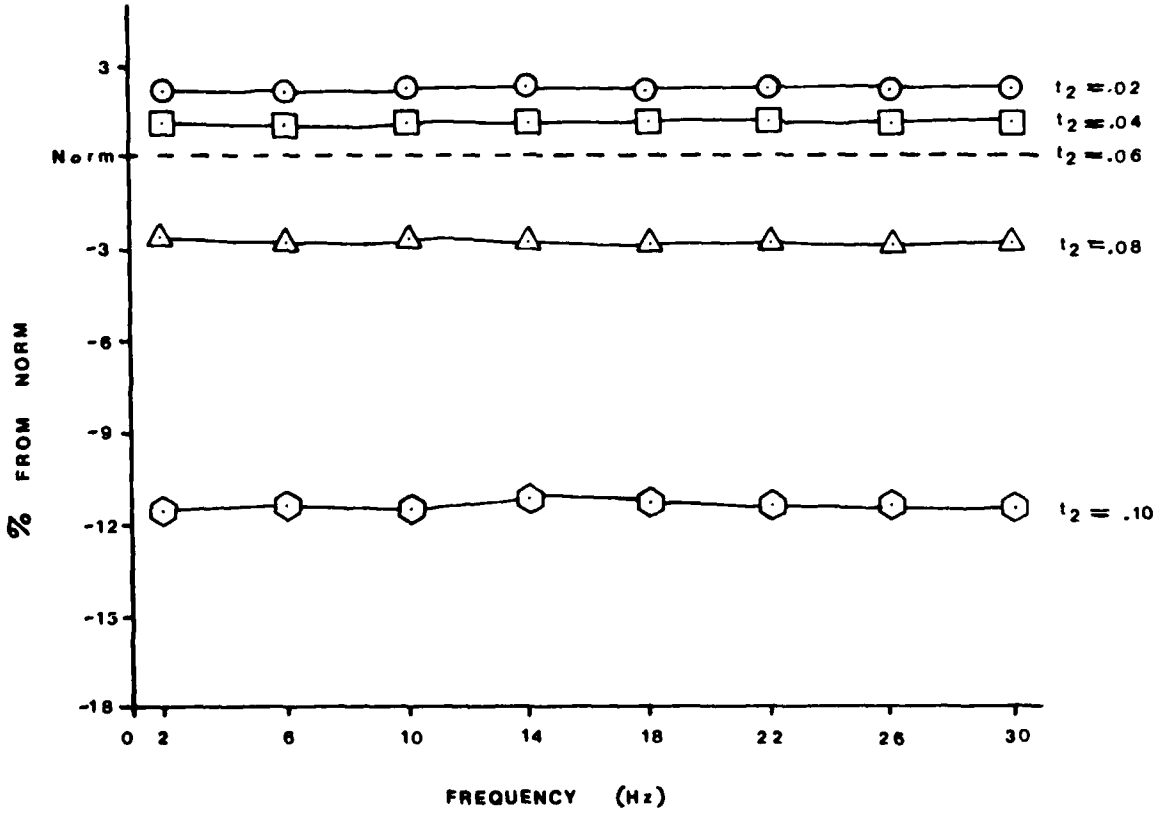

Fig. 35 Percent difference in error ratios.

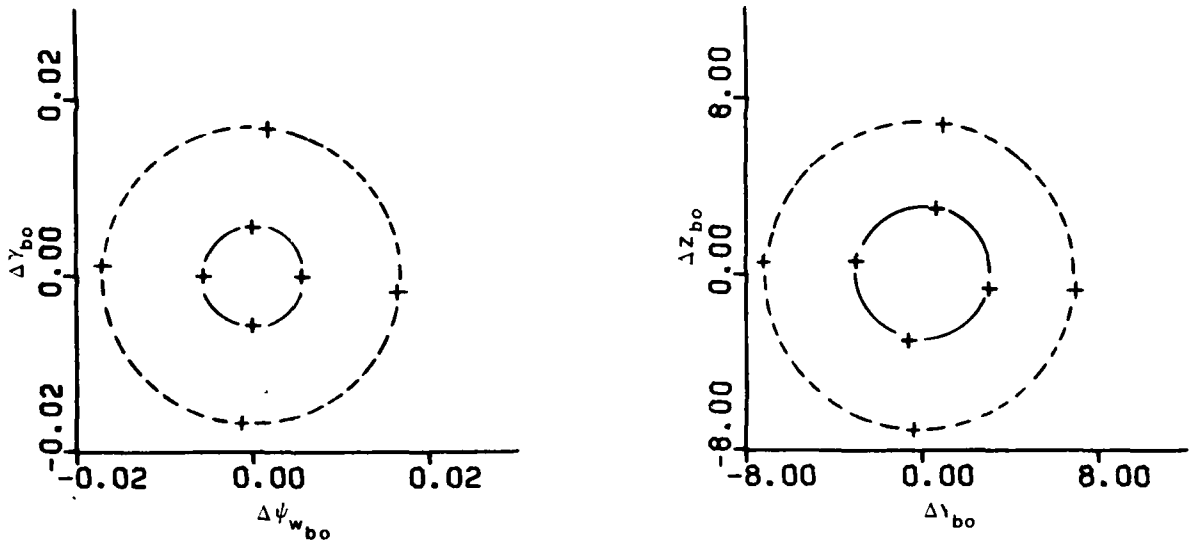

(a)

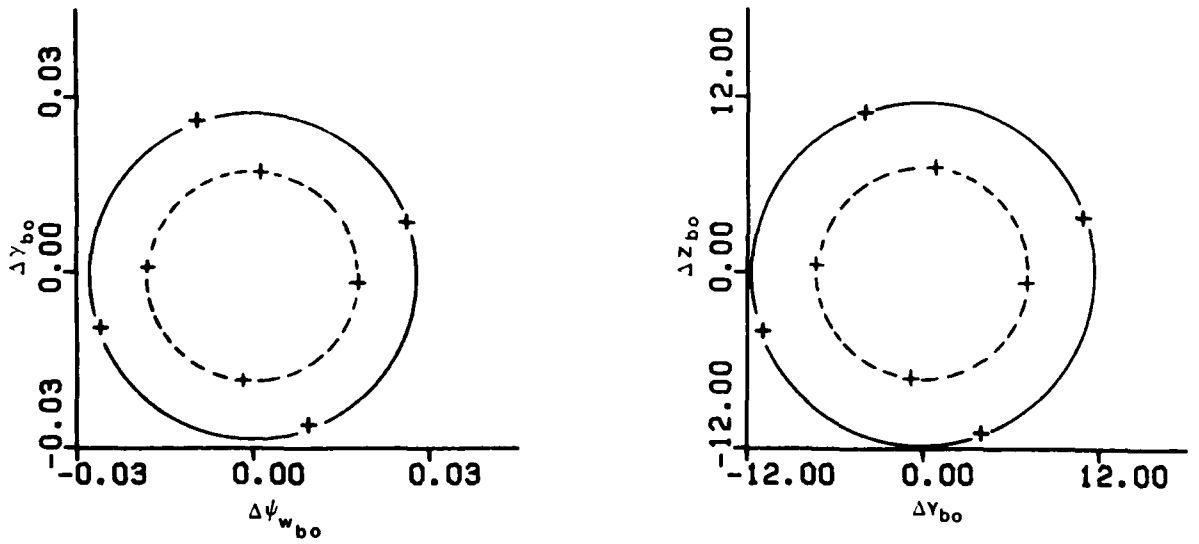

(b)

Fig. 36 Error curves - thrust misalignment.

the pivot point was at the front of the launcher, there was no tip-off and $I_L/I_R = 0.5$. The dashed curves are for a rigid launcher and a rocket with the same thrust misalignment and value of ϕ_{EOG}. A large reduction in total error is clearly evident.

The plots in Fig. 36b are for the same case except $I_L/I_R = 6$. The "overshoot" exhibited in Fig. 31 appears here in the form of flexible launcher error "ellipses" which are larger than their rigid launcher counterparts.

Error curves for a dynamic imbalance case are presented in Fig. 36. For all the curves, $\mu_2 = 0.001$, $\mu_3 = 0$, $\phi_{EOG} = \pi/2$ and a tip-off distance of 0.3048 m. The dashed curves are again for a rigid launcher. To obtain the solid curves, a launcher frequency of 6 Hz and a forward pivot point were used. The dashed curves in Fig. 37a and Fig. 37b are obtained using $I_L/I_R = 0.5$ and $I_L/I_R = 8$, respectively. The large reduction in dispersion for small I_L/I_R and the smaller reduction for I_L/I_R are consistent with previously presented results.

There is no observable bias in the curves presented in Figs. 36 and 37 and they clearly show that the body-fixed orientation of the imperfection does not affect the launcher performance as a passive controller. The effect of varying the magnitude of the imperfection is simply a change in the sizes of both the rigid-launcher and flexible-launcher error curves. Hence, the randomness of the imperfections does not affect the launcher's performance as a passive controller.

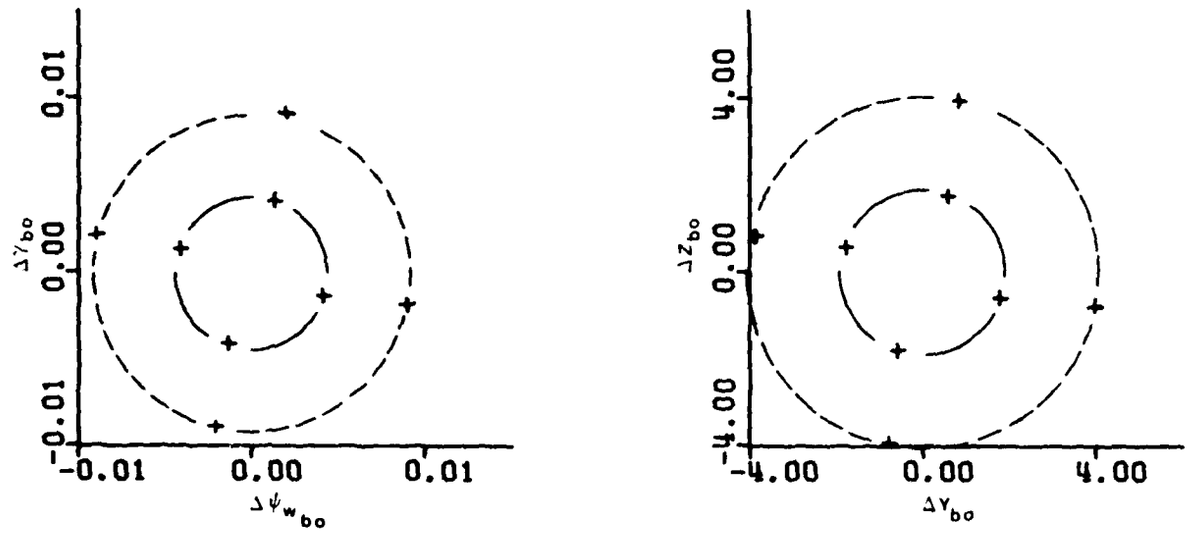

(a)

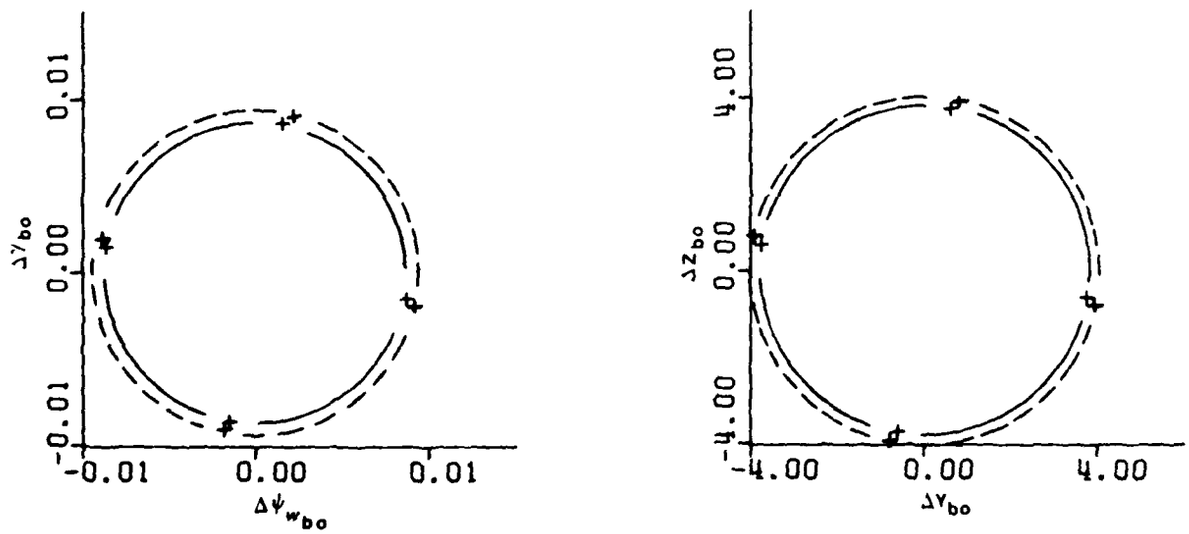

(b)

Fig. 37 Error curves - dynamic imbalance.

SECTION 5. CONCLUSIONS AND RECOMMENDATIONS

5.1 Conclusions

The goal of this investigation was to determine whether a launcher can compensate for random imperfections in free-flight rockets, thereby reducing dispersion. This goal was reached to the extent that reduction of flight errors for particular launcher configurations was demonstrated by numerically solving the equations of motion of the launcher/rocket system model. The reduction in error was found to be as large as eighty percent for launcher natural frequencies and moments of inertia which appear to be physically realizable.

The objectives of modeling the launcher/rocket system and producing quantitative results were attained. The quantitative results indicate that:

1. A forward pivot point for the launcher in general results in more significant response, especially for thrust misalignment; while either forward, or mid-point, pivot is best if dynamic imbalance is present.
2. The natural frequencies of launchers which produce significant reduction in dispersion when thrust misalignment is present are, for some launcher configurations, low enough to be physically realized; while if dynamic imbalance is present it appears that <u>any</u> launcher flexibility is beneficial.
3. Tip-off launchers produce larger reductions of error when the imperfection is thrust misalignment, but do not do so if dynamic imbalance is the imperfection.

4. The effect of increasing launcher inertia is (as intuition implies) to reduce the capability of the launcher to respond to the force and/or torque caused by the imperfection.
5. The effects of small variations in thrust rise time are not significant as far as launcher performance is concerned.
6. The randomness of imperfections does not affect launcher performance.

5.2 Recommendations

On the basis of the investigation, we make the following recommendations:

1. The results obtained herein should be verified by using analog simulations and/or other digital computer codes.
2. A simple experimental launcher should be constructed and tests made under carefully controlled conditions to experimentally substantiate the passive control concept.
3. Additional analytical work should be undertaken to determine the theoretical performance of a passive control launcher which has more degrees of freedom and contains a "sublauncher" (see Fig. 1). The flexibility of the rocket might also be modeled to ascertain its effect on launcher performance.

REFERENCES

1. Davis, L., Follin, J. W., and Blitzer, L., Exterior Ballistics of Rockets, D. Van Nostrand Company, Inc., Princeton, New Jersey, 1958.

2. Anonymous, Engineering Design Handbook - Design of Aerodynamically Stabilized Free Rockets, Headquarters, U.S. Army Material Command, Washington, D.C., July 1968.

3. McCorkle, W. C., "Recent Developments in High Accuracy Free Rocket Weapons System (U)," Carde Report 9AXP/8, Redstone Scientific Information Center, Redstone Arsenal, Alabama, April 1959.

4. Cochran, J. E., Jr., "Launchers as Passive Controllers," Technical Report RL-CR-81-2, Interim Report under Contract DAAH01-80-C-0523, U.S. Army Missile Command, Redstone Arsenal, Alabama, December 1980.

5. Cochran, J. E., Jr., and Christensen, D. E., "Launcher/Rocket Dynamics and Passive Control," AIAA Paper No. AIAA-81-1902, AIAA Atmospheric Flight Mechanics Conference, Albuquerque, New Mexico, August 19, 1981.

6. Beletskii, V. V., "Motion of an Artificial Satellite about Its Center of Mass," NASA TT F-429, 1966.

7. Cochran, J. E., Jr., "Investigation of Factors which Contribute to Mallaunch of Free Rockets," Final Report under U.S. Army Research Office Grant DAHC04-75-0034, Engineering Experiment Station, Auburn University, Alabama, January 1976.

8. Synge, J. L., and Griffith, B. A., Principles of Mechanics, Third Edition, McGraw-Hill Book Company, New York, 1959, pp. 380-383.

APPENDIX A

MATHEMATICAL MODELS

A.1 Introduction

This appendix contains a description of the mathematical models used to obtain the results described in the body of this report. Vector/matrix notation used in the derivation and manipulation of equations of motion is first defined. Then, the physical models for the rocket and the launcher are described. Finally, equations of motion (mathematical model) are derived and cast into the matrix forms which have been programmed for numerical solution.

A.2 Vector/Matrix Notation

The notation used for vector quantities such as position, velocity and angular velocity is typified by

$$\underline{\omega} = \omega_1 \hat{\underline{i}}_L + \omega_2 \hat{\underline{j}}_L + \omega_3 \hat{\underline{k}}_L \ , \tag{A-1}$$

where $\underline{\omega}$ is the angular velocity of a launcher-fixed coordinate frame and $\hat{\underline{i}}_L$, $\hat{\underline{j}}_L$ and $\hat{\underline{k}}_L$ form a set of dextral, orthogonal, unit vectors directed along the coordinate axes. The matrix counterpart of Eq. (A-1) is

$$\underline{\omega} = (\omega_1 \quad \omega_2 \quad \omega_3)^T \ , \tag{A-2}$$

where the superscript T denotes the matrix transpose. Of course, if a matrix is to be used in place of Eq. (A-1) some basis must be adopted. In the case of Eq. (A-2), it is the launcher-fixed basis. Herein, the basis adopted for writing the matrix equivalent of a vector, or dyadic,

should be apparent, in some cases, from the context of the equation in which it appears. In other cases, the basis is defined in the text; and, in still others, the basis used is indicated by the letter L or R written underneath a matrix to denote launcher-fixed (L), or rocket-fixed (R) basis.

Dyadics, such as the inertia dyadic of the launcher are indicated by double underlines. For example, the inertia dyadic of the launcher referenced to the launcher support point 0 is

$$\begin{aligned}\underline{\underline{I}}_L = {} & I_{11}\,\hat{\underline{i}}_L\hat{\underline{i}}_L + I_{12}\,\hat{\underline{i}}_L\hat{\underline{j}}_L + I_{12}\,\hat{\underline{i}}_L\hat{\underline{k}}_L \\ & + I_{12}\,\hat{\underline{j}}_L\hat{\underline{i}}_L + I_{12}\,\hat{\underline{j}}_L\hat{\underline{j}}_L + I_{23}\,\hat{\underline{j}}_L\hat{\underline{k}}_L \\ & + I_{13}\,\hat{\underline{k}}_L\hat{\underline{i}}_L + I_{23}\,\hat{\underline{k}}_L\hat{\underline{j}}_L + I_{33}\,\hat{\underline{k}}_L\hat{\underline{k}}_L \end{aligned} \tag{A-3}$$

where the I_{ij} are moments (i=j) and the negatives of products ($i\neq j$) of inertia of the launcher about 0.

The matrix equivalent of the inertia dyadic $\underline{\underline{I}}_L$ is the inertia matrix,

$$\underline{\underline{I}}_L = \begin{bmatrix} I_{11} & I_{12} & I_{13} \\ I_{12} & I_{22} & I_{23} \\ I_{13} & I_{23} & I_{33} \end{bmatrix} \tag{A-4}$$

where it is obvious that the launcher-fixed basis has been adopted.

The vector cross product, $\underline{\omega}\times\underline{R}$, where $\underline{R} = x_{L_C}\hat{\underline{i}}_L + y_{L_C}\hat{\underline{j}}_L + z_{L_C}\hat{\underline{k}}_L$ has the matrix equivalent $\tilde{\underline{\omega}}\,\underline{R}$, where

$$\tilde{\underline{\omega}} = \begin{bmatrix} 0 & -\omega_3 & \omega_2 \\ \omega_3 & 0 & -\omega_1 \\ -\omega_2 & \omega_3 & 0 \end{bmatrix} \tag{A-5}$$

and $\underline{R} = (x_{L_C} \quad y_{L_C} \quad z_{L_C})^T$.

If it is convenient to use certain bases to write the matrix equivalents of vectors, dyadics and vector products, then the matrix forms must be transformed before matrix products can be formed. For example, let $\underline{\underline{A}}$ denote the direction cosine matrix which defines the orientation of the rocket-fixed system Cxyz with unit vectors $\hat{\underline{i}}$, $\hat{\underline{j}}$ and $\hat{\underline{k}}$ and let $\underline{u}$ denote the matrix equivalent of a rocket-fixed (with respect to rotation) vector, then the matrix product $\tilde{\underline{\omega}}\ \underline{\underline{A}}\ \underline{u}$ and the vector product $\underline{\omega} \times \underline{u}$ are equivalent. Furthermore, the matrix product $\underline{\underline{A}}^T\ \tilde{\underline{u}}\ \underline{\underline{A}}\ \underline{\omega}$ is equivalent to the vector product $\underline{u} \times \underline{\omega}$. The basis of the result in both examples is the launcher-fixed one.

In transforming vector/dyadic equations to matrix equations, care must be taken to make sure that two quantities with different bases are not multiplied, added or subtracted. To illustrate this, we consider the velocity of a point P in the rocket (see Fig. A1). In Fig. A1, O is a fixed point and C_L and C are centers of mass of the launcher and rocket, respectively.

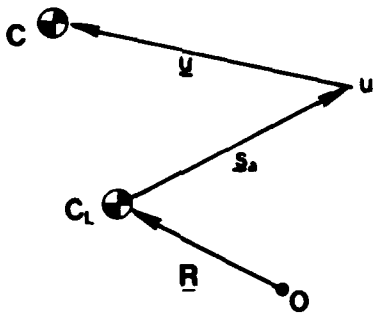

Fig. A1 Definition of vectors.

We let $\underset{L}{R}$ and $\underset{L}{s}_a$ be the launcher-fixed basis equivalents of the vectors $\underline{R}$ and $\underline{s}_a$. We also let $\underset{R}{u}$ and $\underset{R}{\rho}$ denote the rocket-fixed matrix equivalents of the vectors $\underline{u}$ and $\underline{\rho}$. We also use $\underline{\Omega}$ to denote the rocket-fixed basis matrix equivalent of the rocket's angular velocity. Then in matrix form, the position of P (referenced to 0) is given by

$$\underline{r}_P = \underline{R} + \underline{s}_a + \underline{u} + \underline{\rho} \tag{A-6}$$

and the velocity of P is

$$\underline{V}_P = \underline{\omega}x(\underline{R}+\underline{s}_a) + (d\underline{s}_a/dt)_L + \underline{\Omega}x(\underline{u}+\underline{\rho}) + [(d\underline{u}/dt)_R + (d\underline{\rho}/dt)_R] \ , \tag{A-7}$$

where $(d*/dt)_L$ and $(d*/dt)_R$ denote the time-rates-of-change of the launcher-fixed and rocket-fixed components of *; i.e., "local" derivatives.

A matrix equivalent of (A-7) is

$$\underline{V}_P = \tilde{\underline{\omega}}(\underline{R}+\underline{s}_a) + \underline{\underline{A}}^T \tilde{\underline{\Omega}}(\underline{u}+\underline{\rho}) + \underset{L}{\dot{s}}_a + \underline{\underline{A}}^T \underset{R}{\dot{u}} + \underline{\underline{A}}^T \underset{R}{\dot{\rho}} \ , \tag{A-8}$$

where $\underset{L}{\dot{x}}$ and $\underset{R}{\dot{x}}$ denote the matrix equivalents of the local derivatives defined above.

Certain special matrices are used in this appendix. Some are used to extract needed information from a matrix equation in order to remove constraint forces and torques. By definition,

$$\underline{\underline{E}}_1 = \begin{bmatrix} 1 & 0 & 0 \\ 0 & 0 & 0 \\ 0 & 0 & 0 \end{bmatrix} \tag{A-9a}$$

and

$$\underline{\underline{E}}_{23} = \begin{bmatrix} 0 & 0 & 0 \\ 0 & 1 & 0 \\ 0 & 0 & 1 \end{bmatrix} . \qquad \text{(A-9b)}$$

These are recognized as subsets of the identity matrix,

$$\underline{\underline{E}} = \begin{bmatrix} 1 & 0 & 0 \\ 0 & 1 & 0 \\ 0 & 0 & 1 \end{bmatrix} . \qquad \text{(A-10)}$$

Clearly, $\underline{\underline{E}}_1$ can be used to retain only the first element of a 3x1 matrix, while $\underline{\underline{E}}_{23}$ can be used to retain the last two elements of such a matrix.

A.3 Physical Models

Launcher/rocket systems are relatively complex dynamic systems. A typical system consists of a vehicle, the launcher proper and one or more rockets. The vehicle types include massive track vehicles, trucks, towed carriages and human beings. The launchers range from heavy pods, with mechanisms to orient them, to simple hand-held tubes. The rockets may be of several types as far as size and geometric configuration are concerned, but are generally propelled by solid propellant rocket motors. A physical model which incorporates the salient characteristics of all possible systems; i.e., a generic model; would be tremendously complex. For this reason, it appears best to adopt physical models which are most suitable for the investigation of the particular problem of interest, or which are dictated by a specific system concept. Here, we are interested in determining the degree to which a launcher can be expected to act as a passive control device which reduces the flight errors caused by imperfections of the rocket(s) launched from it. Relatively simple models are sufficient for this purpose.

Launcher Model

The physical model adopted for the launcher is a single rigid body with two degrees of rotational freedom (see Fig. A2). Although simple, this launcher model is adequate for light-weight launchers and for the sub-launcher concept described in the body of this report. Only single-round launchers are considered.

Rocket Model

The rocket model is a variable-mass body, composed of a rigid shell, a rigid warhead, solid propellant and the fluid part of burned propellant still within the shell (see Fig. A3). The aerodynamic characteristics are "typical." The principal effects of time-varying mass are that (1) the center of mass of the rocket moves with respect to the rigid body part, (2) the mass and moments of inertia of the rocket change with time and (3) the flow of fluid within the rocket produces jet-damping.

Interface Models

The interface between launcher and rocket is rigid. Hence, the rocket pitches and yaws with the launcher during the "detent" and "guidance" phases. Two methods for imparting spin to the rocket are incorporated. First, spin may be generated by a rocket-fixed torque such as that delivered by spin vanes. Second, and of most application in this report, spin may be imparted by helical rails which cause the rocket to rotate through a specific angle during the guidance phase of flight.

Both non-tip-off launches, in which the rocket becomes totally free of the launcher at one instant of time, and tip-off launches, in which forward support of the rocket is removed at one time and at a later time

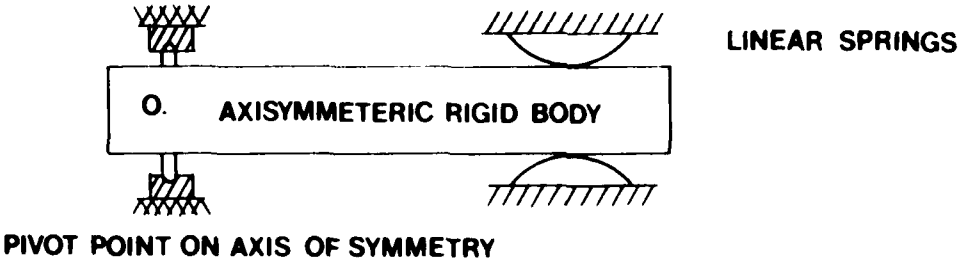

Fig. A2 Launcher physical model.

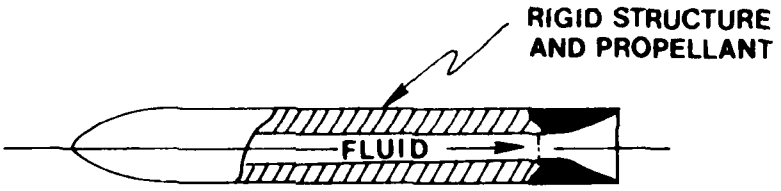

Fig. A3 Rocket physical model.

the rear support is removed, are modeled. The guidance phase ends at the beginning of the tip-off phase (see Fig. A4).

A.4 Equations of Motion

The present derivation of equations of motion follows closely that of Ref. 6. The principal differences are (1) the present derivation is more brief, (2) the use of helical rails to impart spin was not considered then but is now, and (3) some errors in the results given in Ref. 6 have been corrected here. As indicated above, the total time from ignition of the rocket until its impact is divided into four phases: detent, guidance, tip-off and free-flight. The detent phase begins prior to ignition and ends when the mechanism which constrains the rocket's translation along the launcher releases. The guidance phase begins when the detent phase ends and ends when the forward support of the rocket releases; i.e., tip-off begins. The tip-off phase ends when the rocket is no longer in mechanical contact with the launcher.

Because the number of degrees of freedom varies from phase to phase, each is considered separately. However, most of the vector notation and the coordinate systems utilized are shown in Fig. A5. The OXYZ system is an inertial one and has its origin located at the pivot point of the launcher. The launcher has two degrees of freedom in rotation, yaw (angle α_3) and pitch (angle α_2). The launcher-fixed system $C_L x_L y_L z_L$ has its origin at the launcher mass center and its x_L-axis directed parallel to the direction of travel of the rocket. The z_L-axis lies in a vertical plane. Vector $\underline{R}$ locates C_L with respect to O. The rocket-fixed ax'y'z' system has its origin a on the geometric centerline of the rocket at the aft support location. Vector $\underline{s}_a$ locates point a relative to C_L. The x'-axis

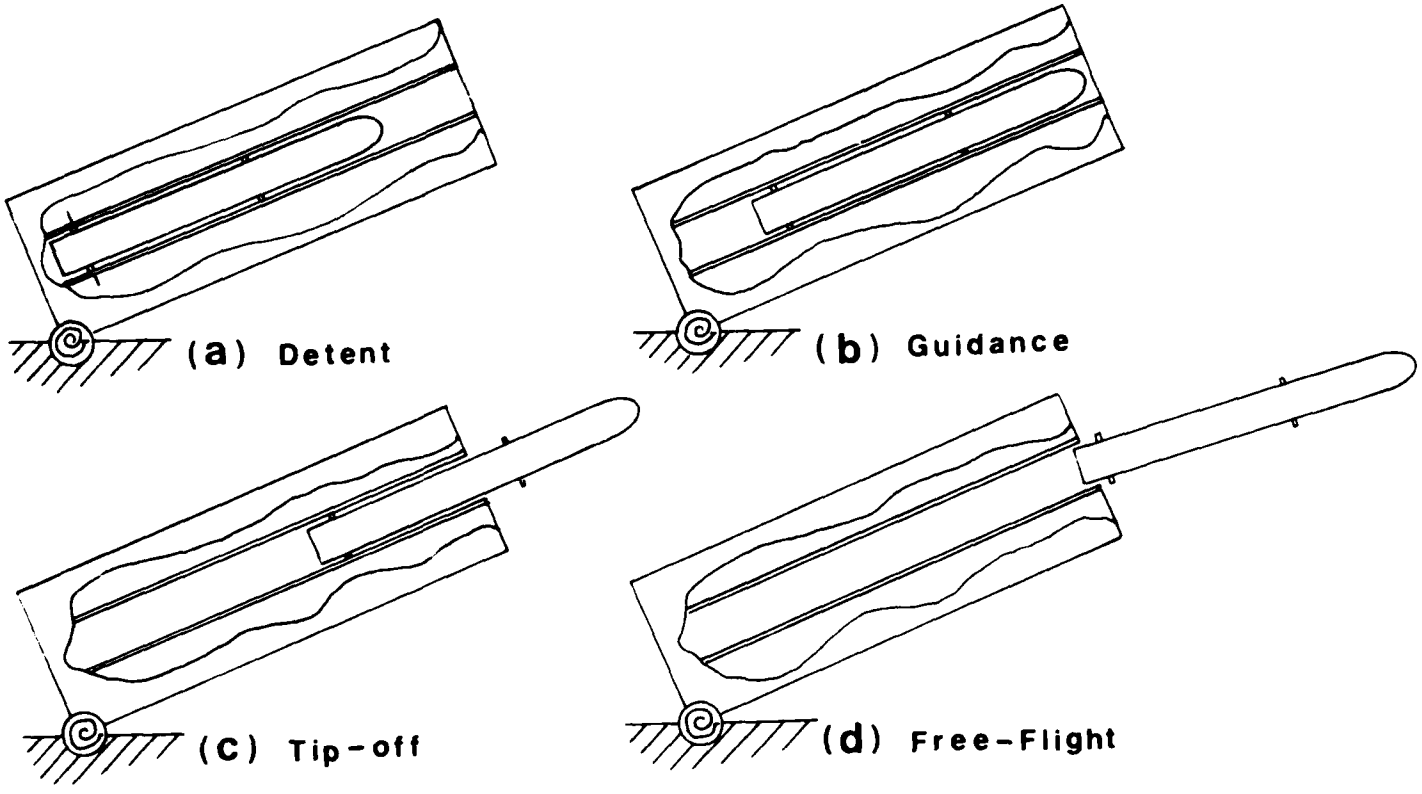

Fig. A4 Phases which are modeled.

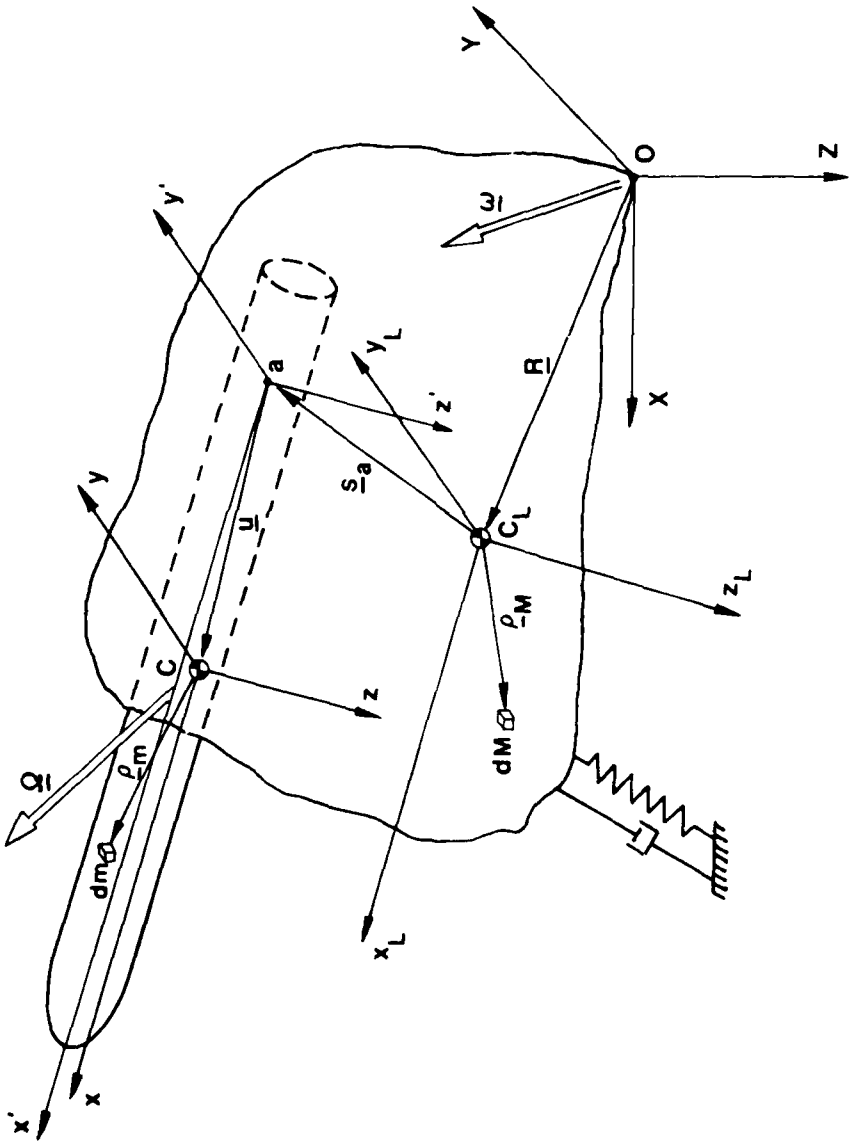

Fig. A5 Notation and reference frames.

lies along the geometric centerline of the rocket. The rocket's center of mass is C and the Cxyz reference frame rotates with the rocket. Because the mass of the rocket varies with time, C translates with respect to a. However, the Cxyz system remains aligned with the ax'y'z' system at all times. The vector $\underline{u}$ locates C relative to point a.

The vectors $\underline{\ell}_T$, $\underline{\rho}_m$, $\underline{\rho}_M$, $\underline{F}_T$, $\underline{\Omega}$ and $\underline{\omega}$ are shown in Fig. A5. A point on the line-of-action of $\underline{F}_T$ is located by $\underline{\ell}_T$. The vectors $\underline{\rho}_m$ and $\underline{\rho}_M$ are generic position vectors which locate elements of mass dm and dM, respectively, in rocket and launcher. Finally, $\underline{\Omega}$ and $\underline{\omega}$ are the angular velocities of the rocket and launcher, respectively.

A.4.2 Detent Phase

During the detent phase, the launcher and rocket move as one body, except the rocket may rotate about the x'-axis. If we let $\underline{\underline{I}}_{L/0}$ and $\underline{\underline{I}}$ denote the inertia dyadics of the launcher about 0 and the rocket about C, respectively, the angular momentum of the system about 0 is

$$\underline{H}_0 = \underline{\underline{I}}_{L/0} \cdot \underline{\omega} + \underline{\underline{I}} \cdot \underline{\Omega} + \underline{r} \times m\dot{\underline{r}} \ , \qquad \text{(A-11)}$$

where $\underline{r} = \underline{R} + \underline{s}_a + \underline{u}$. Because $(d\underline{u}/dt)_R$ and $(d^2\underline{u}/dt^2)_R$ should be small during the brief detent phase, and since $(d\underline{s}_a/dt)_L \equiv (d^2\underline{s}_a/dt^2)_L \equiv 0$ during this phase, the equation of rotational motion of the system about 0 is

$$\underline{T}_0 = \underline{\underline{I}}_{L/0} \cdot (d\underline{\omega}/dt)_L + \underline{\omega} \times \underline{\underline{I}}_{L/0} \cdot \underline{\omega} + \underline{\underline{I}} \cdot (d\underline{\Omega}/dt)_R + \underline{\Omega} \times \underline{\underline{I}} \cdot \underline{\Omega} + \underline{r} \times m\ddot{\underline{r}} \ , \qquad \text{(A-12)}$$

where

$$\ddot{\underline{r}} = (d\underline{\omega}/dt)_L \times (\underline{R}+\underline{s}_a) + \underline{\omega} \times [\underline{\omega} \times (\underline{R}+\underline{s}_a)] + (d\underline{\Omega}/dt)_R + \underline{\Omega} \times (\underline{\Omega} \times \underline{u}) \ . \qquad \text{(A-13)}$$

The torque $\underline{T}_0$ includes a constraint torque which prevents launcher roll. Also, in matrix form, rocket basis,

$$\underline{\Omega} = \underline{\lambda} + \underline{\underline{A}}\,\underline{\omega} \ , \tag{A-14}$$

where $\underline{\lambda} = (p \quad 0 \quad 0)^T$ is the spin rate of the rocket and

$$\underline{\underline{A}} = \begin{bmatrix} 1 & 0 & 0 \\ 0 & c\theta_1 & s\theta_1 \\ 0 & -s\theta_1 & c\theta_1 \end{bmatrix} . \tag{A-15}$$

Here, we have used the shorthand notation, $c\theta_1 \equiv \cos\theta_1$ and $s\theta_1 \equiv \sin\theta_1$. Also,

$$\dot{\theta}_1 = p \ . \tag{A-16}$$

From (A-14) and (A-15) the matrix counterpart of $(d\underline{\Omega}/dt)_R$ is

$$\dot{\underline{\Omega}}_R = \dot{\underline{\lambda}} + \underline{\underline{A}}\,\dot{\underline{\omega}} - \tilde{\underline{\lambda}}\,\underline{\underline{A}}\,\underline{\omega} \tag{A-17}$$

and the equation of rotational motion for the rocket is

$$\underline{\underline{I}}\,(d\underline{\Omega}/dt)_R + \underline{\Omega}\times\underline{\underline{I}}\cdot\underline{\Omega} = \underline{T}_{R/C}, \tag{A-18}$$

where $\underline{T}_{R/C}$ consists of constraint torque, $\underline{T}^c$, and spin torque, $\underline{T}_s$, if present. The constraint torques are orthogonal to the x-axis, so that

$$\underline{T}^c = \underline{\underline{E}}_{23}\{\underline{\underline{I}}\,\dot{\underline{\Omega}}_R + \tilde{\underline{\Omega}}\,\underline{\underline{I}}\,\underline{\Omega}\} \ . \tag{A-19}$$

Also, since $\dot{\underline{\lambda}} = (\dot{p} \quad 0 \quad 0)^T$,

$$\dot{\underline{\lambda}} = \underline{\underline{E}}_1\{-\underline{\underline{A}}\,\dot{\underline{\omega}} + \tilde{\underline{\lambda}}\,\underline{\underline{A}}\,\underline{\omega} - \underline{\underline{I}}^{-1}\underline{\underline{E}}_{23}[\underline{\underline{I}}\,\dot{\underline{\Omega}}_R + \tilde{\underline{\Omega}}\,\underline{\underline{I}}\,\underline{\Omega}] + \underline{\underline{I}}^{-1}\underline{T}_s\} \ . \tag{A-20}$$

Letting I_s denote the moment of inertia of the rocket about the x'-axis and defining

$$\underline{\underline{J}} \equiv \underline{\underline{E}} - \underline{\underline{E}}_1\,\underline{\underline{I}}^{-1}\underline{\underline{E}}_{23}\,\underline{\underline{I}} \ , \tag{A-21}$$

we have

$$\dot{\underline{\lambda}} = \frac{1}{I_s} \{\underline{\underline{E}}_1 \underline{\underline{I}} [\tilde{\underline{\lambda}} \underline{\underline{A}} \underline{\omega} - \underline{\underline{A}} \dot{\underline{\omega}}] - \underline{\underline{J}}^{-1} \underline{\underline{E}}_1 \underline{\underline{I}}^{-1} \underline{\underline{E}}_1 \underline{\underline{\Omega I \Omega}} + (T_s \quad 0 \quad 0)^T\} . \tag{A-22}$$

The translation of C is governed by the equation,

$$m\ddot{\underline{r}} = \underline{F}^{ex} + \underline{F}^{c} \quad , \tag{A-23}$$

where $\underline{F}^{ex}$ is the external force on the rocket and $\underline{F}^{c}$ is a constraint force which includes the detent force. In matrix form, launcher basis,

$$\begin{aligned} \underline{\underline{F}}^{c}_{L} = & - \underline{\underline{F}}^{ex}_{L} + m \{- \tilde{\underline{r}} \dot{\underline{\omega}} + \tilde{\underline{\omega}} \tilde{\underline{\omega}} (\underline{R} + \underline{s}_a) \\ & + \underline{\underline{A}}^T \tilde{\underline{\Omega}} \dot{\underline{\Omega}} \underline{u} - \underline{\underline{A}}^T \tilde{\underline{u}} \dot{\underline{\lambda}} + \underline{\underline{A}}^T \tilde{\underline{u}} \tilde{\underline{\lambda}} \underline{\underline{A}} \underline{\omega}\} , \end{aligned} \tag{A-24}$$

where $\tilde{\underline{r}} = \tilde{\underline{R}} + \tilde{\underline{s}}_a + \underline{\underline{A}}^T \tilde{\underline{u}} \underline{\underline{A}}$.

By using (A-22) in the matrix form of (A-12), we obtain the result,

$$\begin{aligned} \underline{\underline{L}}_1 \dot{\underline{\omega}} = & - \tilde{\underline{\omega}} \underline{\underline{I}}_{L/0} \underline{\omega} + \underline{\underline{A}}^T [\underline{\underline{I}} \tilde{\underline{\lambda}} \underline{\underline{A}} \underline{\omega} - \tilde{\underline{\Omega}} \underline{\underline{I}} \underline{\Omega}] \\ & - m \tilde{\underline{r}} \tilde{\underline{\omega}} \tilde{\underline{\omega}} (\underline{R} + \underline{s}_a) - m \tilde{\underline{r}} \underline{\underline{A}}^T [\tilde{\underline{u}} \tilde{\underline{\lambda}} \underline{\underline{A}} \underline{\omega} + \tilde{\underline{\Omega}} \tilde{\underline{\Omega}} \underline{u}] \\ & - (1/I_s) [\underline{\underline{A}}^T \underline{\underline{I}} - m \tilde{\underline{r}} \underline{\underline{A}} \tilde{\underline{u}}] \{\underline{\underline{E}}_1 [\underline{\underline{I}} \tilde{\underline{\lambda}} \underline{\underline{A}} \underline{\omega} - \underline{\underline{J}}^{-1} \underline{\underline{E}}_1 \underline{\underline{I}}^{-1} \underline{\underline{E}}_1 \underline{\underline{\Omega I \Omega}}] \\ & + (T_s \quad 0 \quad 0)^T\} + \underline{T}_0 , \end{aligned} \tag{A-25}$$

where the "inertia matrix" $\underline{\underline{L}}_1$ is given by

$$\underline{\underline{L}}_1 \equiv \underline{\underline{I}}_{L/0} - m \tilde{\underline{r}} \tilde{\underline{r}} + \underline{\underline{A}}^T \underline{\underline{I}} [\underline{\underline{E}} - (1/I_s) \underline{\underline{I}} \underline{\underline{E}}_1] \underline{\underline{A}} . \tag{A-26}$$

The torque $\underline{T}_0$ is due to gravity, rocket thrust, and the spin torque $\underline{T}_s$. It also includes a constraint torque which prevents rolling of the launcher.

From the geometry of Fig. A6, with $\alpha_1 \neq 0$,

$$\omega_1 = \dot{\alpha}_1 + \dot{\alpha}_2 \sin\alpha_3 ,$$

$$\omega_2 = \dot{\alpha}_2 \cos\alpha_3 \cos\alpha_1 + \dot{\alpha}_3 \sin\alpha_1$$

and

$$\omega_3 = -\dot{\alpha}_2 \cos\alpha_3 \sin\alpha_1 + \dot{\alpha}_3 \cos\alpha_1 .$$

If $\alpha_1 \equiv 0$,

$$\omega_1 = \dot{\alpha}_2 \sin\alpha_3 ,$$

$$\omega_2 = \dot{\alpha}_2 \cos\alpha_3$$

and

$$\omega_3 = \dot{\alpha}_3 . \qquad \text{(A-27)}$$

Hence,

$$\omega_1 = \omega_2 \tan\alpha_3 \qquad \text{(A-28)}$$

and

$$\dot{\omega}_1 = \dot{\omega}_2 \tan\alpha_3 + \omega_2\omega_3/\cos^2\alpha_3 . \qquad \text{(A-29)}$$

By substituting (A-28) and (A-29) into (A-25) one may solve for $\dot{\omega}_2$ and $\dot{\omega}_3$. Then, $\dot{p}$ can be found from (A-22).

The part of $\underline{T}_0$ due to "external" forces is $\underline{T}_0^{ex}$. We assume that the launcher's rotation is restrained by linear springs and viscous dampers. The torque due to these is

$$\underline{T}_{SD} = -\underline{\underline{K}}\,\underline{\alpha} - \underline{\underline{C}}\,\dot{\underline{\alpha}} , \qquad \text{(A-30)}$$

where $\underline{\underline{K}}$ and $\underline{\underline{C}}$ are constant stiffness and damping matrices, respectively, and $\underline{\alpha} = (\alpha_1 \Delta\alpha_2 \ \alpha_3)^T$. Here, $\Delta\alpha_2$ is the difference in α_2 and the quadrant elevation (QE) angle.

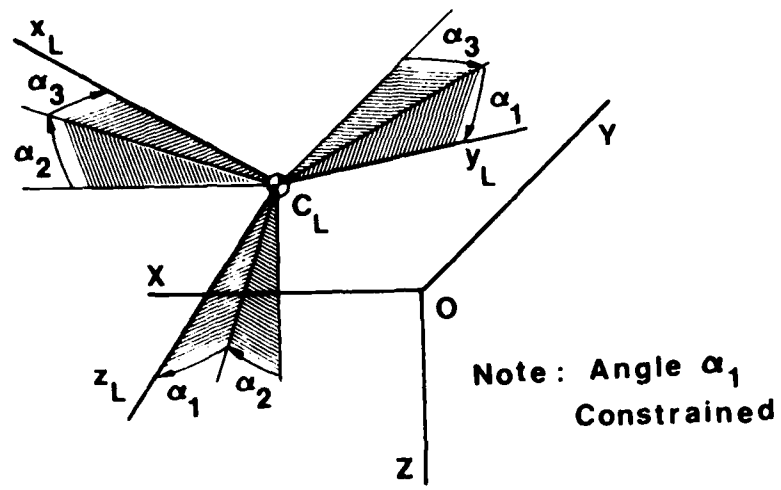

Fig. A6 Launcher orientation.

The torque about 0 due to gravity is

$$\underline{T}_g = m\,\tilde{\underline{r}}\,\underline{\underline{B}}\,\underline{g} + M\,\tilde{\underline{R}}\,\underline{\underline{B}}\,\underline{g}\ , \tag{A-31}$$

where

$$\underline{\underline{B}} = \begin{bmatrix} 1 & 0 & 0 \\ 0 & c\alpha_1 & s\alpha_1 \\ 0 & -s\alpha_1 & c\alpha_1 \end{bmatrix} \begin{bmatrix} c\alpha_3 & s\alpha_3 & 0 \\ -s\alpha_3 & c\alpha_3 & 0 \\ 0 & 0 & 1 \end{bmatrix} \begin{bmatrix} c\alpha_2 & 0 & -s\alpha_2 \\ 0 & 1 & 0 \\ s\alpha_2 & 0 & c\alpha_2 \end{bmatrix}$$

and $\underline{g} = (0 \quad 0 \quad g)^T$. Note that α_1 is not assumed to be identically zero, but is constrained to be zero for this investigation.

Action of the thrust $\underline{F}_T$ on the rocket produces a torque about 0 which is given by

$$\underline{T}_T = (\tilde{\underline{R}} + \tilde{\underline{s}}_a + \underline{\underline{A}}^T\,\tilde{\underline{\ell}}_T\,\underline{\underline{A}})\underline{\underline{A}}^T\,\underline{F}_T\ . \tag{A-32}$$

Finally,

$$\underline{T}_0^{ex} = \underline{T}_{SD} + \underline{T}_g + \underline{T}_T + \underline{T}_s\ . \tag{A-33}$$

The kinematic equations for the launcher for this and subsequent phases are, if $\alpha_1 \equiv 0$,

$$\dot{\alpha}_2 = \omega_2/\cos\alpha_3 \tag{A-34a}$$

and

$$\dot{\alpha}_3 = \omega_3\ . \tag{A-34b}$$

However, the computer code in which the equations are incorporated contains the more general equations,

$$\dot{\alpha}_2 = (\omega_2\cos\alpha_1 - \omega_3\sin\alpha_1)/\cos\alpha_3\ , \tag{A-35a}$$

$$\dot{\alpha}_3 = \omega_2\sin\alpha_1 + \omega_3\cos\alpha_1 \tag{A-35b}$$

and

$$\dot{\alpha}_1 = \omega_1 - \dot{\alpha}_2 \sin\alpha_3 \quad . \tag{A-35c}$$

A.4.3 Guidance Phase Equations

During the guidance phase, allowance is made for spin due to helical rails, or the spin torque $\underline{T}_s$. Two sets of equations are needed because the constraints present when spin is by helical rail are different from those which exist when there is a rocket-fixed spin torque due to spin motor, spin vanes, or a similar device.

Spin Torque Case

When spin is generated by $\underline{T}_s$, the constraints during guidance include a force $\underline{F}^c = (0 \quad F_2^c \quad F_3^c)^T$. We let $\underline{F}^{ex} = (F_1^{ex} \quad F_2^{ex} \quad F_3^{ex})^T$ denote the resultant external force on the rocket. Then, because there can be no motion in the y_L- or z_L-direction,

$$\begin{bmatrix} 0 \\ F_2^{ex} + F_2^c \\ F_3^{ex} + F_3^c \end{bmatrix} = m \underline{\underline{E}}_{23}\{\tilde{\underline{\omega}}\,\tilde{\underline{\omega}}(\underline{R}+\underline{s}_a) - (\tilde{\underline{R}}+\tilde{\underline{s}}_a)\dot{\underline{\omega}}$$

$$+ 2\,\tilde{\underline{\omega}}\,\dot{\underline{s}}_a - \underline{\underline{A}}^T[\tilde{\underline{u}}\,\dot{\underline{\Omega}} + \tilde{\underline{\Omega}}\,\tilde{\underline{\Omega}}\,\underline{u}]\} \ ,$$

where $\underline{s}_a = (x_{L_a} \; y_{L_a} \; z_{L_a})^T$ and only x_{L_a} varies with time. Equation (A-35) can be used along with (A-22) and (A-23) to obtain the following equation for $\underline{\omega}$:

$$\underline{\underline{L}}_2\,\dot{\underline{\omega}} = -\tilde{\underline{\omega}}\,\underline{\underline{I}}_{L/0}\,\underline{\omega} - (1/I_s)[\underline{\underline{A}}^T\,\underline{\underline{1}} - m\tilde{\underline{r}}\,\underline{\underline{E}}_{23}\underline{\underline{A}}^T\tilde{\underline{u}}]\{\underline{\underline{E}}_1\underline{\underline{I}}[\tilde{\underline{\lambda}}\underline{\underline{A}}\,\underline{\omega}$$

$$- \underline{\underline{I}}^{-1}\,\tilde{\underline{\Omega}}\,\underline{\underline{I}}\,\underline{\Omega}]\} + \begin{bmatrix} T_s \\ 0 \\ 0 \end{bmatrix} + \tilde{\underline{r}} \begin{bmatrix} F_1^{ex} \\ 0 \\ 0 \end{bmatrix}$$

$$+ \underline{\underline{A}}^T[\underline{\underline{I}}\,\tilde{\underline{\lambda}}\,\underline{\underline{A}}\,\underline{\omega} - \tilde{\underline{\Omega}}\,\underline{\underline{I}}\,\underline{\Omega}] - m\tilde{\underline{r}}\,\underline{\underline{E}}_{23}[\tilde{\underline{\omega}}\tilde{\underline{\omega}}(\underline{R}+\underline{s}_a) \tag{A-36}$$

$$+ 2\,\tilde{\underline{\omega}}\,\dot{\underline{s}}_a + \underline{\underline{A}}^T(\tilde{\underline{u}}\,\tilde{\underline{\lambda}}\,\underline{\underline{A}}\,\underline{\omega} + \tilde{\underline{\Omega}}\,\tilde{\underline{\Omega}}\,\underline{u})]$$

$$+ \underline{T}_0^{ex}\ , \qquad \text{(A-36 cont.)}$$

where

$$\underline{\underline{L}}_2 = \underline{\underline{I}}_{L/0} + \underline{\underline{A}}^T\,\underline{\underline{I}}\,\underline{\underline{A}} - m\tilde{\underline{r}}\,\underline{\underline{E}}_{23}[\tilde{\underline{r}} - (1/I_s)\underline{\underline{A}}^T\,\tilde{\underline{u}}\,\underline{\underline{E}}_1\,\underline{\underline{I}}\,\underline{\underline{A}}]$$

$$-(1/I_s)\underline{\underline{A}}^T\,\underline{\underline{I}}\,\underline{\underline{E}}_1\,\underline{\underline{I}}\,\underline{\underline{A}}\ . \qquad \text{(A-37)}$$

Translation of the rocket is governed by the equation,

$$m(\ddot{x}_{L_a}\quad 0\quad 0)^T = (F_1^{ex}\quad 0\quad 0)^T - m\,\underline{\underline{E}}_1\{\tilde{\dot{\underline{\omega}}}\underline{\omega}(\underline{R}+\underline{s}_a)$$

$$-(\tilde{\underline{R}}+\tilde{\underline{s}}_a)\dot{\underline{\omega}} + 2\,\tilde{\underline{\omega}}\,\dot{\underline{s}}_a - \underline{\underline{A}}^T\,\tilde{\underline{u}}[\dot{\underline{\lambda}} - \tilde{\underline{\lambda}}\,\underline{\underline{A}}\,\underline{\omega}$$

$$+ \underline{\underline{A}}\,\dot{\underline{\omega}}] + \underline{\underline{A}}^T\,\tilde{\underline{\Omega}}\,\tilde{\underline{\Omega}}\,\underline{u}\ \}\ . \qquad \text{(A-38)}$$

Rotation of the rocket relative to the launcher may be found from (A-22) and $\dot{\theta}_1 = p$.

Helical Rail Case

The helical rail is assumed to have a constant pitch such that if the rocket translates a distance ξ it rotates through an angle $\varepsilon\,\xi$ about its x'-axis. It follows that the rocket angular velocity relative to the launcher is (launcher basis or rocket basis)

$$\underline{\lambda} = (\varepsilon\,\dot{x}_{L_a}\quad 0\quad 0)^T\ . \qquad \text{(A-39)}$$

A portion of the helical rail is shown in Fig. A7. The angle α_H is defined by the following equations:

$$\cos\alpha_H = \varepsilon(d/2)/[1+(\varepsilon d/2)^2]^{\frac{1}{2}} \qquad \text{(A-40a)}$$

$$\sin\alpha_H = 1/[1+(\varepsilon d/2)^2]^{\frac{1}{2}} \qquad \text{(A-40b)}$$

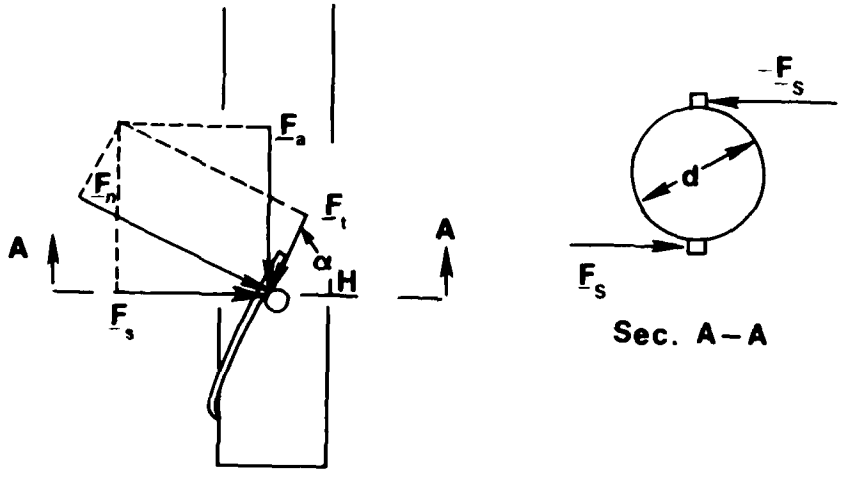

Fig. A7 Helical rail segment and associated forces.

Also shown in Fig. A7 are the $\underline{F}_n$, $\underline{F}_t$, $\underline{F}_a$ and $\underline{F}_s$, the normal, tangential, axial and spin components, respectively, of the force on the rocket due to the rail. Only one rail is shown; however, in most launchers there will normally be two or more. Herein, we assume two diametrically opposed rails, so that the total force on the rocket due to the rails is

$$2(\underline{F}_n + \underline{F}_t) = 2(\underline{F}_a + \underline{F}_s) \ .$$

From the geometry of Fig. A7, we have

$$F_a = -F_t \sin\alpha_H - F_n \cos\alpha_H \tag{A-41a}$$

and

$$F_s = -F_t \cos\alpha_H + F_n \sin\alpha_H . \tag{A-41b}$$

We assume that $F_t = \mu_f F_n$, where μ_f is the coefficient of dynamic friction corresponding to the rail/shoe combination. It then follows that the torque on the rocket due to the rail is given by

$$T_{rail} = F_n[\sin\alpha_H - \mu_f \cos\alpha_H]d \ , \tag{A-42}$$

where d is the rocket's diameter at the shoe location. Equation (A-42) may be used to eliminate F_n from (A-41b) and obtain the axial force on the rocket,

$$F_{axial} = -K_r T_{rail} \ , \tag{A-43a}$$

where

$$K_r = (2/d)(\cos\alpha_H + \mu_f \sin\alpha_H)/(\sin\alpha_H - \mu_f \cos\alpha_H) \ . \tag{A-43b}$$

The equation of rotational motion of the system about 0 is again (A-12) except that $\ddot{\underline{r}}$ has the more general form implied by (A-38); i.e., $\underline{s}_a$ is not constant.

Rotation of the rocket is governed by the equation,

$$\underline{\underline{I}} \cdot (d\underline{\Omega}/dt)_R + \underline{\Omega} \times \underline{\underline{I}} \cdot \underline{\Omega} = \underline{T}^{ex} + \underline{T}^{c} + \underline{T}_{rail}, \tag{A-44}$$

where, as before, $\underline{T}^{ex}$ is the external torque about C and $\underline{T}^{c}$ is the constraint torque which forces the rocket to pitch and yaw with the launcher. Furthermore, the equation which determines the motion of the rocket's center of mass is

$$m\ddot{\underline{r}} = \underline{F}^{ex} + \underline{F}^{c} + \underline{F}_{axial}, \tag{A-45}$$

where $\underline{F}^{ex} = \underline{F}_T + \underline{F}_g$ and $\underline{F}^{c}$ is a force which constrains the motion to be in the x_L-direction.

By writing (A-44) in matrix form (rocket basis) and solving for $\underline{T}_{rail}$, we find that

$$\underline{T}_{rail} = \underline{\underline{E}}_1 [\underline{\underline{I}}(\underline{\underline{A}} \dot{\underline{\omega}}_L - \tilde{\underline{\lambda}}\, \underline{\underline{A}}\, \underline{\omega} + \dot{\underline{\lambda}}) + \tilde{\underline{\Omega}}\, \underline{\underline{I}}\, \underline{\Omega}] . \tag{A-46}$$

This result for $\underline{T}_{rail}$ can be used in the matrix counterpart of (A-45) to get the result,

$$\begin{aligned} \ddot{\underline{s}}_a = \Delta^{-1}\, \underline{\underline{E}}_1 \{ & -2\tilde{\underline{\omega}}\dot{\underline{s}}_a - \tilde{\underline{\omega}}\tilde{\underline{\omega}}\underline{s}_a + \underline{\underline{A}}^T \tilde{\underline{u}}\, \underline{\underline{A}}\, \dot{\underline{\omega}}_L \\ & - \underline{\underline{A}}^T (\ddot{\underline{u}}\tilde{\underline{\lambda}}\underline{\underline{A}}\underline{\omega} + \tilde{\underline{\Omega}}\tilde{\underline{\Omega}}\underline{u} - \underline{F}_T/m) - \underline{\underline{B}}\underline{g} \\ & - K_r\, \underline{\underline{E}}_1\, [\underline{\underline{I}}(\underline{\underline{A}}\dot{\underline{\omega}} - \tilde{\underline{\lambda}}\underline{\underline{A}}\underline{\omega}) + \tilde{\underline{\Omega}}\underline{\underline{I}}\underline{\Omega}]\} , \end{aligned} \tag{A-47}$$

where $\Delta = 1 - \varepsilon(1 \quad 0 \quad 0)\underline{\underline{A}}^T \tilde{\underline{u}}\, \underline{\underline{A}}(1 \quad 0 \quad 0)^T + \varepsilon K_r I_s/m$.

The expression (A-47) can be used in the matrix counterpart of (A-12) to get,

$$\underline{\underline{L}}_{rail}\,\dot{\underline{\omega}}_L = -\tilde{\underline{\omega}}\,\underline{\underline{I}}_{L/0}\,\underline{\omega} - \underline{\underline{A}}^T\,\tilde{\underline{\Omega}}\underline{\underline{I}}\underline{\Omega} + \underline{\underline{A}}^T\,\underline{\underline{I}}\,\tilde{\underline{\lambda}}\,\underline{\underline{A}}\,\underline{\omega}$$

$$-[m\tilde{\underline{r}}(\underline{\underline{E}} - \Lambda^{-1}\underline{\underline{E}}_1) - \varepsilon(\underline{\underline{A}}^T\,\underline{\underline{I}}\,\underline{\underline{A}} - m\tilde{\underline{r}}\,\underline{\underline{A}}^T\,\tilde{\underline{u}}\,\underline{\underline{A}})\Delta^{-1}\underline{\underline{E}}_1]\{2\tilde{\underline{\omega}}\,\dot{\underline{s}}_a$$

$$+ \tilde{\underline{\omega}}\,\tilde{\underline{\omega}}\,\underline{r} + \dot{\tilde{\underline{\omega}}}\,\underline{\underline{A}}^T\,\tilde{\underline{\lambda}}\,\underline{u} + \underline{\underline{A}}^T\,\tilde{\underline{\lambda}}\tilde{\underline{\lambda}}\underline{u}\}$$

$$-[m\tilde{\underline{r}} + \varepsilon(\underline{\underline{A}}^T\,\underline{\underline{I}}\,\underline{\underline{A}} - m\tilde{\underline{r}}\,\underline{\underline{A}}^T\,\tilde{\underline{u}}\underline{\underline{A}})]\Delta^{-1}\,\underline{\underline{E}}_1[\underline{\underline{A}}^T\,\underline{F}_T/m + \underline{\underline{B}}\underline{g}]$$

$$+ \underline{T}_0 \quad . \tag{A-48}$$

Here,

$$\underline{\underline{L}}_{rail} = \underline{\underline{I}}_{L/0} + \underline{\underline{A}}^T\,\underline{\underline{I}}\,\underline{\underline{A}} - m\tilde{\underline{r}}\tilde{\underline{r}}$$

$$+ \Lambda^{-1}[m\tilde{\underline{r}} + \varepsilon(\underline{\underline{A}}^T\,\underline{\underline{I}}\,\underline{\underline{A}} - m\tilde{\underline{r}}\,\underline{\underline{A}}^T\,\tilde{\underline{u}}\,\underline{\underline{A}})]\underline{\underline{E}}_1\,\tilde{\underline{r}}$$

$$- \Lambda^{-1}\,K_r\,\tilde{\underline{r}}\,\underline{\underline{E}}_1\,\underline{\underline{I}}\,\underline{\underline{A}}\,. \tag{A-49}$$

Once $\dot{\underline{\omega}}_L$ has been found, it can be substituted into (A-46) to get $\ddot{\underline{s}}_a$. Then, $\dot{\underline{p}} = \varepsilon\,\ddot{\underline{x}}_{L_a}$.

A.4.4 Tip-Off Phase Equations

During the tip-off phase, if any, the rocket is assumed to rotate with respect to the launcher about the point a. The procedure for finding the equations of motion for this phase is the same as for the previous phases except that, since there is no constraint torque about point a (friction neglected) the derivative $(d\,\underline{\Omega}/dt)_R$ can be computed directly. The main result, from which $\dot{\underline{\omega}}_L$ can be found is

$$\underline{\underline{L}}_3\,\dot{\underline{\omega}}_L = -\tilde{\underline{\omega}}\,\underline{\underline{I}}_{L/0}\,\underline{\omega} - (\tilde{\underline{R}} + \tilde{\underline{s}}_a)\underline{\underline{E}}^*\,m\{2\,\dot{\tilde{\underline{\omega}}}\,\dot{\underline{s}}_a$$

$$+ \tilde{\underline{\omega}}\tilde{\underline{\omega}}(\underline{R}+\underline{s}_a) + \underline{\underline{A}}^T\tilde{\underline{\Omega}}\tilde{\underline{\Omega}}\underline{u} - \underline{\underline{B}}\underline{g} - \underline{\underline{A}}^T\underline{F}_T/m\} \tag{A-50}$$

$$+ (\tilde{\underline{R}}+\tilde{\underline{s}}_a)\underline{\underline{E}}_{23}\, m\, \underline{\underline{A}}^T\, \tilde{\underline{u}}\, \underline{\underline{I}}_a^{-1}\{-\tilde{\underline{\Omega}}\, \underline{\underline{I}}\, \underline{\Omega} + (\tilde{\underline{\ell}}_T - \tilde{\underline{u}})\underline{F}_T + \underline{T}_s\}$$

$$+ \underline{T}_0 - m\tilde{\underline{r}}\, \underline{\underline{Bg}} - \underline{T}_T - \underline{T}_s \ , \qquad \text{(A-50, Cont.)}$$

where

$$\underline{\underline{L}}_3 = \underline{\underline{I}}_{L/0} - m(\underline{R}+\underline{s}_a)\underline{\underline{E}}^*(\underline{R}+\underline{s}_a) \qquad \text{(A-51a)}$$

$$\underline{\underline{E}}^* = \underline{\underline{E}}_{23} + \underline{\underline{E}}_{23}\, \underline{\underline{A}}^T\, m\tilde{\underline{u}}\, \underline{\underline{I}}_a^{-1}\, \tilde{\underline{u}}\, \underline{\underline{A}}\, \underline{\underline{E}}_{23}, \qquad \text{(A-51b)}$$

$$\underline{\underline{I}}_a = \underline{\underline{I}} - m\tilde{\underline{u}}\, \underline{\underline{A}}\, \underline{\underline{E}}_{23}\, \underline{\underline{A}}^T\, \underline{u} \ , \qquad \text{(A-51c)}$$

$$\underline{\underline{A}} = \underline{\underline{C}}\, \underline{\underline{B}}^T \ , \qquad \text{(A-51d)}$$

$$\underline{\underline{C}} = \begin{bmatrix} 1 & 0 & 0 \\ 0 & c\Phi & s\Phi \\ 0 & -s\Phi & c\Phi \end{bmatrix} \begin{bmatrix} c\Theta & 0 & -s\Theta \\ 0 & 1 & 0 \\ s\Theta & 0 & c\Theta \end{bmatrix} \begin{bmatrix} c\Psi & s\Psi & 0 \\ -s\Psi & c\Psi & 0 \\ 0 & 0 & 1 \end{bmatrix} \ , \qquad \text{(A-51e)}$$

and M is the launcher mass. The Euler angles appearing in $\underline{\underline{C}}$ are the yaw (Ψ), pitch (Θ) and roll (Φ) angles of the rocket with respect to the fixed reference frame OXYZ (see Fig. A8).

The equation for $\dot{\underline{\Omega}}_{\underline{R}}$ is

$$\dot{\underline{\Omega}}_{\underline{R}} = \underline{\underline{I}}_a^{-1}\{-\tilde{\underline{\Omega}}\, \underline{\underline{I}}_a\, \underline{\Omega} + (\tilde{\underline{\ell}}_T - \underline{u}\, \underline{\underline{A}}\, \underline{\underline{E}}_1\, \underline{\underline{A}}^T)\underline{F}_T$$

$$+ \underline{T}_s + m\, \tilde{\underline{u}}\, \underline{\underline{A}}\, \underline{\underline{E}}_{23}[\underline{\underline{Bg}} + (\underline{R}+\underline{s}_a)\dot{\underline{\omega}}_{\underline{L}}$$

$$- \tilde{\underline{\omega}}\tilde{\underline{\omega}}(\underline{R}+\underline{s}_a) - 2\, \tilde{\underline{\omega}}\, \dot{\underline{s}}_a)\} \ ; \qquad \text{(A-52)}$$

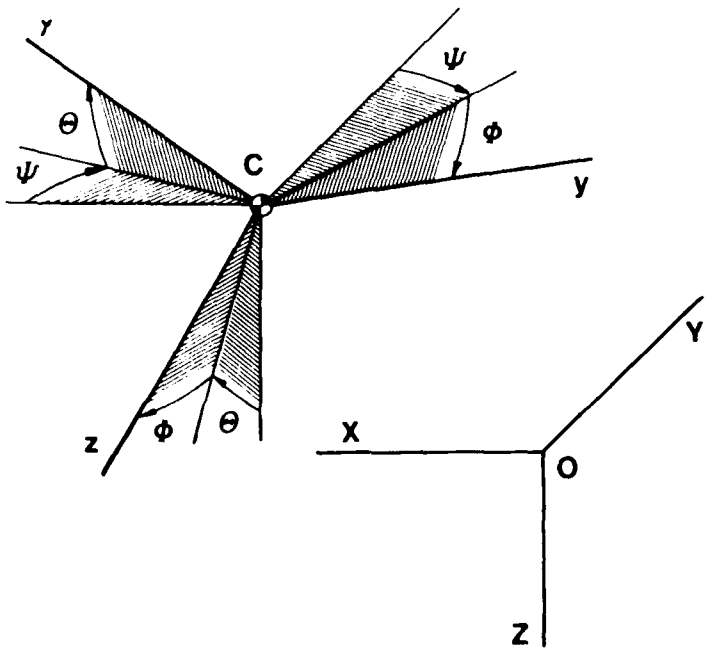

Fig. A8 Euler angles for definition of rocket orientation.